The role of the uncoupling protein2 -866G/A polymorphism in oxidative stress markers associated with air pollution exposure during pregnancy

By

SAVANIA NAGIAH

B.Sc. B. Med. Sc. (Hons) (UKZN)

Submitted in fulfilment of the requirements for the degree of M. Med. Sci

in the

Discipline of Medical Biochemistry and Chemical Pathology

School of Laboratory Medicine and Medical Sciences

College of Health Sciences

University of KwaZulu-Natal

Durban

2012

ABSTRACT

Consistently high levels of air pollutants such as sulphur dioxide, particle matter and nitric oxides have been observed in the Durban South (DS) industrial basin. The adverse health outcomes associated with ambient air pollution (AAP) exposure have underlying molecular mechanisms. Oxidative stress is a known outcome of AAP exposure and contributes to the exacerbation of adverse AAP related outcomes such as chronic obstructive pulmonary disorder (COPD) and asthma. Pregnant women are at increased risk of developing oxidative stress due to increased energy expenditure. Oxidative stress during pregnancy is linked to adverse birth outcomes such as intrauterine growth retardation and low birth weight. The mitochondria are the most abundant source of endogenous reactive oxygen species (ROS), making these organelles extremely susceptible to oxidative damage. Alterations in mitochondrial function by air pollutants can contribute to oxidative stress. Uncoupling protein2 (UCP2) is an anion carrier located on the inner mitochondrial membrane that regulates mitochondrial ROS production by reducing mitochondrial membrane potential ($\Delta\psi_m$) through mild uncoupling. Genetic variation in genes that play a role in oxidative stress response is likely to influence susceptibility to oxidative stress related health outcomes. The aim of this study was to evaluate air pollution associated oxidative stress response in women from the DS industrial basin and determine the functional relevance of a common -866G/A promoter polymorphism in the UCP2 gene. Fifty pregnant women from DS and 50 from north Durban (DN; control) were recruited. The thiobarbituric acid assay (TBARS) and comet assay were performed to measure oxidative stress and DNA fragmentation. Mitochondrial function was evaluated by JC-1 Mitoscreen and ATP luminometry. Quantitative PCR (qPCR) was performed to measure mitochondrial DNA (mtDNA) damage. Antioxidant response was determined by qPCR to measure mRNA expression of superoxide

dismutase 2 (SOD2), nuclear factor erythroid 2-related factor 2 (Nrf2) and UCP2 mRNA expression. Western blots were performed to quantify UCP2 and Nrf2 protein expression. The samples were genotyped using PCR - restriction fragment length polymorphism. Results from the TBARS assay showed women from DS displayed elevated levels of MDA, a marker for oxidative stress (0.07±0.06µM; p = 0.56). ATP (1.89 fold) and $\Delta\psi_m$ (45.3±17.2%; p = 0.8) were also elevated in women from DS, favouring free radical production. DNA fragmentation, as indicated by comet tail length was also higher in DS when compared to the control group (0.57±0.16µm; p = 0.037). Analysis of mtDNA viability showed a 0.49 fold change in mtDNA amplification in women from the industrialized DS. All antioxidant genes, i.e. Nrf2 (0.73 fold), UCP2 (1.58 fold), SOD2 (1.23 fold), were up regulated in women from DS. Analysis of protein expression showed a significant increase in UCP2 expression (0.08±0.03RBI; p = 0.049) and a significant decline in Nrf2 levels (1.68±0.84RBI; p = 0.03). The homozygous G genotype was significantly more frequent in DS (37.5%) than in DN (18.6%; p = 0.047; OR: 2.57; 95% CI: 1.353 to 4.885). This genotype exhibited higher MDA levels, comet tail length, $\Delta\psi_m$, SOD2, Nrf2, and UCP2 expression than the AA/GA in genotype in women from DS (p > 0.05). This study found that pregnant women from a more industrialized area exhibit higher markers for oxidative stress and conditions that favour mitochondrial free radical production.

DECLARATION

This study represents the original work by the author and has not been submitted in any form to another university. The use of work by others has been duly acknowledged in the text.

The research described in this study was carried out in the Discipline of Medical Biochemistry, Faculty of Health Sciences, University of KwaZulu-Natal, Durban, under the supervision of Prof. A.A. Chuturgoon and Miss Alisa Phulukdaree.

……

S. Nagiah

ACKNOWLEDGEMENTS

Prof A. A. Chuturgoon

Thank you for your guidance, support and motivation throughout the past two years. Most of all thank you for instilling in me a love for science and research.

Ms Alisa Phulukdaree

Thank you for being an exceptional mentor and friend to me. Your passion for your work has become an inspiration to me as a researcher.

Medical Science Masters Class 2012

Thank you for your assistance and making it a pleasure to work in the lab every day.

Senior PhD students

Thank you for your assistance and advice throughout the course of the year.

Patients in the EPoCH study

Thank you for willingly participating in this study and providing blood samples.

My family

Thank you for your patience and support.

The National Research Foundation and College of Health Science, UKZN

Scholarships and funding.

PRESENTATIONS

The role of mitochondria in air pollution associated oxidative stress response in pregnant women

S. Nagiah, A. Phulukdaree, D. Naidoo, K. Ramcharan, R. Naidoo, and A. Chuturgoon

College of Health Science Research Symposium, UKZN (*September 2012*)

Durban, South Africa

ABBREVIATIONS

$\Delta\psi_m$	Mitochondrial depolarisation
15d-PGJ$_2$	15-deoxy-D$^{12, 14}$-prostaglandin J$_2$
AAP	Ambient air pollution
ADP	Adenosine diphosphate
ARE	Antioxidant response element
ATP	Adenosine-5'-triphosphate
BCA	Bicinchonic acid
BHT	Butylated hydroxytoulene solution
BLAST	Basic local alignment search tool
BSA	Bovine serum albumin
CAT	Catalase
cDNA	Complementary DNA
CI	Confidence interval
CO	Carbon monoxide
CO_2	Carbon dioxide
COPD	Chronic obstructive pulmonary disorder

CSIR	Council for Scientific and Industrial Research
Ct	Comparative threshold
Cul3	Cullin3
DJ-1	Parkinson disease 7 (also known as PARK7)
DMSO	Dimethyl sulfoxide
DN	Durban North
DNA	Deoxyribose nucleic acid
dNTPs	Deoxyribonucleotide
DS	Durban South
dsDNA	Double stranded DNA
EDTA	Ethylenediaminetetraacetic acid
ELISA	Enzyme linked immune-sorbent assay
EtBr	Ethidium bromide
ETC	Electron transport chain
FADH	Flavin adenine dinucleotide
g	Gravitational force
GDP	Guanosine diphosphate
GP_x	Glutathione peroxidase

GSH	Reduced glutathione
GST	Glutathione-*S*-transferase
HO-1	Heme oxygenase 1
HRP	Horse radish peroxidase
HWE	Hardy Weinberg equilibrium
IUGR	Intrauterine growth retardation
Keap1	Kelch like ECH-associated protein 1
LMPA	Low melting point agarose
MDA	Malondialdehyde
$MgCl_2$	Magnesium chloride
MPP	Multi Point Plan
MRA	Merebank Residents Association
mRNA	messenger RNA
mtDNA	Mitochondrial DNA
NADH	Nicotinamide adenine dinucleotide
NADPH	Nicotinamide adenine dinucleotide phosphate
NCBI	National Centre for Biotechnology Information
NO	Nitrogen oxide

NO_2	Nitrogen dioxide
NOx	Nitric oxide; nitrogen dioxide
NQO1	NADPH:quinone oxidoreductase
Nrf2	Nuclear factor erythroid 2-related factor 2
$O_2^{-\bullet}$	Superoxide anion radical
O_3	Ozone
OR	Odds ratio
qPCR	Quantitative PCR
PAH	Polycyclic aromatic hydrocarbons
PBMCs	Peripheral blood mononuclear cells
PBS	Phosphate saline buffer
PCR	Polymerase chain reaction
PM_{10}	Particulate matter (diameter 10μm)
PPARγ	Peroxisome proliferator activated receptor γ
RBI	Relative band intensity
RLU	Relative light units
RNA	Ribose nucleic acid
RNS	Reactive nitrogen species

ROS	Reactive oxygen species
SD	Standard deviation
SDCEA	South Durban Community Environmental Alliance
SDS	Sodium dodecyl sulfate
SDS-PAGE	SDS-Polyacrylamide gel electrophoresis
SNP	Single nucleotide polymorphism
SO_2	Sulphur dioxide
SOD	Superoxide dismutase
ssDNA	Single stranded DNA
TBA	Thiobarbituric acid
TBARS	Thiobarbituric acid reactive substances
TEMED	Tetramethylethylenediamine
Tris-HCl	Tris(hydroxymethyl)aminomethane hydrochloric acid
TRS	Total reduced sulphur
TTBS	Tween 20 Tris-buffered saline
UCP	Uncoupling protein
UV	Ultra violet

LIST OF FIGURES

CHAPTER 1

CHAPTER 2

CHAPTER 3

LIST OF TABLES

CHAPTER 2

CHAPTER 3

TABLE OF CONTENTS

INTRODUCTION

The Durban South (DS) industrial basin in the province of KwaZulu Natal, South Africa (SA), comprises of a mix of closely situated heavy industrial and residential areas. Studies have evaluated the association of high air pollutant levels and the incidence of adverse respiratory health outcomes in the DS basin (Kistnasamy 2005; Niranjan 2005; Guastella 2007). Although air pollutant levels fell below international and national guidelines, high sulphur dioxide (SO_2) and particulate matter (PM_{10}) in DS was associated with acute changes in health status and moderate to severe asthma in children of school going age (Kistnasamy 2005). An estimate of 600 "smokestack" industries are situated in the DS basin including the largest oil refinery in SA, petroleum, paper, refined sugar, and asbestos product industries. The health concerns raised due to the toxic emissions from these industries has led to the monitoring of air pollutant levels in the DS area. Sulphur dioxide levels have been a concern in the DS area due to consistently high levels (Kistnasamy 2005; Guastella 2007). Recently, other air pollutants such as nitrogen dioxide and nitrogen oxide (collectively known as NOx), carbon monoxide (CO), PM_{10}, ozone (O_3) and lead have been detected at high levels in the DSB (Guastella 2007).

The health risk that long term exposure to AAP poses to humans increased due to the rapid expansion of industries. Adverse health effects include asthma, chronic obstructive pulmonary disorders, decreased lung function, cardiovascular disease, cystic fibrosis, inflammation, cancer, mitochondrial dysfunction and oxidative stress (Künzli, Kaiser et al. 2000; Kelly 2003; Bobak 2005; Liu, Poon et al. 2008; Yang and Omaye 2009; Shrey, Suchit et al. 2011). Exposure to AAP during pregnancy has been associated with birth outcomes such as low birth weight, premature birth, pre eclampsia and intra-uterine growth retardation (IUGR) (Wang, Ding et al. 1997; Bobak 2000; Maroziene and Grazuleviciene 2002;

Maisonet, Correa et al. 2004). The mechanism by which AAP results in adverse health outcomes is still not clearly understood. Several adverse birth and health outcomes associated with AAP exposure have been attributed to oxidative stress (Chahine 2007; Kamdar, Le et al. 2008; Liu, Poon et al. 2008; Castro-Giner 2009; Xu, Xu et al. 2011). Pregnant women have increased susceptibility to oxidative stress due to altered physiological processes and increased energy expenditure (Kelly 2003; Sastre-Serra 2010). The DS industrial basin presents the opportunity to investigate the health implications of long term AAP exposure, especially in pregnant mothers.

Common air pollutants such as PM_{10}, SO_2, CO, O_3 and NOx have all been implicated in free radical production (Kelly 2003; Risom, Møller et al. 2005; Campen 2009; Yang and Omaye 2009). These pollutants generate free radicals by being oxidants themselves, altering mitochondrial and NADPH oxidase function or initiating an inflammatory response (Kelly 2003).

Reactive oxygen species (ROS) are a natural by product of mitochondrial respiration. The electron transport chain (ETC), on the inner mitochondrial membrane, drives ATP synthesis via a proton gradient created by electron flow across the mitochondrial membrane. Oxidative phosphorylation is the process that drives electron flow through each complex of the ETC. However, electron "leakage" occurs, mainly at complex I and III, resulting in the production of superoxide ($O_2^{\bullet-}$) anion radical. When electron transfer at complex I and III is slow or when mitochondrial membrane potential ($\Delta\psi_m$) is elevated, $O_2^{\bullet-}$ anion radical production is increased (Giardina, Steer et al. 2008; Emre and Nubel 2010).

Endogenous antioxidant systems exist to prevent cellular damage by ROS. The major antioxidant enzymes such as superoxide dismutase (SOD), glutathione peroxidase (GPx), glutathione reductase (GR), and catalase (CAT) are regulated at the transcriptional level by

nuclear factor erythroid 2-related factor 2 (Nrf2). When intracellular ROS levels rise, Nrf2 translocates from the cytoplasm to the nucleus. Nrf2 binds to the antioxidant response element (ARE) in the nucleus and initiates transcription of antioxidant genes (Motohashi and Yamamoto 2004). When ROS production exceeds the antioxidant capacity of the cell, oxidative stress occurs.

Mitochondria are highly susceptible to oxidative damage as they are the main endogenous ROS producers. Mitochondrial DNA (mtDNA) lacks the repair mechanisms that nuclear DNA possesses, making mtDNA extremely susceptible to oxidative insult. Damage to mtDNA often results in mitochondrial dysfunction and increased mitochondrial ROS production (Sies 1997; Li, Sioutas et al. 2002).

A group of mitochondrial anion carriers known as uncoupling proteins (UCPs) found in the inner mitochondrial membrane uncouple oxidative phosphorylation from ATP synthesis (Pecqueur, Alves-Guerra et al. 2001). Uncoupling proteins increase the rate of electron transfer across the mitochondrial membrane and reduce $\Delta\psi_m$ (Nedergaard, Ricquier et al. 2005). Several homologues have been discovered, each displaying different tissue specificity and biological functions.

Uncoupling protein 2 (UCP2) is the most widely expressed UCP and negatively regulates mitochondrial ROS production. Studies have shown that $O_2^{\bullet-}$ anion radical and products of lipid peroxidation are potent inducers of UCP2 expression (Echtay, Roussel et al. 2002; Bo 2008; Giardina, Steer et al. 2008; Stephens 2008). Uncoupling protein2 has also been implicated in reducing hydrogen peroxide production and oxidative burst in macrophages (Negre-Salvayre 1997; Rudofsky, Schroedter et al. 2006; Jun, Kim et al. 2008; Lee, Ryu et al. 2008; Emre and Nubel 2010).

A common G/A polymorphic variant in the -866 region of the promoter of the UCP2 gene has been implicated in the expression and function of this protein (Stephens, Dhamrait et al. 2008; Emre and Nubel 2010). Variation in genes involved in oxidative stress response can possibly influence susceptibility to adverse health outcomes associated with AAP (Kim and Hong 2012). Despite the rapid pace of industrialisation in Africa, very few studies have been conducted investigating gene-environment interactions regarding AAP.

This pilot study sought to firstly evaluate oxidative stress markers in women from the DS industrial basin and compare these to women from the less industrialized Durban North (DN). Secondly, the functional relevance of the UCP2 -866G/A promoter polymorphism in the oxidative stress response of women from DS was investigated. The objective of this study was to determine whether women exposed to higher levels of air pollutants displayed higher markers for oxidative stress and whether genetic variability in the UCP2 gene affected susceptibility of these women to oxidative stress. The antioxidant response of women in the DS basin was also investigated. This is the first study investigating the involvement of UCP2 in air pollution associated oxidative stress, and will give insight into mitochondrial response to oxidative stress. By identifying genetic and environmental risk factors, more targeted therapeutic interventions can be put in to place, such as antioxidant administration.

CHAPTER 1

LITERATURE REVIEW

1.1 Durban South Industrial Basin

The Durban South (DS) basin is the largest industrial hub of KwaZulu-Natal, contributing 8% of the gross domestic profit. It is located on the east coast of the SA, extending from the Durban Central Business District to Umbogintwini. The DS basin is home to some 200 000 inhabitants (Guastella 2007). It consists of the residential areas of Merebank, Wentworth, Bluff, Clairwood, Isipingo, and Lamontville and the industrial areas of Prospecton and Jacobs (Fig 1.1). The residential areas are located adjacent to the industrial areas.

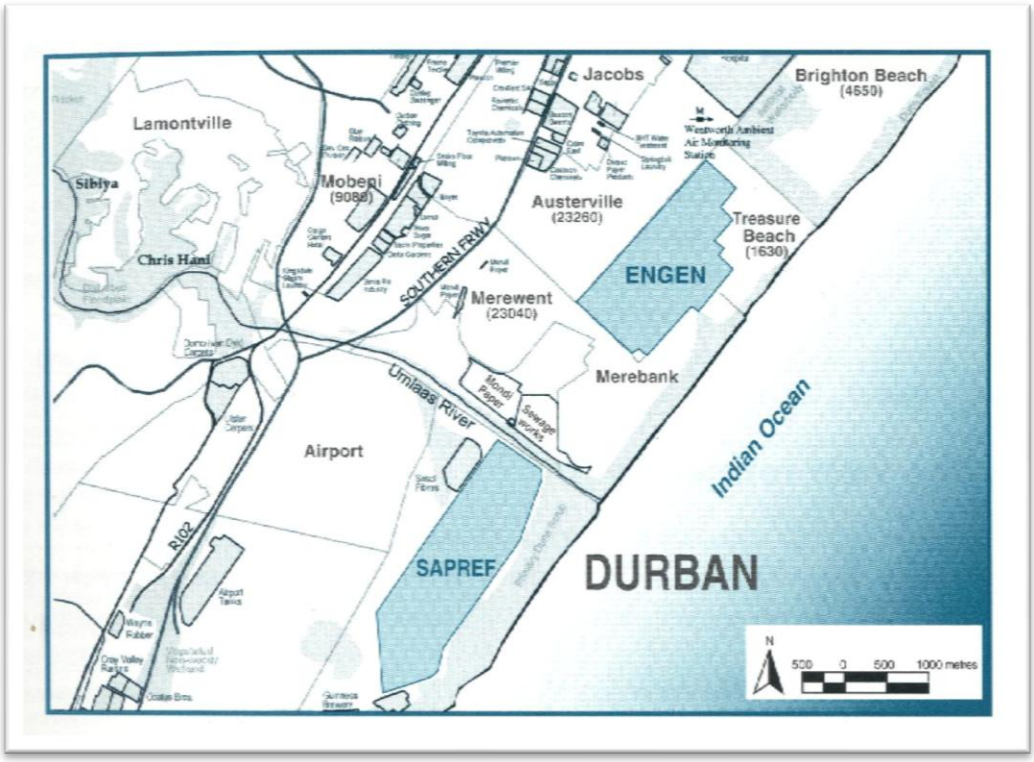

Figure 1.1: Map of Durban South industrial basin located on the east coast of South Africa (Kistnasamy 2005).

Among what is estimated to be 120 "smokestack" industries located in the DS region are the largest crude oil refinery in Southern Africa, Sapref; ENGEN petroleum company (Fig 1.2B); Mondi paper company (Fig 1.2A); Hulett sugar refinery; and various chemical producing companies. Other companies include plastics, chromium, asbestos, textiles, paint products and sewage works. Hulett, SAPREF and Mondi are collectively responsible for 80% of sulphur dioxide (SO_2) emissions in DS (Kistnasamy 2005; Guastella 2007). The DS industrial basin is also central to major transport routes, including a harbour, railway line and highways. These vehicular emissions exacerbate the deterioration of air quality in DS (Guastella 2007).

The toxic emissions that are characteristic of heavy industries have been a pressing concern for residents of DS for many decades. The DS industrial basin is an existing legacy of environmental injustice by the apartheid regime. Since the 1950's, the industrialisation of this site was coupled with the forced relocation of non-Whites in accordance with the Group Areas Act. Apartheid politicians deliberately located low income black townships in close proximity to industries to provide easy access to cheap labour (Niranjan 2005). The health implications of this situation were not taken in to account.

In the 1960's, the Council for Scientific and Industrial Research (CSIR) began a nationwide initiative to measure SO_2 levels across the country at 48 and 72 hour intervals. Sulphur dioxide is a common indicator used in air pollution studies and elevated levels are associated with respiratory problems and oxidative stress (Gumus 2000; Yang and Omaye 2009). During this initiative the DS industrial basin was recognized as an area of concern due to the high levels of SO_2 observed by the CSIR. Residents had also started to voice various complaints attributed to the emissions from the industries including odours, nausea, loss of apetite, sleeplessness, increased blood pressure, asthma, respiratory infections, bronchodialation, rashes, headaches and bronchial pneumonia (Kistnasamy 2005). The lack of substantial research in determining the health implications of long term air pollution

exposure in DS and protective legislature heightened tension between residents and industry stakeholders (Guastella 2007).

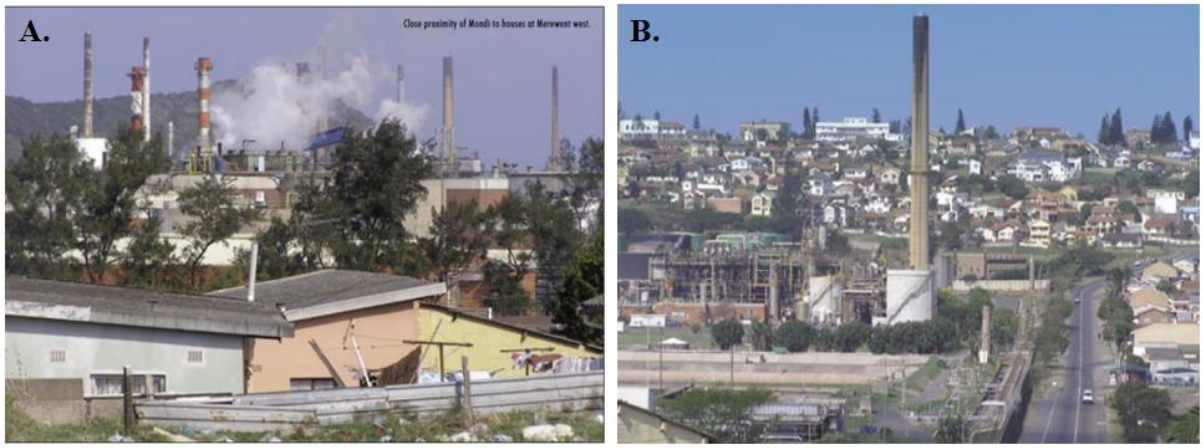

Figure 1.2: Close proximity of Mondi paper mill in Merewent (A) and ENGEN petrol refinery (B) in Austerville (Guastella, 2007).

The community's efforts to address the growing concern over air pollution in the DSB intensified in the 1980's and 1990's. In 1997, the South Durban Community Environmental Alliance (SDCEA) was formed to unify the community's efforts to address air pollution concerns. This consisted of a conglomerate of pre-existing organisations such as the Merebank Residents' Association (MRA), Bluff Ratepayers Association and Wentworth Developmental Forum. The SDCEA represented the community on the South Durban Sulphur Dioxide Management System Steering Committee (Kistnasamy 2005; Guastella 2007). This committee functioned to monitor SO_2 levels and implement management strategies to lower SO_2 levels. Monitoring stations were set up in Wentworth, Athlone Park, AECI and Southern Sewage Works. The monitoring system, now known as the eThekwini Air Quality Management Association, also recognised ozone (O_3); and nitric oxide and nitrogen dioxide (collectively known as NO_x) as pollutants that required attention. Eventually carbon monoxide (CO), particulate matter (PM_{10}) and total reduced sulphur (TRS) were added to the list of pollutants being monitered in DS (Guastella 2007).

In 2003, the eThekwini Air Quality Management Association was replaced by the South Durban Basin Multi-Point Plan. The Multi-Point Plan (MPP), which extended efforts to implement change in the regulation of emissions by industries in the DS basin. The DS industrial basin was recognised as having one of the highest SO_2 levels in the country and media coverage was given on heightened incidences of cancer and respiratory disease in the region. This was substantiated by a study in 1991 by Dr B Kistnasamy, who showed a higher incidence of respiratory illnesses in a school in Merebank when compared to a school in Chatsworth (Kistnasamy 1991). In 2004 a study was undertaken to investigate the incidence of asthma in the Settlers' School in Merebank. It was found that elevated levels of SO_2 and PM_{10} increased the risk of asthma in the school when compared to a control school in Chatsworth (Kistnasamy 2005). Since the implementation of the MPP, the Wentworth, Southern Works and Settler's monitering stations were recognized as 'hotspots" regarding SO_2 levels (Fig 1.3). The MPP is still in place, continuing efforts to reduce pollutant emissions from industries without compromising economic development. Currently, four pollutants are being monitored on a daily basis in DS i.e. SO_2, PM_{10}, nitrous oxide and ozone.

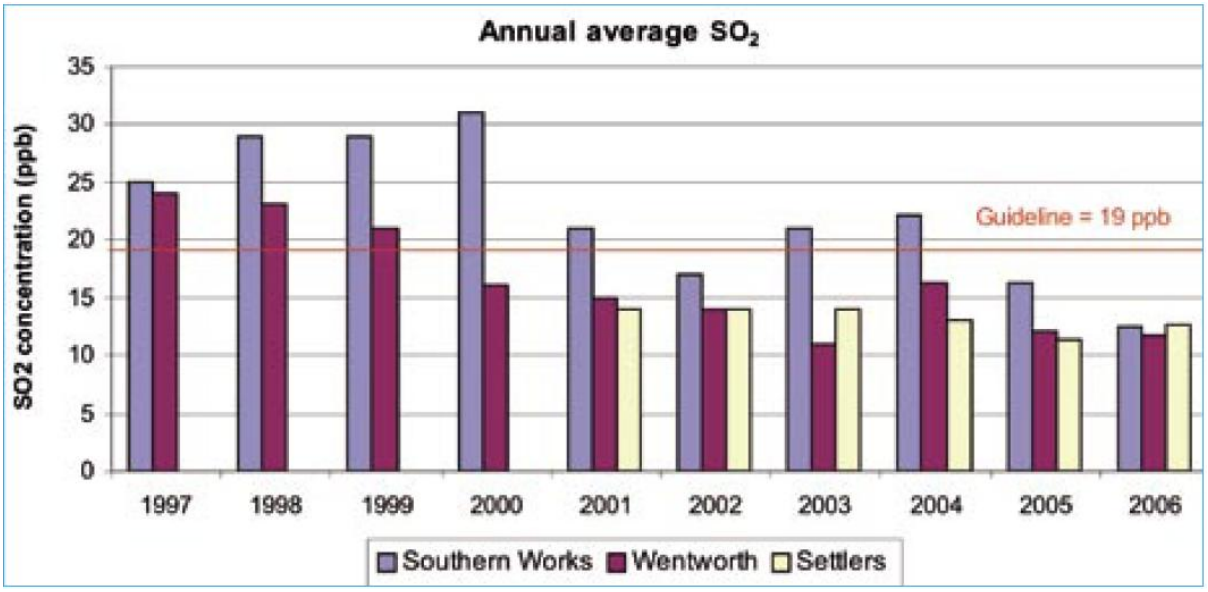

Figure 1.3: Sulphur dioxide distribution at the three monitoring stations with the highest SO_2 readings from 1997-2006 (Guastella, 2007).

The DS industrial basin provides an opportunity to investigate health implications of long term exposure to ambient air pollution. Studies have already been done regarding the social effects (Jaggernath 2010) and health outcomes (Kistnasamy 2005; Niranjan 2005). However, no studies have been performed investigating genetic and biological risk factors.

1.2 Health Implications of Ambient Air Pollution Exposure

Air pollution caused by industrialisation is not a problem isolated to DS. It is a globally recognized concern, with interest peaking in recent years due to the rapid expansion of industries (Brunekreef 2002). The health outcomes of ambient air pollution (AAP) exposure have been well discussed in literature. A correlation between AAP exposure and increased morbidity and mortality has been observed in epidemiological studies (Künzli, Kaiser et al. 2000). Exposure to AAP has been associated with asthma (Li 2003; Li, Hao et al. 2003; Kistnasamy 2005; Castro-Giner 2009), COPD (Li 1996; Yang and Omaye 2009), decreased

lung function (Li 1996; Pope 2002; Liu, Poon et al. 2008), cardiovascular disease (Stephens 2008; Shrey, Suchit et al. 2011), cystic fibrosis (Kamdar, Le et al. 2008), inflammation (Li 1996; Liu, Poon et al. 2008), cancer (Pope 2002), mitochondrial dysfunction (Xu, Xu et al. 2011) and oxidative stress (Kelly 2003; Risom, Møller et al. 2005; Castro-Giner 2009; Yang and Omaye 2009; Bigagli 2011).

The most commonly studied air pollutants are SO_2, NO_x, PM_{10}, CO and recently O_3. The exact mechanism by which air pollution exposure exerts toxicity is difficult to determine as pollutant levels vary among microenvironments, and possible interactions between pollutants need to be taken in to account.

1.2 .1 Particulate matter (PM_{10})

Particulate matter can be solid or liquid, or a mixture of solid and liquid particles suspended in the air (Brunekreef 2002). It is a by product of fossil fuel combustion and commonly used as an indicator of air pollution (Künzli, Kaiser et al. 2000). Particulate matter is usually defined by its size in diameter, e. g. PM_{10} =10µm in diameter. Particulate matter equal to or less than 10µm in diameter have been associated with increased morbidity and mortality (Li 2003). Exposure to PM_{10} has been implicated in life-shortening, non-malignant respiratory and cardiopulmonary deaths, lung cancer and asthma (Brunekreef 2002). One proposed mechanism by which PM_{10} exerts toxicity is via the induction of oxidative stress (Li 1996). These particulates can contain soluble metals, including transition metals that are capable of redox reactions. Polycylclic aromatic hydrocarbons (PAHs) that are adsorbed in PM_{10} are capable of forming DNA adducts, and of being biotransformed by cytochrome P450 enzymes to free radicals (Kelly 2003). Particulate matter is also capable of generating ROS by altering mitocondrial function or NADPH oxidase activity, initiating an inflammatory response or direct generation from the particles surface. Oxidative stress induced by PM_{10} has been found

to result in DNA damage (Risom, Møller et al. 2005). Particulates have also been found to induce proinflammatory (Li 1996) and allergic response that can contribute to acute asthma attacks (Li 2003) and increased blood viscosity (Maisonet, Correa et al. 2004).

1.2.2 Sulphur dioxide (SO_2)

Sulphur dioxide occurs ubiquitously in the air and is a characteristic emission of industrial processes (Gumus 2000; Pope 2002; Yang and Omaye 2009). This gas has been linked with cardiopulmonary disease and various respiratory disorders including bronchoconstriction in asthmatics, allergic reactions and lung cancer (Ziqiang Meng 2003). It is inhaled through the respiratory tract and enters the blood stream, allowing distribution through out the body. In an aqueous environment, SO_2 is converted to its free radical form, $SO_2^{-\bullet}$ (Gumus 2000). Health implications of SO_2 exposure include allergic reactions, bronchoconstriction in asthmatics; ischeamic cardiac events and lung cancer (Meng 2007). Although the exact mechanism by which SO_2 exerts its toxicity is unclear, oxidative stress plays a role in SO_2 toxicity. Meng et al. found that SO_2 (112mg/m^3) decreased antioxidants superoxide dismutase (SOD) and glutathione peroxidase (GP_x) expression in mice. At lower concentrations SO_2 was found to increase antioxidant response as well as ROS generation (Meng, Qin et al. 2003). Other studies have shown that SO_2 caused elevated lipid peroxidation in mice brains, liver (Meng, Qin et al. 2003), lungs, heart (Meng, Qin et al. 2003), and testicles (Meng and Bai 2004). It has also been found to be genotoxic to humans (Ziemann, Hansen et al. 2010) and decrease serum vitamin C and ceruloplasmin (Gumus 2000). Sulphur dioxide has gene altering capabilities, particularly with regard to genes involved in the electron transport chain. It has been found to upregulate the expression of ATPase inhibitor genes and decrease the expression of the cytochrome c oxidase gene. Inhibition of the electron transport chain promotes formation of mitochondrial-derived ROS (Meng 2007).

1.2.3 Nitric oxide and nitrous oxide (NO_x)

The major source of NO_x emmissions are vehicles. Concentrations of NO_x peak during high traffic hours in the morning and in the afternoon. Unlike PM_{10} and SO_2, NO_x is not a spatially distributed pollutant. Nitric oxide (NO) exists endogenously, and plays a vasodilatory function in endothelial cells and smooth muscle (Loh, Stamler et al. 1994). Nitric oxide itself is not toxic, however secondary reactive nitrogen species (RNS) can be derived when NO interacts with other free radicals. Nitric oxide can react with O_3 to form NO_2 or it can be converted to peroxynitrite by $O_2^{\bullet-}$ (Campen 2009). Exposure to NO has been associated with lung disease and atherosclerosis (Barnes 1993; Quyyumi 1995). Nitrogen dioxide is soluble in aqueous solutions and forms a nitrogen centred free radical when dissolved in lung lining fluid (Kelly 2003). Nitrogen dioxide activates oxidant pathways, resulting in T lymphocyte and macrophage recruitment. It increases the risk of infection by impairing the function of alveolar macrophages (Brunekreef 2002).

1.2.4 Carbon monoxide

Carbon monoxide is a common pollutant produced from vehicle emissions, industrial processes and burning of fossil fuels. This gas exerts its toxicity by competitive inhibition of oxygen transport. Carbon monoxide has a higher affinity for haemoglobin than oxygen. Carbon monoxide binds to haemoglobin, forming carboxyhaemoglobin, and thus reduces oxygen transport by haemoglobin. Health manifestations of CO exposure include headaches, fatigue and cardiovascular disorders (Shrey, Suchit et al. 2011).

1.2.5 Ozone

In recent years, concerted efforts have been made to reduce air pollutants released from burning of fossil fuels. However, concern has been raised over photochemical pollutants, such as O_3.

Ozone is the product of a sunlight reacting with NO_2 or hydrocarbons. Nitric oxide, a common pollutant from vehicles, is converted to NO_2 by O_3. The uptake of O_3 is directly related to the amount of substrate available. In the lung lining fluid, O_3 forms ozonation free radical products (Kelly 2003). Being a potent oxidizing agent, O_3 activates stress signalling pathways, causing a proinflammatory response in lung epithelial cells and alveolar macrophages. The inflammatory response can result in bronchoconstriction, which is characteristic of asthma. Ozone also increases IgE production, causing hypersensitivity (Brunekreef 2002). Other symptoms of O_3 include decreased lung function, pulmonary inflammation and exacerbation of symptoms in asthmatics (Kelly 2003).

1.3 Air Pollution and Pregnancy Outcomes

Exposure to AAP during pregnancy has been associated with adverse birth outcomes such as low birth weight, pre-term delivery (< 37 weeks gestation) and intra-uterine growth retardation (IUGR) (Wang, Ding et al. 1997; Dejmek 2000; Maroziene and Grazuleviciene 2002; Maisonet, Correa et al. 2004; Bobak 2005). The mechanisms by which AAP exposure affects pregnancy outcomes is still not clearly understood. Carbon monoxide can retard foetal growth due to reduced oxygen transport to the foetus. Particle matter has been found to increase blood viscosity thus compromising placental function (Maisonet, Correa et al. 2004). Exposure to PAHs that are adsorbed in PM_{10} results in the formation of DNA adducts. It was found that PAHs can pass through the placenta, exposing the foetus to PAHs. Babies with higher PAH-DNA adducts had impaired growth when compared to those with lower adduct

levels (Maisonet, Correa et al. 2004). Taking these factors in to account could explain impaired foetal growth. Furthermore, exposure to air pollution during childhood also has adverse health outcomes. The first 6 years of childhood are critical for lung and immune development. Childhood exposure to air pollution has been found to result in decreased lung development, cardiovascular and pulmonar disorders and asthma (Schwartz 2004).

Oxidative stress during pregnancy has been observed to have similar birth outcomes to those associated with AAP exposure (Al-Gubory 2010). Pregnant women are at an increased risk of developing oxidative stress due to the offset of physiological processes, hormonal changes and increased energy expenditure (Masaki 1999; Kelly 2003). Increases in oestrogen levels during pregnancy have been found to increase ROS production by mitochondria (Sastre-Serra 2010). Oxidative stress during pregnancy has been implicated in birth outcomes such as preeclampsia, embryonic resorption, spontaneous pregnancy loss, IUGR and foetal death (Al-Gubory 2010). Considering exposure to common air pollutants such as SO_2, PM_{10}, CO, NO_x, O_3 all induce oxidative stress, this could be a possible mechanism by which air pollutants cause adverse birth outcomes.

1.4 Oxidative Stress

Gaining an understanding of the biological mechanisms by which specific pollutants exert adverse health outcomes will allow a targeted approach (e.g. antioxidant administration) to prevention and treatment of AAP induced health problems. Many of the discussed pollutants are either free radicals in nature or have the ability to drive free radical production. This implicates oxidative stress as a possible mechanism of AAP exposure toxicity.

Oxidative stress is a term first used by Sies in 1991(Sies 1991). This term refers to a condition whereby the balance between circulating free radicals and antioxidants are disrupted, favouring the former (Fig 1.4). Free radicals, which include reactive oxygen species (ROS) and reactive nitrogen species (RNS), have an unpaired valence electron, making them extremely reactive. The free electron is capable of oxidising neighbouring molecules by "stealing" electrons (Kelly 2003; Ježek and Hlavatá 2005). The oxidizing potential of free radicals pose as a potential threat as they could alter the structure, and thus function, of cellular components such as lipids, proteins and DNA. Free radical damage is associated with elevated intracellular calcium levels, DNA strand breaks and base modification (Poston and Raijmakers 2004).

Reactive oxygen species are natural by products of cellular respiration, hence mitochondria are the most abundant endogenous source (Turrens 2003; Ježek and Hlavatá 2005). They play a role in normal physiological functions of the cell such as cell signalling, apoptosis and immunity (Hensley, Robinson et al. 2000; Thannickal and Fanburg 2000; Turrens 2003; Ježek and Hlavatá 2005; Sanjuán-Pla, Cervera et al. 2005). To counteract the potentially dangerous effects of ROS, an antioxidant defence mechanism is in place to scavenge free radicals. Antioxidants can occur intracellularly or be administered by dietary means (Seifried, Anderson et al. 2007; Al-Gubory 2010). Oxidative stress occurs when there is an overproduction of ROS, owed to increased endogenous production, exposure to a toxin, or a depletion of antioxidants.

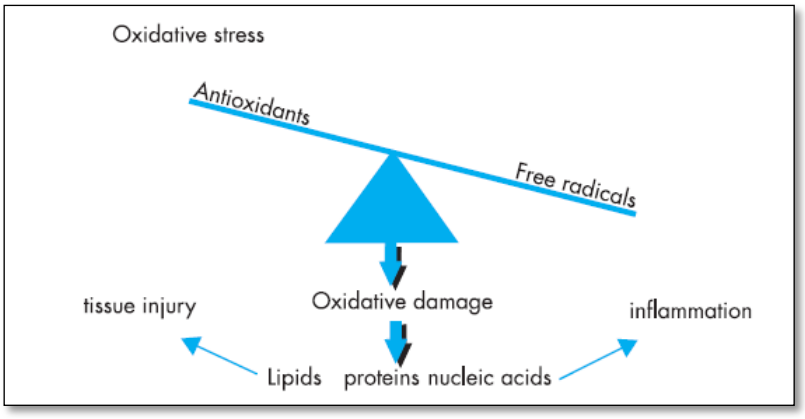

Figure 1.4: Schematic representation of oxidative stress mechanism of toxicity. When free radical content exceeds antioxidant capacity, more free radicals are free to oxidize neighbouring molecules, resulting in oxidative damage (Kelly, 2003).

Oxidative stress has been implicated in various pathological conditions such as atherosclerosis, hypertension, ischemia reperfusion injury, cystic fibrosis, cancer, type 2 diabetes, inflammation, neurodegenerative diseases and aging (Nordberg and Arnér 2001; Kelly 2003; Ježek and Hlavatá 2005; Bo 2008; Stephens 2008; Salpea, Talmud et al. 2010). The mechanism by which free radicals exert toxicity is due to the oxidizing of DNA, proteins and lipids.

Attack of lipid membranes by free radicals results in lipid peroxidation. Oxidation of fatty acids leads to the production of fatty acid free radicals that are capable of oxidizing neighbouring fatty acids. This results in a chain reaction in lipid membranes, with neighbouring fatty acid radicals generating more free radicals (Poston and Raijmakers 2004). The cell membrane becomes compromised and this leads to increased apoptosis or necrosis. Mitochondrial swelling and the release of hydrolytic enzymes from lysosomes have also been observed as events following lipid peroxidation (Meng 2007).

Reactive oxygen species are capable of iniating caspase activity thus increasing cell death. Free radical interaction with DNA causes mutations and strand breaks (Poston and

Raijmakers 2004). This is a possible mechanism for oncogenesis. Oxidative stress also results in mitochondrial damage by attack of mtDNA which has implications for metabolism, cell death and further generation of ROS. (Turrens 2003; Ježek and Hlavatá 2005).

1.5 Transcriptional regulation of antioxidant response

Since most cells have had to evolve in an oxygen environment, intricate and tightly regulated antioxidant defence systems have developed to minimize ROS toxicity. Antioxidant systems include phenolic compounds, vitamins A, E and C, and various enzymatic antioxidants (Sies 1997; Nordberg and Arnér 2001; Ziqiang Meng 2003; Sanjuán-Pla, Cervera et al. 2005; Seifried, Anderson et al. 2007; Al-Gubory 2010).

Recent studies have recognised a transcription factor, nuclear factor erythroid 2-related factor 2 (Nrf2), as an indespensible regulator in the inducible expression of numerous important detoxifying and antioxidant enzymes. This transcription factor belongs to the Cap 'n' Collar family of bZIP transcription factors. The transcription of various phase II detoxifying enzymes and various antioxidant enzymes such as glutathione-*S*-transferase (GST), GP_x, heme oxygenase 1 (HO-1), SOD, thioredoxin reductase and peroxidase, catalase (CAT) and NADPH:quinone oxidoreductase (NQO1) are all induced by activation by Nrf2 (Motohashi and Yamamoto 2004; Jung 2010; Taguchi 2011).

The mechanism by which Nrf2 induces the transcription of stress response genes is shown in Figure 1.5. This process is tightly regulated. Under normal conditions, Nrf2 remains bound to Kelch like ECH-associated protein 1 (Keap1) in the cytoplasm. Kelch like ECH-associated protein 1 is an actin binding protein that binds to the N terminal of the Neh2 domain of Nrf2, tethering it in the cytoplasm (Ishii 2000). This represses translational activity of Nrf2. Kelch

like ECH-associated protein 1 acts as an adaptor for a Cullin 3 (Cul3)-dependant ubiquitin ligase complex. The ubiquitin ligase marks Nrf2 for degradation by cytoplasmic proteasomes (Motohashi and Yamamoto 2004).

The cysteine residues on Keap1 act as a sensor for electrophiles. When ROS levels rise, Keap1 interacts with Cul3 so that the sulfhydryl group of Keap1 is degraded, compromising the bond between Nrf2 and Keap1 and the degradation process of Nrf2 ceases. 15-deoxy-$D^{12,14}$-prostaglandin J_2 (15d-PGJ_2) covalently binds to Keap1, facilitating the translocation of Nrf2 in to the nucleus. Like all Cap 'n' Collar transcription factors, Nrf2 needs to form a heterodimer with a partner protein to function. In the nucleus, Nrf2 forms a heterodimer with small Maf proteins and binds to the antioxidant response element (ARE), initiating the transcription of Nrf2 target genes (Motohashi and Yamamoto 2004; Taguchi 2011).

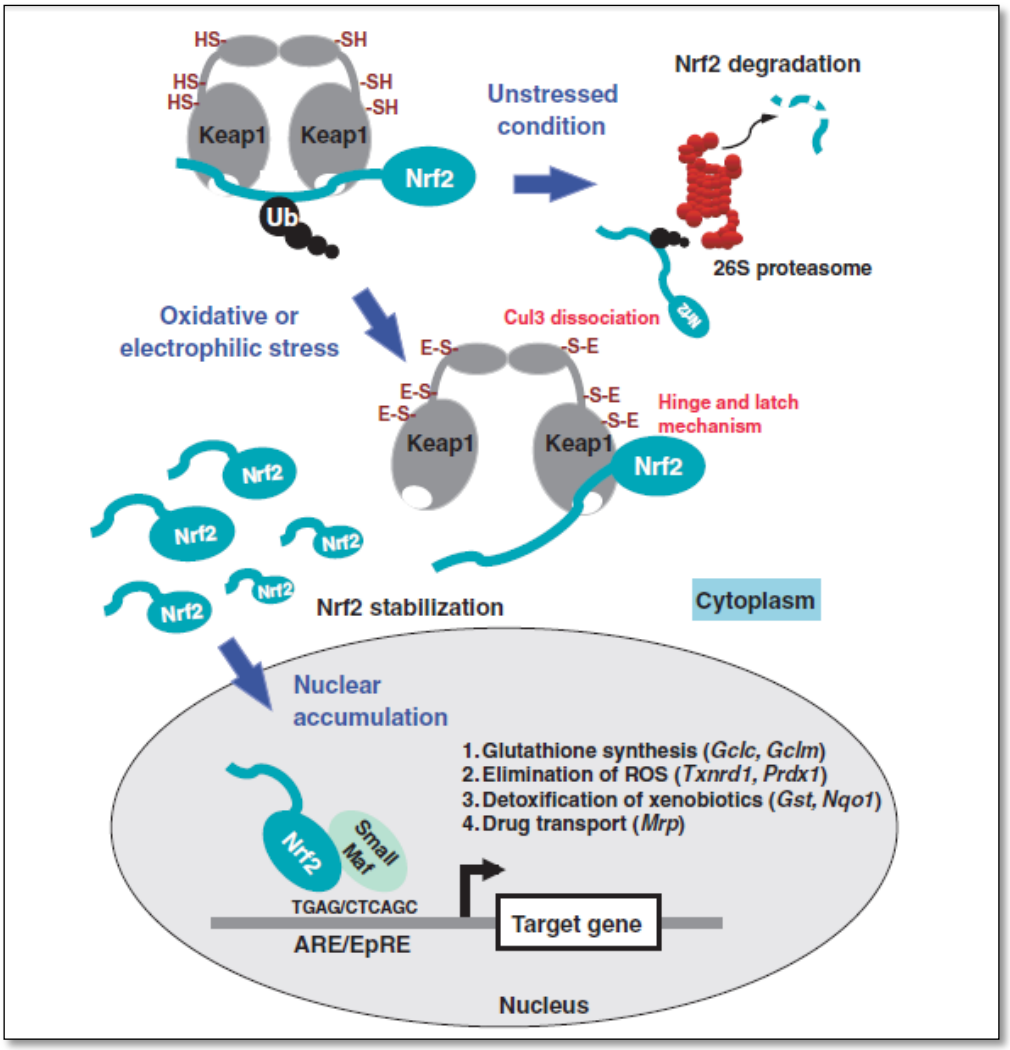

Figure 1.5: The Keap1-Nrf2 pathway (Taguchi 2011).

The ARE is situated on the 5' flanking region of antioxidant response and phase II detoxifying enzymes. The consensus binding sequence of the ARE shares a high similarity with the sequence of erythroid transcription factor NF-E2. Nrf2 is a subunit of NF-E2. Furthermore the expression profile of Nrf2 strongly correlates with that of GST and NQO1 (Ishii 2000). Increases in intracellular reduced glutathione (GSH), a potent antioxidant, has been affiliated with increased Nrf2 activity (Suh, Shenvi et al. 2004). Xenobiotic conjugation and excretion have also been attributed to Nrf2 mediated pathways (Motohashi and Yamamoto 2004).

Considering the major role Nrf2 plays in antioxidant response, the Keap1-Nrf2 mechanism has become a target for therapies for oxidative stress related diseases. The role of Nrf2 in the pathogenesis of COPD has been evaluated. It was found that the stabilizer protein, DJ-1, was expressed at extremely low levels in patients with COPD. This resulted impaired Nrf2 mediated antioxidant response, contributing to the pathogenesis of COPD (Malhotra, Thimmulappa et al. 2008). Long term exposure to oxidative stress can also deplete DJ-1 levels and could have possible implications for Nrf2 function (Giaime 2012). Disruption or impairment of Nrf2 function was also found to increase sensitivity to allergen induced asthma (Li 2004; Rangasamy 2005) and diesel exhaust induced DNA damage (Aoki 2001).

Decreased sensitivity to apoptosis has also been observed as an outcome of Nrf2 activity, possibly implicating Nrf2 in cell survival (Ishii 2000). One of the Nrf2 target genes, *Pparg*, encodes for peroxisome proliferator activated receptors (PPARs) which plays a role in cell cycle regulation. Peroxisome proliferator activated receptors are a super family of ligand-activated nuclear hormone receptor transcription factors. They are divided into 3 isomers (α; β; γ). Peroxisome proliferator activated receptor γ (PPARγ) regulates several genes involved in plays inflammatory and oxidative stress response (Fig 1.6). Major antioxidants such as CAT and HO-1 are transcriptionally regulated by PPARγ. Increased activity of PPARγ also induces expression of the mitochondrial ROS regulator uncoupling protein 2 (Polvani 2012). The effects of this protein will be discussed later. Peroxisome proliferator activated receptor γ is also an agonist against 15d-PGJ_2, suggesting a synergistic relationship between Nrf2 and PPARγ. Lower expression or absence of Nrf2 and PPARγ has been found to result in oxidative stress (Polvani 2012)

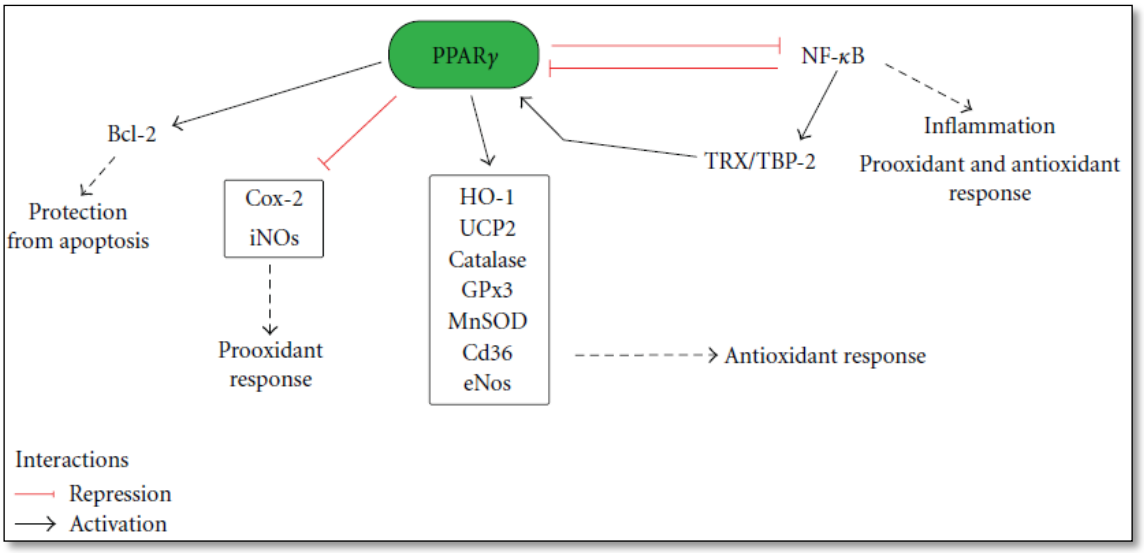

Figure 1.6: Gene targets of PPARγ (Polvani 2012).

1.6 Mitochondrial production of ROS

The mitochondrion is the energy generating organelle of the cell. Its main function is ATP synthesis. ATP synthesis is driven by an electrochemical potential gradient across the inner mitochondrial membrane, thus allowing the re-entry of protons into the mitochondrial matrix (Cadenas 2004). This gradient is created by the transfer of electrons from a reduced substrate, mainly NADH and FADH, through a consecutive series of complexes located on the inner mitochondrial membrane (Fig 1.7). As electrons are passed from one complex to the next, the electrochemical potential gradient increases. The final acceptor of the electron is oxygen (O_2), with water being the end product. The enzymatic transfer of electrons is known as oxidative phosphorylation. This process of oxidative phosphorylation is not water tight, hence not all of the electrons derived from NADH or FADH go towards ATP production. A small percentage of electrons escape. These electrons can react with O_2 to form superoxide ($O_2^{\bullet-}$) anion radical (Brand 2004).

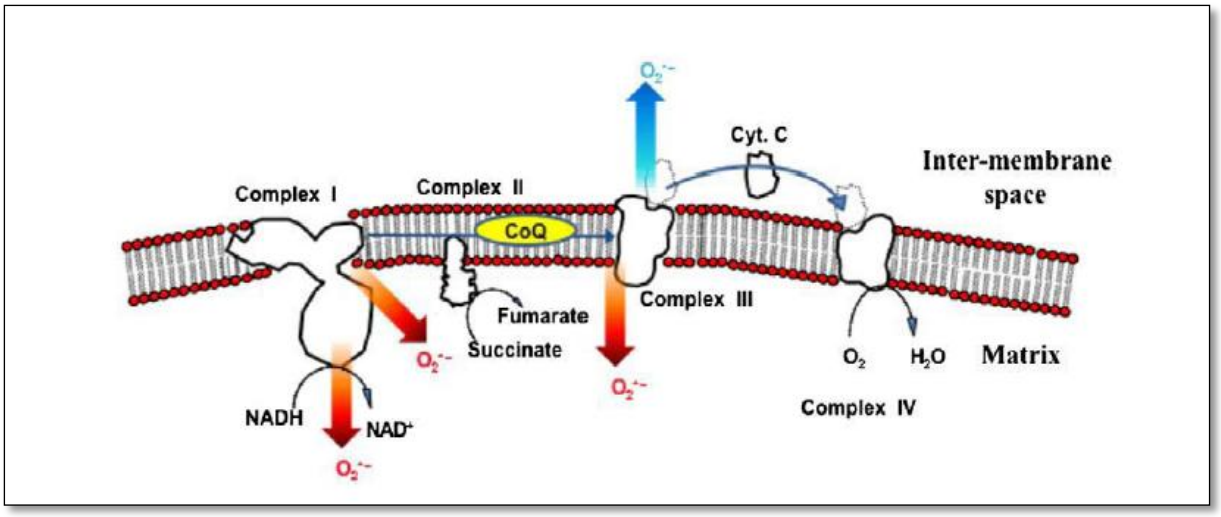

Figure 1.7: The electron transport chain. Complex I and III have been identified as the main source of superoxide production due to electron leakage at these points. Complex I releases superoxide into the mitochondrial matrix. Complex III releases superoxide into both the matrix and intermembrane space (Matsuzaki et al. 2009).

The production of $O_2^{\bullet-}$ anion radical by mitochondria is a naturally occurring process and plays a physiological role, particularly with regard to cell signalling (Cadenas 2004; Matsuzaki, Szweda et al. 2009). However, when there is an influx of oxygen, or a blockage or defect in the functioning of the complexes, the number of electrons that escape increases (Giardina, Steer et al. 2008). This leads to more $O_2^{\bullet-}$ anion radical production. Complex I and III are the points in the electron transport chain (ETC) with the highest escape of electrons (Echtay, Roussel et al. 2002; Brand 2004; Cadenas 2004). Many toxins exert their toxicity by altering the functioning of the complexes and enzymes involved in the ETC (Giardina, Steer et al. 2008). Impaired functioning of ATPase and cytochrome c oxidase favour ROS production (Meng 2007).

Superoxide is the most common mitocondrially derived free radical. The antioxidant enzyme Mn-SOD is responsible for converting $O_2^{\bullet-}$ anion radicals to hydrogen peroxide (H_2O_2) in the mitochondrial matrix (Cadenas 2004). Hydrogen peroxide is then converted to water and

oxygen by either CAT or GP_x. Although H_2O_2 is not highly reactive, in the presence of ferrous ions it can form hydroxyl radicals via the Fenton reaction (Nègre-Salvayre 1997; Brand 2004; Giardina, Steer et al. 2008). Overproduction of $O_2^{\bullet-}$ by mitochondria can also lead to mitochondrial DNA damage and mutations. Implications of mitochondrial DNA damage include impaired respiration, apoptosis via the intrinsic pathway and increased mitochondrial derived ROS (Meng 2007). Since mitochondria are the main source of endogenous ROS, many diseases and pathological conditions associated with oxidative damage have been linked to defective mitochondria (Matsuzaki, Szweda et al. 2009).

1.7 Uncoupling Proteins

Mitochondria are the main endogenous source of ROS (Giardina, Steer et al. 2008). Naturally, a regulatory system needs to be in place to control ROS production by mitochondria. A family of anion carriers, known as uncoupling proteins (UCPs) are located on the inner mitochondrial membrane. These proteins function to uncouple oxidative phosphorylation from ATP synthesis by increasing proton conductance across the mitochondrial membrane, resulting in energy being dissipated as heat as shown in Figure 1.8 (Kovacs 2005; Rudofsky, Schroedter et al. 2006; Emre and Nubel 2010). Various homologues of this protein have been identified. The most commonly studied mammalian UCPs are UCP1, UCP2, UCP3, and to a lesser extent UCP4 and UCP5. Expression and function of the different UCPs vary among different tissues. Mild uncoupling by UCPs plays a role in various physiological processes including thermogenesis (Boss 1998), metabolism (Masaki, Yoshimatsu et al. 1999; de Souza 2012), the regulation of mitochondrial ROS production (Echtay, Roussel et al. 2002; Krauss, Zhang et al. 2002; Bo 2008) and ATP synthesis (Krauss, Zhang et al. 2002).

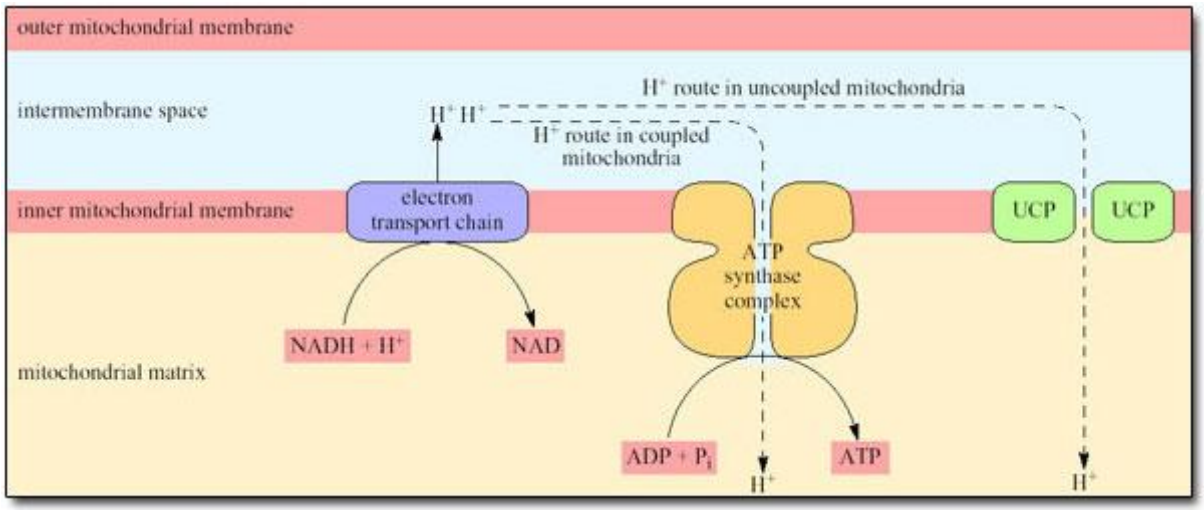

Figure 1.8: Diagramatic representation of the mechanism by which UCPs reduce mitochondrial membrane potential. The electron transport chain creates an electrochemical potential gradient across the inner mitochondrial membran by releasing protons into the inter mitochondrial space. This gradient favours the passing of protons through the ATP synthase complex, facilitating ATP production. Uncoupling proteins increase conductance of protons into the mitochondrial matrix, lowering mitochondrial membrane potential and ATP synthesis (Space 2012).

Uncoupling protein 1 is the most well characterised of the UCPs. This protein is exclusively expressed in brown adipose tissue. This protein is regulated at the transcriptional level and it is regulated by the sympathetic nervous system. The main function of UCP1 is in thermogenesis by uncoupling substrate oxidation from ATP synthesis (Nedergaard, Ricquier et al. 2005). Purine nucleotides (e. g. GDP, ATP and ADP) inhibit UCP1 and regulate activity of this protein. Under cold conditions, intracellular triacylglycerides release fatty acids. These fatty acids overcome purine nucleotide inhibition of UCP1, allowing heat production (Brand 2004; Nedergaard, Ricquier et al. 2005).

Up until 1997, UCP1 was the only identified UCP (Boss 1998). Thereafter, 4 more homologues were discovered (UCP2, UCP3, UCP4, UCP5). The homologues of UCP1 share

similar nucleotide sequences, but evidence for similar function in thermogenesis is weak (Nedergaard, Ricquier et al. 2005). Both UCP2 and UCP3 are expressed in different tissues than UCP1. Uncoupling protein 3 is mainly expressed in skeletal muscle (Bo 2008) while UCP2 is ubiquitously expressed. The role of UCPs in processes other than thermogenesis became evident.

Expression of both UCP2 and UCP3 were found to be induced in the presence of $O_2^{\bullet-}$ anion radicals (Nedergaard, Ricquier et al. 2005). This lead to the hypothesis that they play a role in the negative regulation of ROS production by mitochondria and energy expenditure (Brand 2004). Mild uncoupling by UCP2 and UCP3 increases proton conductance, thus lowering mitochondrial membrane potential while increasing O_2 utilization, leading to reduced mitochondrial ROS production. Uncoupling protein4 and UCP5 play a similarly protective role in neuronal cells. They have also been found to have cytoprotective properties in these cells (Nedergaard, Ricquier et al. 2005).

1.8 Uncoupling Protein 2

Uncoupling protein 2 is ubiquitously expressed throughout the body in tissues such as lung, spleen, brain, kidney, intestine and cells such as macrophages, lymphocytes, and pancreatic islet cells (Reis, Dubois-Laforgue et al. 2004; Nedergaard, Ricquier et al. 2005; De Souza, Araújo et al. 2007; Emre and Nubel 2010). It has a much shorter half life than UCP1 (Rousset, Mozo et al. 2007) and is tightly regulated at a translational level (Pecqueur, Alves-Guerra et al. 2001; Hurtaud, Gelly et al. 2006; Giardina, Steer et al. 2008; Emre and Nubel 2010). Peroxisome proliferator-activator receptorγ (PPARγ) , sterol regulatory element-binding protein 1 (SREBP-1c), $O_2^{\bullet-}$ anion radicals, and free fatty acids are all potent stimulators of UCP2 expression (Nedergaard, Ricquier et al. 2005; Baffy 2010). Thyroid

hormones, TNF-α, plasma glucose, corticosteroids, prostaglandins and leptin have also been found to influnce UCP2 expression (Masaki 1999).

Although UCP2 is regulated at a translational level, most studies investigated UCP2 mRNA expression, rather than protein expression of UCP2 as no reliable anti-UCP2 antibody had been developed until recently (Fleury and Sanchis 1999; Pecqueur, Alves-Guerra et al. 2001). No correlation in UCP2 gene, mRNA and protein expression has been identified (Pecqueur, Alves-Guerra et al. 2001; Giardina, Steer et al. 2008).

Uncoupling protein 2 has gained attention in recent years due to its role in energy metabolism. Expression of UCP2 has been found to favour oxidation of fatty acids and glutamine over glucose-derived pyruvate (De Souza, Araújo et al. 2007; Emre and Nubel 2010) and inhibit lipogenesis (Reis, Dubois-Laforgue et al. 2004). This led to interest in the role of UCP2 in obesity (De Souza, Araújo et al. 2007; Jun, Kim et al. 2008). It has been found to negatively regulate insulin secretion and has been linked to beta cell dysfunction, thus making it a target for diabetes studies (Kovacs 2005). The role of UCP2 in energy expenditure is also identified in late pregnancy, due to upregulation of UCP2 in the uterus during pregnancy (Masaki 1999).

Uncoupling protein 2 has been identified as the major UCP expressed in immune cells and has thus been implicated in immune and inflammatory response. It is down regulated during oxidative burst in macrophages (Emre and Nubel 2010). Macrophages from UCP2-null mice were found to produce excessive amounts of $O_2^{\bullet -}$ anion radicals (Nedergaard, Ricquier et al. 2005). Expression of UCP2 reduces ATP production, thus affecting ATP-dependant inflammatory processes such as exocytosis of lysozymes and cytokine production are reduced (Emre and Nubel 2010). Uncoupling protein 2 also regulates NO production by macrophages in response to lipopolysaccharides (Vogler 2005). This has led to interest in the involvement

of UCP2 in inflammatory diseases such as rheumatoid atherosclerosis, systemic lupus erythematosus, and Crohn's disease (Emre and Nubel 2010; Salpea, Talmud et al. 2010).

Evidence that UCP2 functions to regulate ROS production has been growing in recent years. Superoxide production causes the accumulation of UCP2 in the mitochondria (Giardina, Steer et al. 2008), while UCP2 up regulation reduces H_2O_2 production by mitochondria (Nègre-Salvayre 1997). The over expression of UCP2 in cardiomyocytes was found to protect against ROS-induced apoptosis (Bo 2008). The proposed mechanism is that $O_2^{\bullet-}$ anion radicals and products of lipid peroxidation stimulate UCP2 expression, which increases the proton conductance of the inner mitochondrial membrane, thus reducing membrane potential and lowering ROS production. The increased consumption of O_2 due to uncoupling results in less O_2 being available for one electron reduction to a $O_2^{\bullet-}$ anion radical (Boss 1998).

Many studies have investigated the protective role of UCP2 against diseases and disorders associated with oxidative damage such as retinopathy and neuropathy in diabetics (Rudofsky, Schroedter et al. 2006; de Souza 2012), coronary heart disease (Stephens 2008), neurodegenerative disorders like Alzheimer's and multiple sclerosis (Vogler 2005; Emre and Nubel 2010; Salpea, Talmud et al. 2010), and recently cancer (Baffy 2010; Sastre-Serra 2010).

Four single nucleotide polymorphisms (SNPs) have been identified in the UCP2 gene (Lee, Ryu et al. 2008). The most common SNP is the UCP2-866G/A SNP in the promoter of the UCP2 gene has been studied in relation to its potential role in diseases such as diabetes, obesity and metabolic syndrome (Lim 2012). This genetic variant has been implicated in the expression, functioning and stability of UCP2 (Reis, Dubois-Laforgue et al. 2004; Vogler 2005; Rudofsky, Schroedter et al. 2006). Results from studies on this polymorphism have been controversial. The homozygous A genotype is the least frequent SNP and is associated

with increased mRNA expression in adipose tissue (Reis, Dubois-Laforgue et al. 2004) but lower expression in pancreatic β cells (Stephens, Dhamrait et al. 2008). The same genotype was found to have lower expression than the homozygous G genotype in human retina (De Souza 2012). This genotype was found to decrease insulin secretion in Caucasians in an Italian study, but increased insulin secretion in Caucasians in Northern Europe (Kovacs 2005). This genotype was also associated with higher markers for oxidative stress in smokers when compared to the wild type GG genotype (Stephens, Dhamrait et al. 2008).

The homozygous G genotype has been associated with reduced risk of developing type 2 diabetes in middle-aged obese humans (Kovacs 2005), increased insulin response to glucose, and decreased circulating triacylglycerides and LDL cholesterol in diabetics (Reis, Dubois-Laforgue et al. 2004). This genotype has also been implicated in inflammatory disorders, as this SNP is linked to decreased UCP2 expression in macrophages and lymphocytes (Vogler 2005; Emre and Nubel 2010). Lower UCP2 expression leads to excessive production of $O_2^{\bullet-}$ anion radicals by immune cells, thus contributing to increased susceptibility to inflammatory diseases like carotid atherosclerosis, multiple sclerosis, rheumatoid arthritis, and lupus. The GG genotype has also been found to favour neuropathy in type 1 diabetes (Emre and Nubel 2010).

The GA polymorphism is a commonly observed SNP. There are conflicting results regarding the role of this SNP on UCP2 expression. Some authors suggest this genotype is associated with lower mRNA expression in adipose cells (Salpea, Talmud et al. 2010) while others have observed increased mRNA expression of UCP2 (Kovacs 2005; Rudofsky, Schroedter et al. 2006). This genotype has been associated with inflammatory markers (Emre and Nubel 2010), increased markers for oxidative stress in diabetic smokers (Salpea, Talmud et al. 2010) and increased susceptibility marker for type 2 diabetes (Lee, Ryu et al. 2008).

The function of this protein in energy expenditure and regulation of mitochondrial ROS has lead to intense research into its potential as a therapeutic target. However, it appears that its function and expression is tissue specific as results differ between different tissue types. To date, no studies have been done investigating the expression of UCP2 over long term AAP exposure or the role of the UCP2-866G/A polymorphism in the susceptibility of air pollution associated with oxidative stress.

The aim of this study was to measure markers for oxidative stress and damage in pregnant women from the industrialised DS basin and compare and compare the results to women from the less industrialised Durban North (DN). Furthermore, the functional relevance of the -866G/A promoter polymorphism in the UCP2 gene in the oxidative stress response of these women was evaluated. The objective of the study was determine if pregnant women exposed to higher air pollutant levels displayed higher markers for oxidative stress and to determine the antioxidant response of these women. Variation in the expression and regulatory function between the 2 UCP2 genotypes were also investigated as a possible genetic risk factor for oxidative stress.

CHAPTER 2

MATERIALS AND METHOD

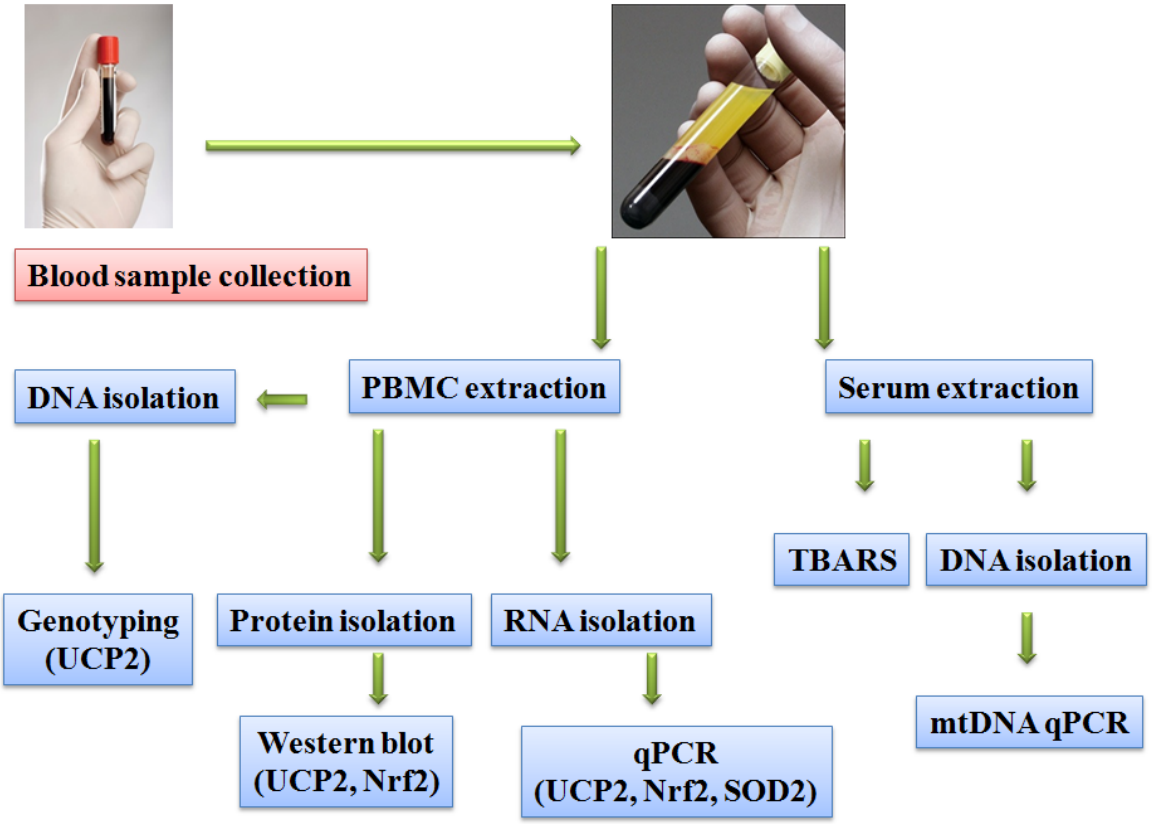

Figure 2.1: Overview of methods and experimental design.

2.1. Patient recruitment

Pregnant women attending public sector ante-natal clinics in DS (Merebank, Wentworth, Bluff; n=50) and the less industrial north Durban (DN; n=50) were recruited as part of the Environmental Pollution and Child Health (EPoCH) pilot study. These communities were selected according to the presence (DS) or absence (DN) of heavy industry. Institutional ethical approval was obtained (BF023/09) and informed consent was obtained from the

participants of the study. The pregnant women selected for the study would have to reside in the given geographical location for the full duration of the pregnancy. Preference was given to women at less than 20 weeks of the gestational period. Women with hypertension, diabetes, placenta pervia, genital tract infections and multiple pregnancies were excluded.

2.2. Sample preparation

2.2.1. Peripheral blood mononuclear cell (PBMC) and serum isolation

Peripheral blood mononuclear cells (PBMCs) and serum were isolated from blood by density gradient centrifugation. Equal volumes of blood and Histopaque 1077 (Sigma, Germany) were aliquoted into 15ml sterilin tubes and centrifuged (400 *g*; 30 min). Sample serum was aspirated and stored -80°C. The buffy layer containing the PBMCs was aspirated and washed twice in 0.1M phosphate saline buffer (PBS). The cells were then transferred to cryovials and stored at -80°C.

2.2.2. DNA isolation

Genomic DNA was isolated from sample serum and whole blood using a commercially available kit (Quick-*g*-DNA MiniPrep Kit, Catalogue no. D3007, Zymo research, USA). Briefly, 800µl of Genomic Lysis Buffer was added to 200µl of whole blood/serum and vortexed vigorously. The samples were allowed to stand for 10 min and then transferred to a Zymo-Spin^{TM} Column in a Collection Tube. The samples were centrifuged (10, 000 *g*, 1 min) and the flow in the Collection Tube was discarded. 200µl of DNA Pre-Wash Buffer was added to the Zymo-Spin^{TM} Column and centrifuged (10, 000 *g*, 1 min). The DNA was washed once more with 500µl of g-DNA Wash buffer (10, 000 *g*, 1 min). The spin column

was then transferred to a fresh eppendorf tube and 50µl of DNA Elution Buffer was added. The tubes were then centrifuged for 30 sec at 10, 000 *g*.

The DNA was quantified (ng/µl) using the Nanodrop 2000 spectrophotometer (λ=260nm). DNA from serum was standardised to 5ng/µl for mtDNA quantitative PCR (qPCR). DNA from whole blood was standardised to 15ng/µl for conventional PCR. Samples were stored at -80°C.

2.2.3. RNA isolation

Sample RNA was extracted from PBMCs using the TRIzol method. TRIzol lyses the cells and disrupts cellular components, while maintaining the integrity of RNA. Equal volumes of TRIzol and cell suspension were mixed in 1.5ml eppendorf tubes and incubated overnight at -80°C. Samples were allowed to thaw and 100µl of chloroform was added. Samples were centrifuged (12, 000 *g*; 15 min; 4°C) and the solution split into an organic phase and aqueous phase. The aqueous phase, containing the RNA was transferred to fresh eppendorf tubes containing 250µl of isopropanol. Isopropanol is added to precipitate the sample RNA. Samples were incubated in isopropanol overnight at -80°C to increase RNA yields (Chomczynski 1987). Following incubation, samples were thawed and then centrifuged (12, 000 *g*; 20 min; 4°C) to pellet the RNA in the tube. The supernatant was decanted and RNA was washed with 75% ethanol (7, 400 *g*, 15 min; 4°C). The ethanol was then decanted and samples were allowed to air dry. Sample RNA was then reconstituted in 12.5µl of nuclease free water.

RNA concentrations (ng/µl) were determined by using the Nanodrop 2000 spectrophotometer and standardised to 25ng/µl for conversion to cDNA. Samples were stored at -80°C.

2.2.4. Protein isolation

Protein was isolated from PBMCs. Stored cell suspension was reconstituted in RPMI and rinsed twice in 0.1M PBS. 200µl of Cytobuster (Novagen), supplemented with phosphotase and protease inhibitors (Roche), was added to the cell pellet and kept on ice for 30 min. Cytobuster disrupts cells and cellular components without disrupting the integrity of the proteins. Disruption of cellular components results in the release of the cells natural phosphotases and proteases. Inhibitors are required to conserve the integrity of the proteins and phosphate groups. The samples were centrifuged (13, 000 *g*; 10 min) and the supernatant containing the crude protein extract was aspirated and stored at -80°C.

Sample protein was quantified by performing the bicinchoninic (BCA) assay. The BCA assay is a colometric assay that measures protein content by a colour change from green to purple. A working solution of 198µl of BCA (containing sodium carbonate, sodium bicarbonate and sodium tartrate) and 4µl of cupric sulphate pentahydrate (Cu_2SO_4) was made up per sample. 200µl of the working solution were added to 25µl of protein sample in a 96-well microtitre ELISA plate. Protein standards (0; 0.2; 0.4; 0.6; 0.8, 1mg/ml) were made up using bovine serum albumin (BSA).The plate was then incubated for 1 hr at 37°C. Absorbance was read on the µQuant BioTek ELISA plate reader (λ = 562nm). The absorbance from the standards was used to construct a standard curve to calculate protein concentrations of the samples (Appendix 1).

The BCA assay relies on the reduction of Cu^{2+} in Cu_2SO_4 to Cu^{+} by peptide bonds found in protein. Under alkaline conditions, in a temperature dependant reaction, BCA forms a purple complex with Cu^{+}. Therefore, samples with higher protein concentrations would reduce more Cu^{2+} to Cu^{+}, thus increasing the formation of the purple complex with BCA (Smith, Krohn et al. 1985).

Following protein quantification, proteins were standardised to 5mg/ml in Cytobuster.

2.3. Detection of UCP2 -866G/A polymorphism

2.3.1. Polymerase chain reaction (PCR)

Polymerase chain reaction (PCR) is the technique used to exponentially amplify a target gene for further analysis. Concentrations of the various components of the PCR reaction mix have to be optimized for specific gene targets. The components of a PCR reaction include a

- 2 primers (forward and reverse) - complementary to the 3' ends of the sense and antisense strands of the target gene, bind to the flanking regions of the target gene allowing specificity of DNA amplification
- Deoxynucleoside triphosphates (dNTPs) – the building blocks required for the synthesis of a new DNA strand (A, T, C, G)
- *Taq* polymerase – enzyme responsible for addition of complementary dNTPs to the DNA template
- $MgCl_2$ – polymerase requires a divalent cation to function optimally, also stabilizes the DNA strand
- Buffer solution – maintains optimal conditions (e.g. pH) during PCR reaction

The method relies on 3 temperature dependant stages (Fig 2.2);

i) Denaturation (94-96°C) – melting of dsDNA into single stranded DNA (ssDNA)

ii) Annealing (55-60°C) – optimum temperature for binding of specific primers

iii) Extension (72-75°C) – addition of complementary dNTPs to ssDNA template, resulting in the formation of new dsDNA

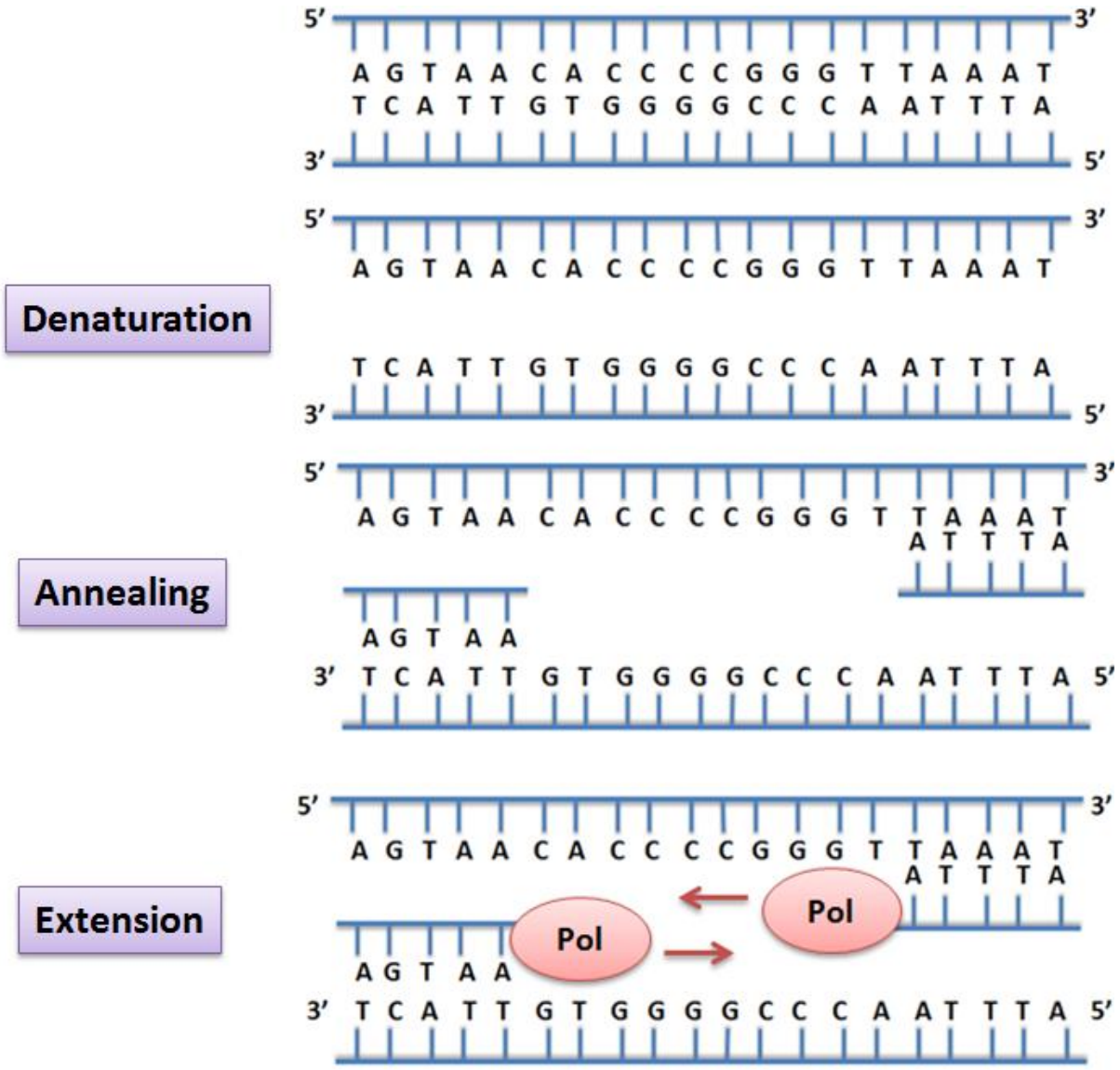

Figure 2.2: Three steps of PCR reaction.

The UCP2 gene in the pregnant women from DS and DN was amplified by using PCR. A 360 base pair product was amplified by using a PCR reaction volume of 25µl consisting of the following optimised conditions: 5µl of 5x Green GoTaq ® Flexi Buffer, 200µM of each dNTP, 1.5mM $MgCl_2$, 0.75 units of Taq Polymerase, 10*p*mol of forward (5'-CACGCTGCTTCTGCCAGGAC-3') and reverse primer (5'-AGGCGTCAGGATGGACCG-3') and 45ng of genomic DNA template. Primer specificity and efficiency was evaluated

using the National Centre for Biotechnology Information (NCBI) basic local alignment search tool (BLAST; www.ncbi.nlm.nih.gov/BLAST/.)

Samples were held at 96°C for 5 min before undergoing 35 cycles of denaturation (96°C; 30 sec), annealing (68°C; 30 sec) and extension (72°C; 30 sec). This was followed by a final extension step at (72°C; 7 min).

DNA verification was performed by electrophoresing the PCR product (15µl) on a 1.8% agarose gel (30 min; 150V) stained with ethidium bromide (EtBr). Ethidium bromide intercalates between the DNA base pairs of dsDNA and emits a fluorescent signal when exposed to UV light. Gels were viewed using the Alliance 2.7 apparatus (Uvitech).

2.3.2 Restriction fragment length polymorphism (RFLP)

Polymerase chain reaction-Restriction fragment length polymorphism (PCR-RFLP) was used to detect the UCP2 -866G/A polymorphism in the birth cohort. A restriction endonuclease is an enzyme that is used to detect specific DNA sequences. Once it recognises a consensus sequence (restriction site) it cleaves the dsDNA, resulting in DNA fragments. If the consensus sequence is not present, the restriction enzyme will not cleave the DNA, and the DNA will remain undigested.

The PCR product was subject to a fast digest with restriction endonuclease *MluI* (Fermentas). The fast digestion was conducted (37°C; 30 min) in a 30µl reaction volume containing 10µl of PCR product, 2µl 10X Green Flexi Buffer, 1µl fast digest *MluI* enzyme and 17µl nuclease free deionised water. The consensus sequence and cleave sites were:

5 ’- G ↓ G A T C C - 3’

3’ – C C A T G ↑ G – 5’

The amplicons that were homozygous for the G allele underwent complete digestion by the restriction enzyme and produced 2 restriction fragments (290bp and 70bp). Amplicons that were heterozygous (GA) were not completely digested and produced 3 fragments (360bp, 290bp and 70bp). Amplicons that were homozygous for the A allele remained undigested (Fig 2.3). The smaller fragments will travel further along the gel as it is easier for them to move through the gel matrix. The larger fragments will be positioned closer to the loading well.

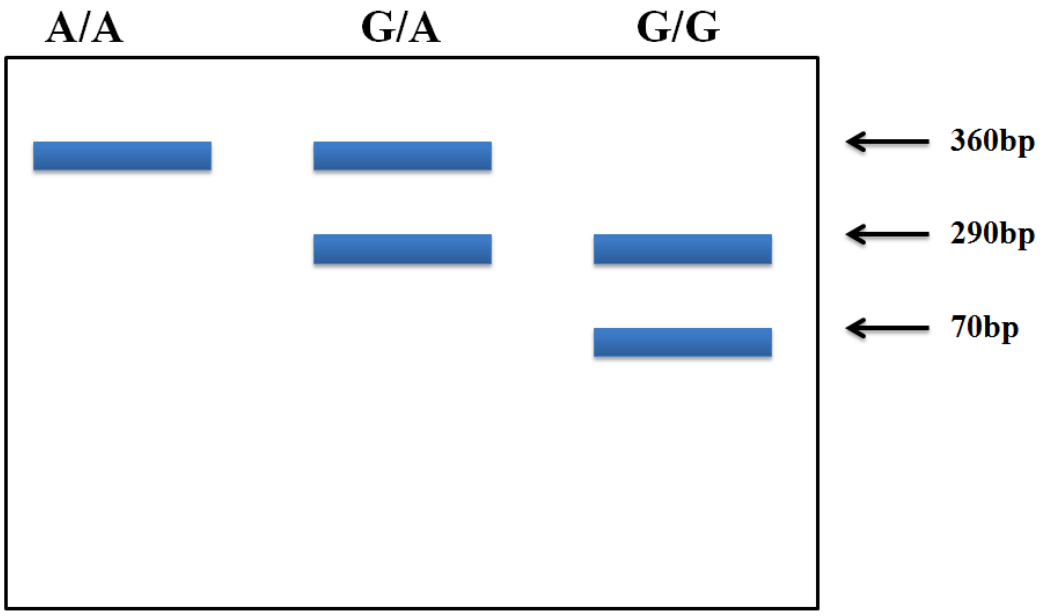

Figure 2.3: Restriction fragments of *MluI* fast digest.

The digested product was electrophoresed on a 3% agarose gel containing 0.5mg/ml EtBr for (30 min; 120V). The Uvitech Alliance 2.7 gel documentation system was used to visualise the digested product.

2.4. Thiobarbituric acid reactive substances assay

Endogenous ROS levels are difficult to measure directly as they have extremely short half-lives. Products of ROS interaction with cellular components are often used as indicators of oxidative stress. Lipid peroxidation involves the degradation of lipid components of the cell due to oxidative damage by free radicals (Fig 2.4). Polyunsaturated fatty acids are the most susceptible to free radical attack. The methylene bonds found between the double bonds in polyunsaturated fatty acids are highly reactive with free radicals. The first step in lipid peroxidation is the oxidation of an unsaturated lipid by ROS resulting in the formation of a fatty acid radical and water. The fatty acid radical is extremely reactive and reacts with O_2 creating a peroxyl-fatty acid radical. This creates a chain reaction of free radical production as the peroxyl-fatty acid radical then oxidizes another lipid, producing a fatty acid radical and lipid peroxide (Södergren 2000). Malondialdehyde (MDA) is one of the end products of lipid peroxidation.

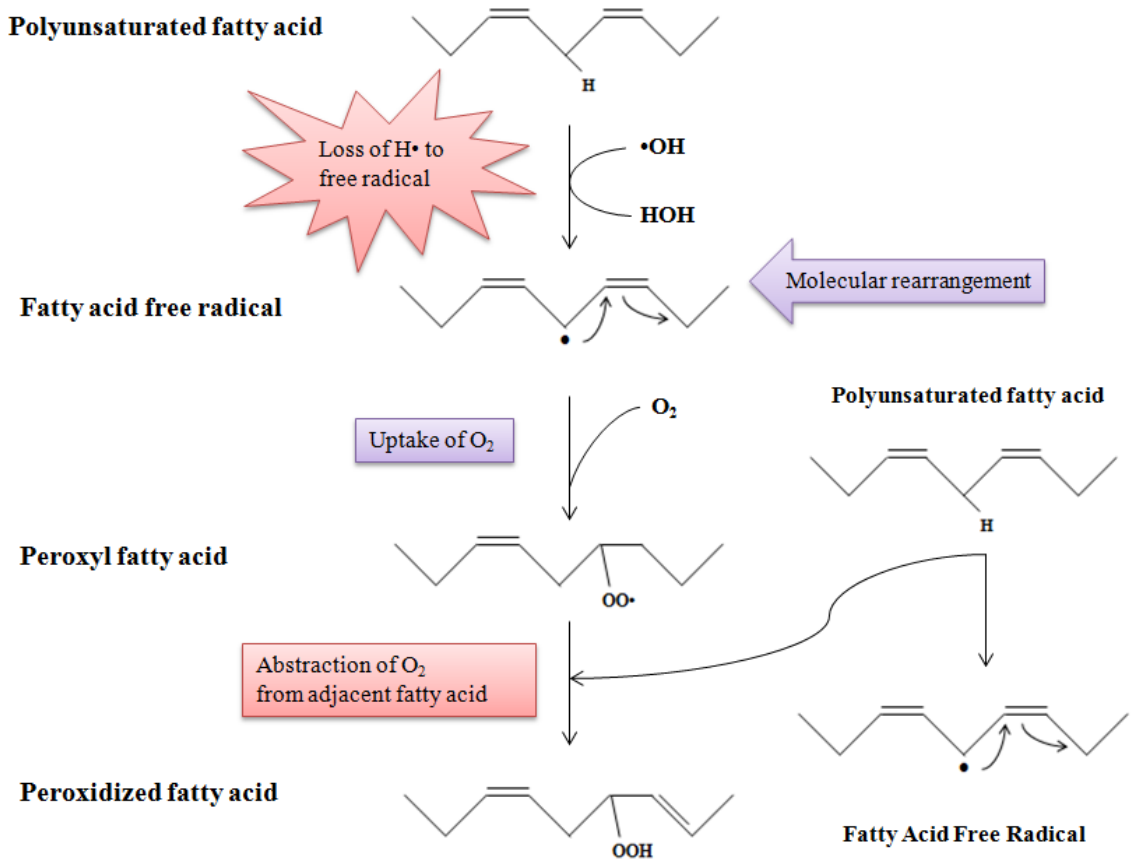

Figure 2.4: Initiation and propagation of lipid peroxidation. Free radicals "steal" H• from the methylene group in polyunsaturated fatty acids, resulting in the formation of a fatty acid radical and water. The fatty acid radical reacts with O_2 to form a peroxyl fatty acid that oxidizes adjacent fatty acids creating a chain reaction.

The thiobarbituric acid reactive substances assay (TBARS) is based on the principle that under acidic conditions, thiobarbituric acid (TBA) reacts with MDA when heat is applied, forming a coloured complex that absorbs light at λ = 530-540nm (Fig 2.5). The addition of butanol to the samples is an extraction method for the TBA-MDA complex. The intensity of the colour at λ = 532nm is proportional to the level of lipid peroxidation.

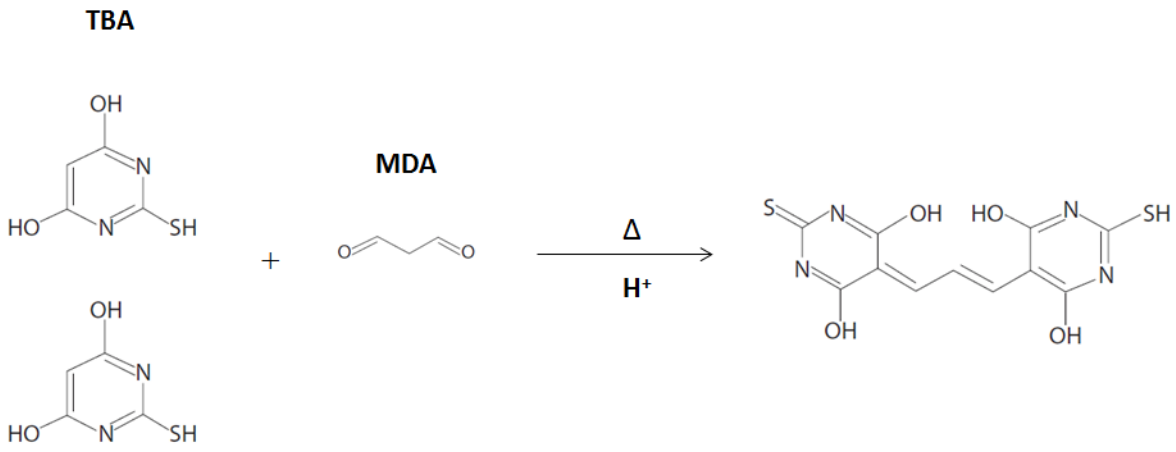

Figure 2.5: Under acidic conditions, when heat is applied, 2 molecules of TBA react with 1 molecule of MDA to form a coloured complex that is used to quantify MDA levels.

500µl of serum from each patient was aliquoted into clean glass tubes. A blank sample was prepared with 400µl of 3mM HCl and a positive control was prepared with 1µl of 1% MDA. To each tube the following was added: 200µl of 2% H_3PO_4, 400µl of 7% H_3PO_4 and thiobarbituric acid (1% w/v)/ 0.1mM butylated hydroxytoluene solution (BHT). The samples were boiled for 15 min then allowed to cool to RT. Butanol (1.5ml) was added to the cooled samples and the tubes were vortexed vigorously. The solution was then allowed to settle in to 2 phases. The butanol phase was aspirated and centrifuged (840 *g*, 10 min). The samples (200µl) were then transferred to a 96-well microtitre plate. Absorbance was read using a spectrophotometer, λ = 532/600nm (BioTek µQuant). The concentration of MDA was calculated by dividing the mean absorbance of the samples by the absorption coefficient ($156mM^{-1}$).

2.5. ATP luminometry

Adenosine-5'-triphosphate (ATP) transports chemical energy in cells and is used to measure cell metabolism. Cellular respiration is responsible for ATP synthesis. In the inner mitochondrial membrane, the electron transport chain creates an electrochemical potential

gradient that drives ATP synthesis. ATP levels can be used as an indication of cellular or pathological processes and mitochondrial function.

ATP can be quantified by bioluminescence. The ATP levels of PBMCs from the pregnant women in the birth cohort were measured using the CellTiter-Glo® Luminescent Cell Viability Assay (Promega, Madison, USA). This assay is based on the properties of the UltraGlo™ Recombinant Luciferase that emits a luminescent signal. The luciferase reaction is depicted in the Figure 2.6.

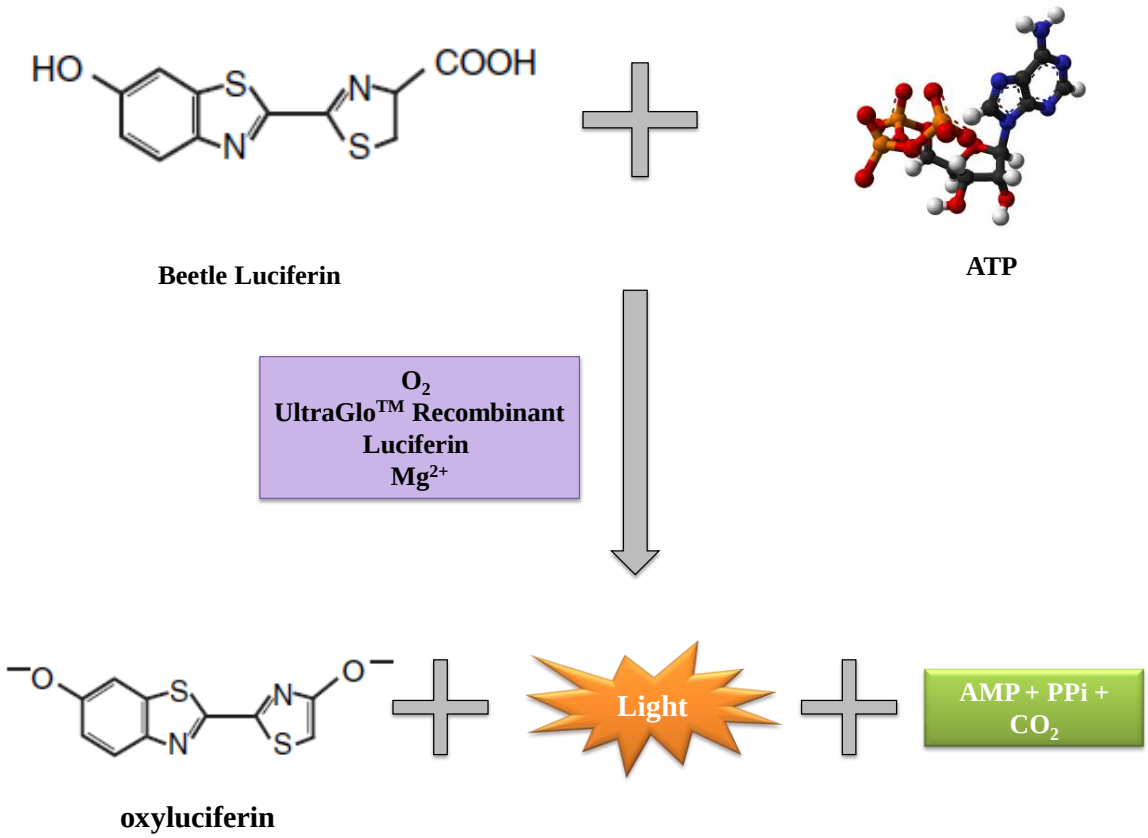

Figure 2.6: The luciferase reaction is catalyzed by ATP, O_2 and Mg^{2+}. The luminescent signal is proportional to the amount of ATP present.

Briefly, 20 000 cells were aliquot into each well in a white microtiter plate. The ATP Cell Titer-Glo® Reagent (Promega), consisting of Cell Titer-Glo® Buffer and Cell Titer-Glo® Reagent, was added to the cells in a 1:2 ratio. The plate was incubated in the dark for 30 min

at RT. Luminescence was measured on a Modulus^{TM} microplate luminometer (Turner Biosystems, Sunnyvale, USA). Luminescence was proportional to ATP content and expressed as relative light units (RLU). The RLU values were used to calculate fold change.

2.6. JC-1 Mitoscreen

Mitochondrial membrane potential ($\Delta\Psi$m) is useful as an indicator of apoptosis and mitochondrial function. A spike in $\Delta\Psi$m is associated with elevated mitochondrial ROS production and a decline in $\Delta\Psi$m is associated with apoptosis. A sensitive way to detect polarized mitochondria in cells is by the JC-1 Mitoscreen. The JC-1 Mitoscreen relies on flow cytometry.

Flow cytometry allows the analysis of individual cells by ordering the cells into a stream of single cells to be evaluated by the machine's detection system. The flow cytometer achieves this by a fluidics system that uses hydrodynamic focussing to arrange cells into a stream of single cells (Fig 2.7).

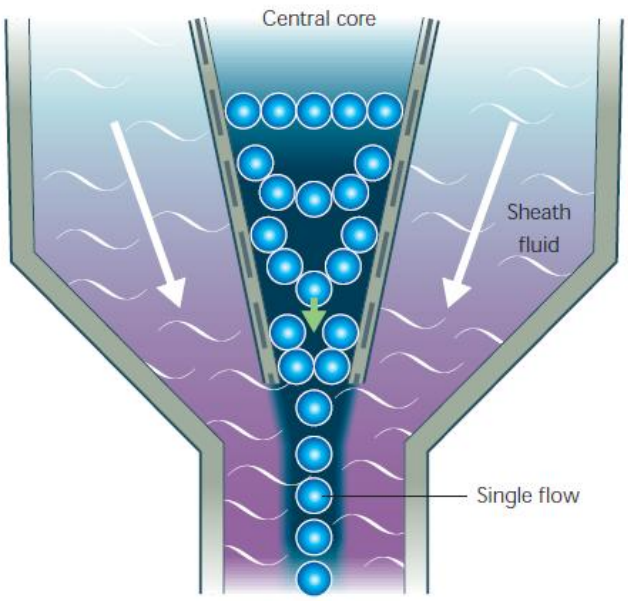

Figure 2.7: Hydrodynamic focussing (Rahman 2006).

The sample containing the cells is injected into the central core. The sheath fluid outside of the central core is flowing at a faster rate than the fluid in the central core. A drag effect is created on the narrow central core, so that fluid at the centre of the core has the fastest velocity and fluid near the wall of the core have a velocity of zero. This results in a single flow of cells and is known as hydrodynamic focussing.

Each cell/particle that passes through the core is interrogated by one or more beams of light. If the cell has been labelled with a fluorochrome, it emits a fluorescent signal that is picked up by the machine's detection system. Flow cytometers have fluorescence (FL-) channels that detect fluorescence and will measure the signal at different wavelengths to gain qualitative and quantitative data.

JC-1 is a fluorescent labelled dye (fluorochrome). Fluorochromes are able to absorb light energy and emit light at a longer wavelength. The JC-1 dye is a lipophilic fluorochrome that penetrates the cell membrane. The dye forms JC-1 aggregates when it is at high concentrations and monomers at lower concentrations. The mitochondria of healthy cells are

polarized, and therefore take up the JC-1 dye, resulting in JC-1 aggregate formation. The aggregates undergo a red spectral shift and emit red fluorescence that is detected in FL-2. The monomers, which occur when the dye is unable to enter depolarized mitochondria, exhibit green fluorescence that is detected in FL-1.

Briefly, JC-1 stock solution was diluted in pre-warmed 1X Assay Buffer (37°C) to make up a working solution. Approximately 10 000 cells from each sample were transferred to polystyrene cytometry tubes. JC-1 dye (150µl) was added to each tube and the cells were incubated for 10 minutes at 37°C, 5% CO_2. Cells were washed in JC-1 Mitoscreen wash buffer (400 *g*, 5 min). Cells were then resuspended in 300µl of flow cytometry sheath fluid. A FACSCalibur (BD Biosciences) flow cytometer and CellQuest PRO v4.02 software (BD Biosciences) were used to capture data of the stained cells. Cells were gated using FlowJo v7.1 software (Tree Star Inc., Ashland, USA).

2.7. Comet assay

The comet assay was used to determine DNA fragmentation. The 3 steps of the comet assay are encapsulation of the cells, cell lysis and finally electrophoresis of the lysed cells. The comet assay works on the principle that undamaged DNA remains in a highly intact structure and will be too large to migrate through the gel. Damaged DNA loses its intact organisation and individual strands start to break free and are tiny enough to migrate from the cavity that encapsulated the cell.

Partially frosted glass slides were prepared by spreading 700µl of 1% low melting point agarose (LMPA) dissolved in 1M PBS. This was allowed to solidify at 4°C for 10 min. A second layer consisting of 25µl of cell suspension (~20 000 cells) mixed with 525µl of 0.5%

LMPA was then applied on to the first layer. The molten agarose was covered with a glass cover slip and allowed to set for 10 min at 4°C.

The cover slips were then removed and the slides were submerged in cold cell lysis buffer [2.5M NaCl, 100mM EDTA, 1% Triton X-100, 10mM Tris (pH10), 10% DMSO] for 1 hr at 4°C. The lysis buffer contains detergent and a high salt content. This allows degradation of the cell membrane as well as all protein, RNA, and nucloesomal components of the cell, leaving only the DNA in a cavity that was occupied by the cell.

Slides were removed from the cell lysis solution and placed in an electrophoresis tank. The tank was filled with electrophoresis buffer [300mM NaOH, 1mM Na_2EDTA (pH13)] so that all the slides were submerged. The slides were allowed to equilibrate in the electrophoresis buffer for 20 min. Thereafter a current of 300mA was applied for 35 min. DNA, which is negatively charged, will migrate towards the positively charged cathode. Uncompromised DNA would remain in its highly organised structure and be too large to migrate from the cavity. DNA with strand breaks would break away from their organized structure and slowly migrate, with smaller strands migrating further.

The slides were then removed from the tank and gently washed 3 times for 5 min each with neutralisation buffer (0.4M Tris; pH 7.4). This was followed by a staining step with EtBR (20µg/ml). Ethidium bromide intercalates between base pairs in dsDNA and allows for visualisation of the comets. Undamaged DNA would remain double stranded and would emit a stronger signal. The gels were covered with glass cover slips and left to incubate overnight at 4°C. Images were captured using a fluorescent microscope (filter 4) [Olympus IXSI inverted microscope] with 510-560 excitation and 590 emission filters. Images had to include at least 50 cells per sample. The Soft Imaging System [Life Science – Olympus Soft Imaging Solutions version 5] was used to measure comet tail length in µm.

2.8. Quantitative PCR

Quantitative PCR (qPCR) contains all the basic elements of conventional PCR, but differs in that it not only facilitates amplification, but also quantification of a target gene. The use of a fluorescent reporter dye, SYBR green, allows amplified DNA to be detected as the reaction progresses over time. SYBR green binds to dsDNA and emits a fluorescent signal. The intensity of the signal is proportional to the amount of dsDNA amplified. The fluorescence emitted is plotted on a graph after each cycle and allows quantification of the initial amount of dsDNA present. The graph provides a comparative threshold (Ct) value for each sample. The Ct values from where the curve becomes exponential are compared to a simultaneously run housekeeping gene are used to calculate the amount of DNA present.

The Livak method is used to calculate fold change of samples compared to a control group. The Ct value of the housekeeping gene is subtracted from the Ct value of the target gene to standardise the results (ΔCt). Next, ΔCt of the control group is subtracted from ΔCt of the experimental group (ΔΔCt). Fold change is calculated as $2^{-\Delta\Delta Ct}$ (Appendix 2).

2.8.1. Mitochondrial DNA damage

Mitochondrial DNA (mtDNA) damage was measured by performing qPCR. DNA was isolated from serum using a commercially available kit (Quick-*g*-DNA MiniPrep Kit, Zymo Research, USA). Sample DNA was quantified using the Nanodrop 2000 spectrophotometer and standardized to 5ng/µl.

A reaction volume of 25µl consisting of 12.5µl SYBR Green Supermix (BioRad), 10*p*mol of forward and reverse primer (Table 2.1), and ~10ng genomic DNA template made up in nuclease free water. A reference gene, β-Globin (Table 2.1) was amplified under the same

conditions. Initial denaturation was applied (94°C; 3 min), followed by 28 cycles of denaturation (94°C; 20 sec); annealing (58°C; 10 min), extension (72°C; 10 min) and a plate read. This was followed by a melt curve and a final hold (25°C; 5 min). Fold change of mtDNA amplification was calculated using the Livak method.

The principle of this assay is that viable mtDNA will not have DNA strand breaks or lesions and will amplify accordingly. Compromised or damaged mtDNA with breaks will result in the incomplete DNA template and thus the polymerase will not be able to fully amplify the gene. Therefore, mtDNA amplification is inversely proportional to mtDNA damage.

2.8.2. mRNA expression

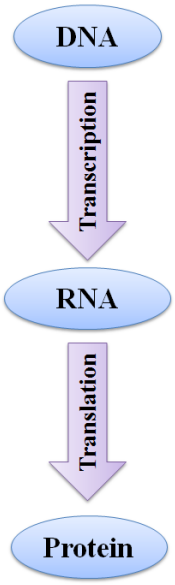

Figure 2.8: The central dogma of molecular biology.

Under stressful conditions, the cell responds by induction or up regulation proteins involved in stress response. Most protein synthesis is regulated by gene expression as shown in Figure 2.8. Quantitative PCR was performed to evaluate mRNA expression of 3 key proteins in relation to oxidative stress response (UCP2, Nrf2, and SOD2).

To perform qPCR, the isolated RNA had to be converted to cDNA. The iScript™ cDNA Synthesis kit (BioRad; catalog no. 107-8890) was used to synthesize cDNA from the RNA isolated from the PBMCs. A reaction volume of 20µl containing 4µl of 5X iScript reaction mix, 1µl of iScript reverse transcriptase and ~250ng of RNA template were made up in nuclease free water. Thermocycler conditions for cDNA synthesis were 25°C for 5 min, 42°C for 30 min, 85°C for 5 min and a final hold at 4°C.

The synthesis of cDNA from an mRNA template is catalyzed by the enzymes reverse transcriptase and DNA polymerase. The cDNA strands synthesized will be complementary to the RNA base pairs of the mRNA template strand.

The iScript™ One-Step RT-PCR kit with SYBR® Green (BioRad, 170-8892) was used to perform qPCR to measure mRNA expression of UCP2, Nrf2 and SOD2. Briefly 4µl of cDNA sample was added to 30nM of sense primer, 30nM antisense primer (Table 2.1), 5X iScript reaction mix and nuclease free water in a final reaction volume of 25µl. GAPDH was used as a reference gene. The primers were tested for specificity and efficiency by using the NCBI's BLAST on their website. Initial denaturation was conducted at 95°C for 4 min, followed by 37 cycles of denaturation (95°C; 15 sec), annealing (57°C; 40 sec), extension (72°C; 30 sec) and a plate read for 37 cycles.

All qPCR was conducted in the BioRad Chromo4 thermocycler and Ct values were read using MJ Opticon Moniter Version 3.1 analysis software.

Table 2.1: Primer sequences for qPCR

Primer	Primer sequence
UCP2 sense	5'-GACCTATGACCTCATCAAGG-3'
UCP2 antisense	5'-ATAGGTGACGAACATCACCACG-3'
Nrf2 sense	5’-AGTGGATCTGCCAACTACTC-3'
Nrf2 antisense	5'-CATCTACAAACGGGAATGTCTG-3'
SOD2 sense	5’-GAGATGTTACACGCCCAGATAGC-3’
SOD2 antisense	5-AATCCCCAGCAGTGGAATAAGG-3’
GAPDH sense	5’-TCCACCACCCTGTTGCTGTA-3’
GAPDH antisense	5’-ACCACAGTCCATGCCATCAC-3’
β-Globin forward	5’-ACATGATTAGCAAAGGGCCTAGCTTGACTCAGA-3’
β-Globin reverse	5’-TGCACCTGCTCTGTGATTATGACTATCCCACAGTC-3’
mtDNA forward	5’-TGAGGCCAAATATCATTCTGAGGGC-3’
mtDNA reverse	5’-TGCACCTGCTCTCTGTGATTATGACTATCCCACAGTC-3’

2.9. Western Blots

Western blots are one of the most sensitive methods to quantify protein expression. This technique is based on the separation of protein samples according to size by electrophoresis. The separated proteins are then transferred to a membrane and probed with specific antibodies to detect the presence and quantity of a specific protein. Protein expression of UCP2 and Nrf2 in PBMCs from pregnant women in the birth cohort was quantified using this technique.

2.9.1. Sample preparation

Firstly, the standardised protein samples had to be prepared in Laemmeli buffer [dH_2O, 0.5M Tris-HCl (pH 6.8), glycerol, 10% SDS, β-mercaptoethanol, 1% bromophenol blue]. 5X Laemelli buffer was added (1:4 ratio) to the protein samples and boiled for 5 min. Boiling the samples activates the SDS which denatures the proteins and breaks up the hydrophobic regions so that they lose their secondary and tertiary structure. This facilitates separation of the proteins based on size rather than shape. Another function of SDS is to bind to the

positive charges, creating an overall negative charge on the protein, so that charge of the protein does not affect its migration through the gel. β-mercaptoethanol breaks inter and intra-molecular disulfide bonds to accommodate proper separation of the bands according to size. The function of glycerol in the buffer is to add density to the sample, so that when loading into the gel, the sample sinks to the bottom of the well. This reduces sample loss in the running buffer during loading. Bromophenol blue is used as a tracking dye to monitor the migration of the proteins during electrophoresis.

2.9.2. SDS-Polyacrylamide gel electrophoresis (SDS-PAGE)

Once the samples have been prepared, they are cooled to room temperature and ready to be loaded. A 10% SDS-polyacrylamide resolving gel and a 4% stacking gel was prepared (dH_2O, Tris, SDS, Bis/Acrylamide, 10% Ammonium phosphate sulphide, TEMED). N,N'-methylene-bis-acrylamide acts as a cross linking agent, facilitating polymerization of the acrylamide gel. This reaction is initiated by TEMED. The cross-linked matrix formed by the polymerized acrylamide creates a porous structure through which the proteins will migrate. The smaller proteins will migrate faster through the matrix, and thus travel further down the gel. The larger proteins will have difficulty moving through the porous structure and will remain higher up on the gel.

The samples were loaded into the gel and electrophoresed for 1 hr; 120V. The negative charge of the proteins would cause the protein to migrate to the positive node.

2.9.3. Transfer

The gels were then equilibrated in transfer buffer (dH_2O, Tris, glycine, methanol) and the separated proteins were transferred to a nitrocellulose membrane using the BioRad TransBlot Turbo Transfer System (400mA, 45 min). The equilibrated gels and membranes were

sandwiched between fibre pads soaked in transfer buffer (Fig 2.9). Application of an electric current allows the proteins to migrate from the gel to the membrane, while still maintaining the structural organisation they had in the gel.

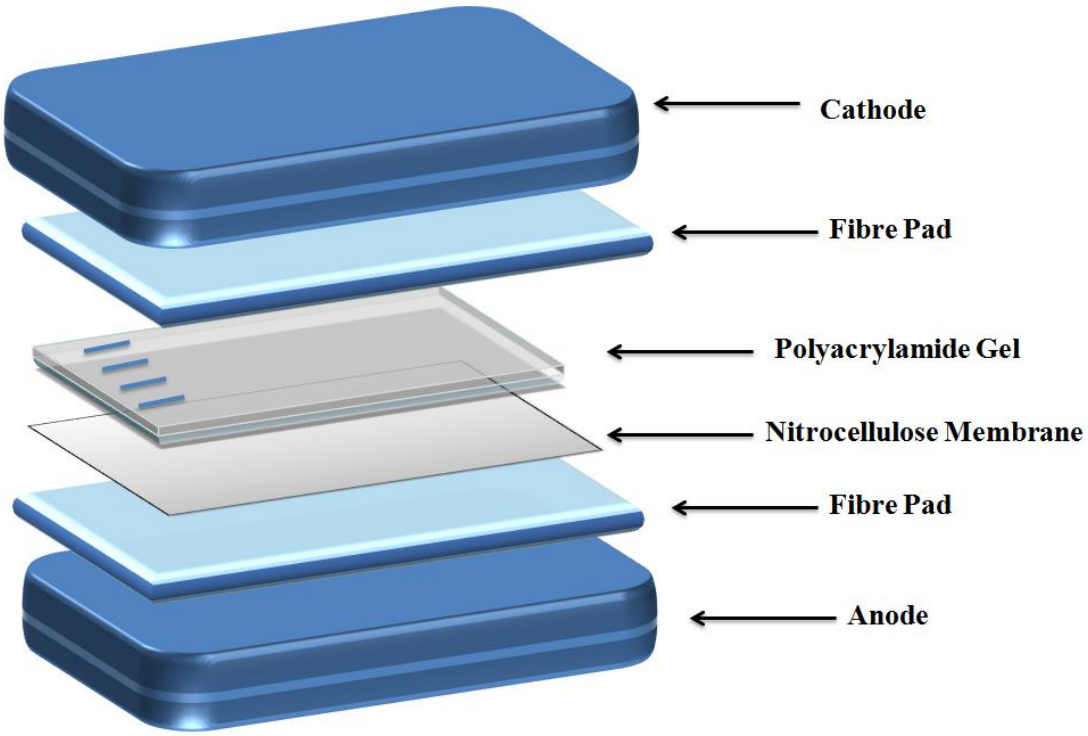

Figure 2.9: Arrangement for transfer of proteins from gel to nitrocellulose. The fibre pads, membrane and gels were equilibrated in transfer buffer for 10 min before the transfer.

Once the transfer was complete, the membranes were incubated in a blocking solution of 3% BSA made up in Tris Buffer Saline with Tween-20 (TTBS) for 1 hr at RT on a shaker. The protein in the BSA solution binds to all parts of the membrane where the target protein has not bound, thus preventing non-specific binding.

2.9.4. Probing/Detection

Probing for specific proteins is achieved via 2 steps as shown in Figure 2.10. The first step is incubation with a primary antibody. This antibody is specific to the target protein that is being detected and binds accordingly, forming an antibody-antigen complex. Goat anti-UCP2 (ab77363) and rabbit anti-Nrf2 (ab31163) were used to detect UCP2 and Nrf2 protein expression respectively (1: 5 000 dilution in 1% BSA). The membranes were incubated in primary antibody for 1 hr on a shaker at RT and then overnight at 4°C. The membranes were then subject to 5 X 10 min washes in TTBS before incubation with secondary antibody. The secondary antibody is conjugated to horse radish peroxidase (HRP) and is specific to the primary antibody. The secondary antibody binds to the bound primary antibody. The HRP-conjugated secondary antibody emits a chemiluminescent signal that can be used for detection and quantification of a target protein. Rabbit anti-goat (ab6742) and goat anti-rabbit (ab6112) were used for UCP2 and Nrf2 respectively (1: 10 000 dilution in 1% BSA). The membranes were incubated with secondary antibody for 1 hr at RT on a shaker. The membranes were then rinsed subject to 5X 10 min washes.

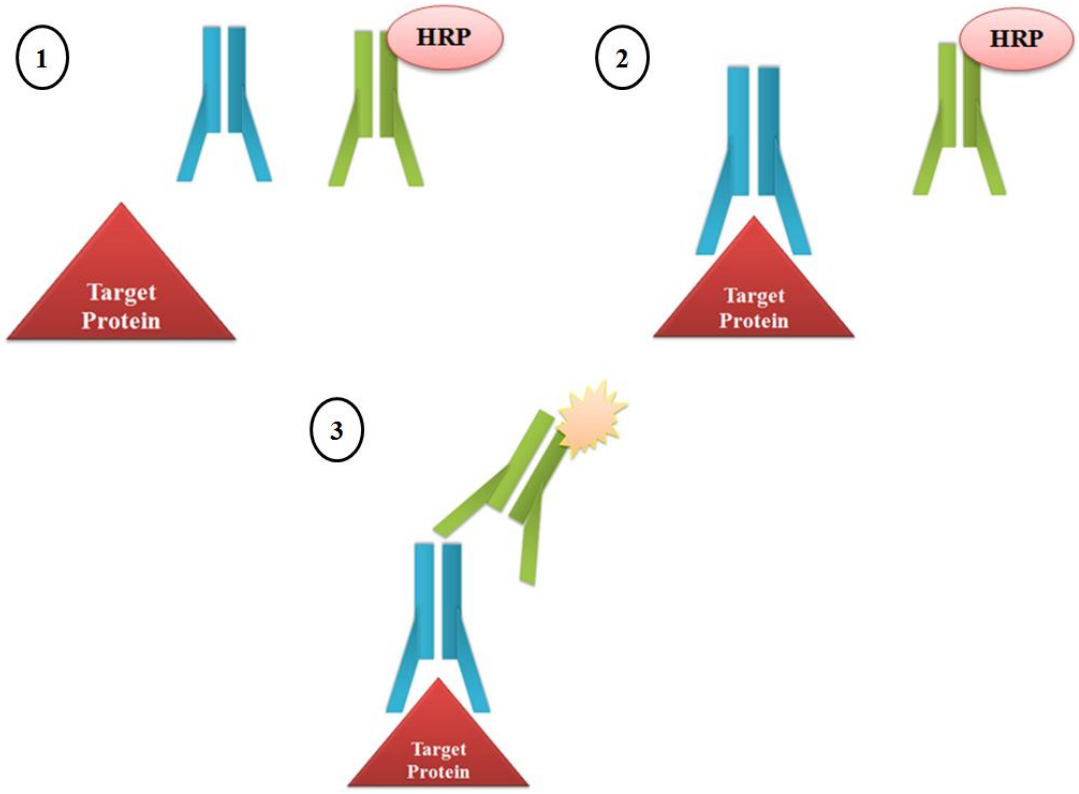

Figure 2.10: Detection of target protein with antibodies. The primary antibody (blue) is specific to the target protein. The primary antibody binds to the target protein forming the antigen-antibody complex (2). The HRP-conjugated secondary antibody binds to the primary antibody and emits a luminescent signal (3).

LumiGLO® chemiluminescent substrate system (KPL) was used to detect protein bands. Membranes were visualised by measuring chemiluminescence using the Alliance 2.7 apparatus (UviTech). Analysis of relative band density (RBI) of the bands was done using Uvitech Alliance Acquisition software.

Membranes were stripped with 5% hydrogen peroxide, incubated in blocking solution (3% BSA; 1 hr; RT), rinsed twice in TTBS and probed with HRP-conjugated anti-β-actin (house-keeping protein). Relative band density was reflected as a ratio of the relative band density of the proteins divided by the relative band density of β-actin.

2.10. Statistical analysis

Statistical analyses were performed using the GraphPad Prism software package (GraphPad Software Inc.) The Hardy-Weinberg equilibrium model was used to test the UCP2 genotype frequencies. Statistical significance was relative to p value < 0.05

CHAPTER THREE

RESULTS

3.1. Uncoupling protein2 -866G/A promoter polymorphism

The UCP2 -866G/A promoter polymorphism was detected using PCR-RFLP (Fig 3.1).

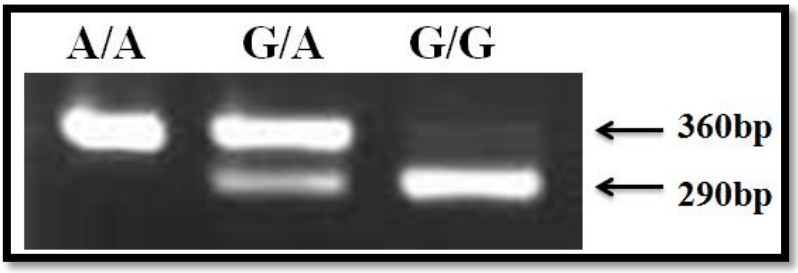

Figure 3.1 Restriction fragment length polymorphism for the UCP2 -866G/A polymorphism. Fast digest of the amplicons resulted in a 360bp undigested product in the homozygous A genotype, a completely digested 290bp product for the homozygous G genotype and the heterozygous genotype produced two fragments.

Since the AA genotype is rare, the results from this genotype were grouped with the GA genotype. Frequencies of the genotypes and alleles are displayed in Table 3.1. The G allele was more frequent in pregnant women from DS (48.7%) than women from DN (44.3%; p = 0.26; OR: 1.44; 95% CI: 0.82 to 2.51). Fishers exact test results showed a significantly higher frequency of the GG genotype in the pregnant women from DS (37.5%) than those from DN (20.9%; p value < 0.05; OR: 2.57; 95% CI: 1.353 10 4.885). The genotype frequency was tested against the Hardy Weinberg equation (HWE) as quality control. The genotype frequencies were found to be consistent with the HWE (DN: p = 0.17, X^2 = 1.9; DS: p = 0.32, X^2 = 0.98; Chi square test).

Table 3.1: Genotype and allelic frequencies of UCP2 -866G/A promoter SNP in pregnant women from Durban North and Durban South

		Frequency	
		North (n = 43)	South (n = 48)
Allelotype	G	35 (*44.3%*)	38 (*48.7%*)
	A	44 (*55.7%*)	40 (*51.3%*)
Genotype	AA/GA	34 (*79.1%*)	**30 (*62.5%*)
	GG	9 (*20.9%*)	**18 (*37.5%*)
	X^2 value	1.9	0.98
	p value	0.17	0.32

***p* < 0.005 compared to DN

3.2. Thiobarbituric acid reactive substances assay

The TBARS assay was done to quantify MDA as an indicator of oxidative stress. Pregnant women from DS displayed elevated levels of MDA when compared to women from DN (DN: 0.05±0.03 vs DS: 0.07±0.06µM; *p* = 0.56; Mann-Whitney test). The difference was not statistically significant (*p*>0.05; Figure 3.2).

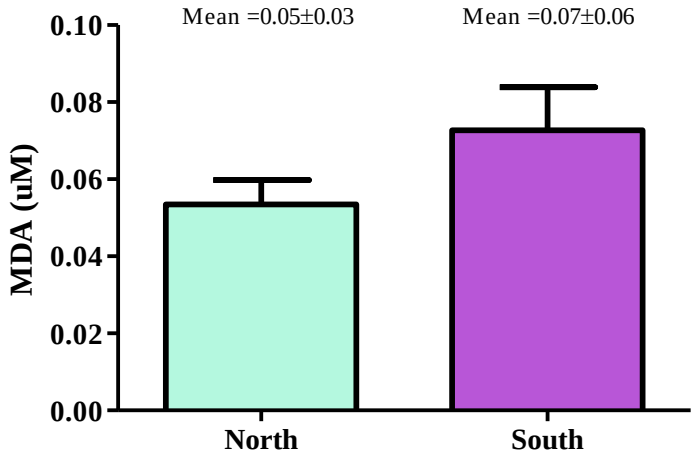

Figure 3.2: Extracellular MDA levels for women from Durban North and Durban South (*p* > 0.05).

The results from the TBARS assay were then stratified according to the UCP2 genotypes of the pregnant women. No significant differences were observed between the genotypes ($p > 0.05$; ANOVA). The GG genotype in women from DS exhibited higher MDA levels than the AA/GA genotype in the same group as shown in Figure 3.3 (GG: 0.07±0.06 vs AA/GA: 0.05±0.03µM; $p = 0.59$).

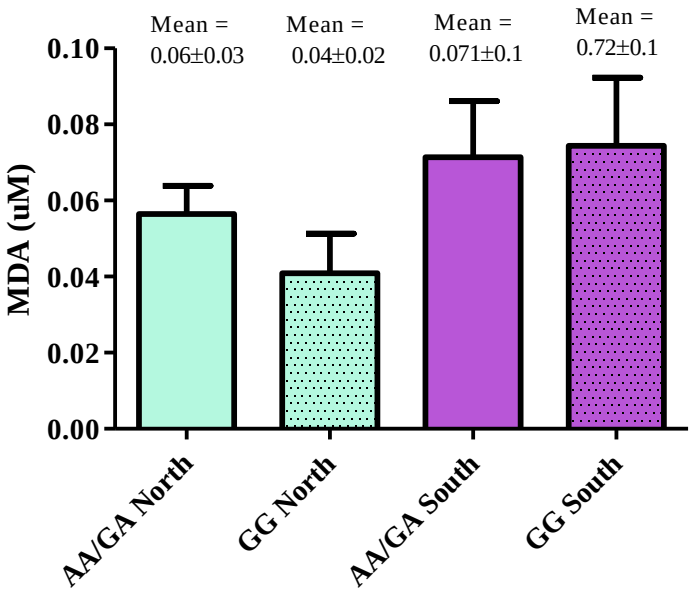

Figure 3.3: Stratified results of TBARS assay according to UCP2 genotypes ($p > 0.05$).

3.3. ATP luminometry

ATP levels of the PBMCs isolated from women in the DN and DS were measured using the CellTiter Glo® Assay. Luminescence was used as a measure of ATP content of PBMCs. Luminescence was measured as relative light units (RLU) and converted to fold change compared to the control group. Statistics done on the RLU values, as shown in Figure 3.4, showed that ATP levels were significantly higher in DS ($3.7\pm3.02x10^3$RLU) compared to DN (7.01 ± 1.97RLU$x10^3$; $p = 0.001$; Mann Whitney). The mean ATP level in PBMCs from pregnant women from DS was 1.89 fold higher than the mean ATP level of women from DN (Fig 3.5).

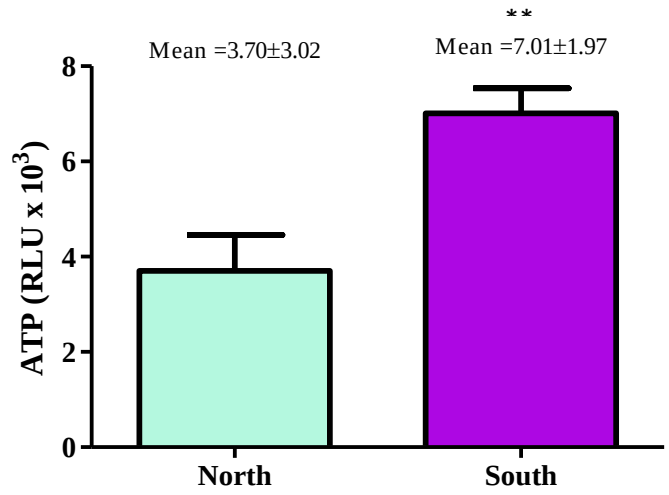

Figure 3.4: Luminescence measured for CellTiter Glo® Assay in relative light units (RLU; **$p < 0.005$).

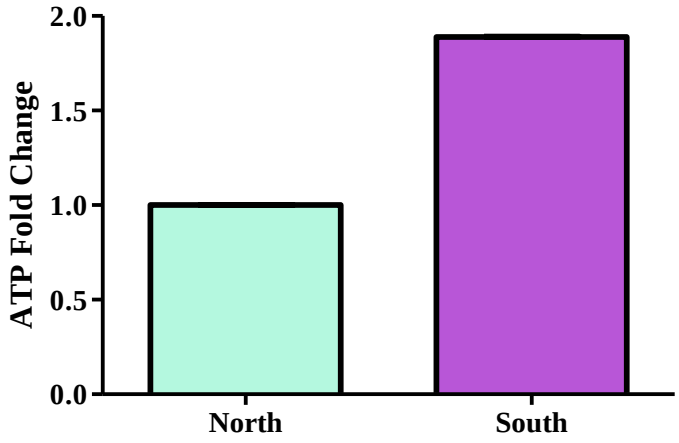

Figure 3.5: ATP fold change in PBMCs from pregnant women from Durban North and Durban South.

The ATP results were then stratified according to the UCP2 genotypes of the pregnant women. The AA/GA genotype in women from DS exhibited the highest ATP levels (Fig 3.6) and was significantly higher than the same genotype in DN ($p = 0.01$; ANOVA). Fold change of ATP levels were then calculated using the GG genotype as reference (1 fold) in each

geographical group. The AA/GA genotype displayed higher ATP levels in DS (1.28 fold) than the GG genotype (Fig 3.7). The AA/GA genotype in the control group had slightly lower ATP levels (0.88 fold) when compared to the GG genotype in the same group.

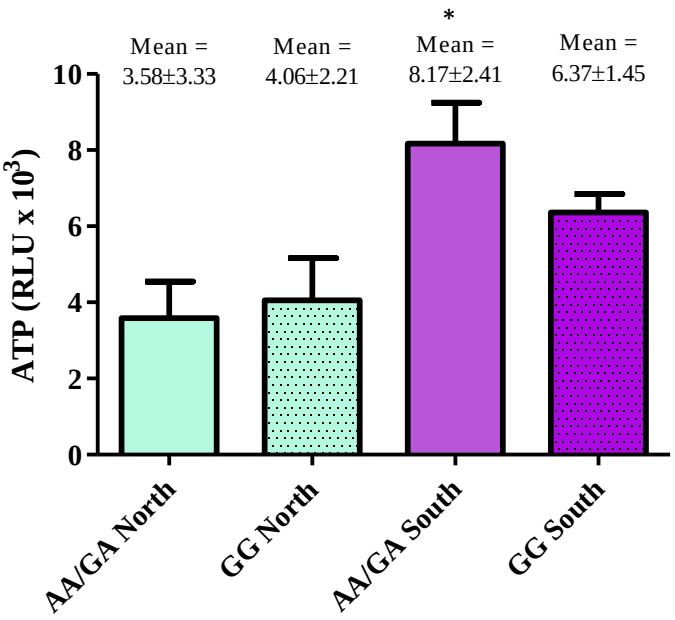

Figure 3.6: Results from ATP luminometry stratified according to UCP2 genotypes in PBMCs from pregnant women living in Durban North and Durban South. ATP levels in the AA/GA genotype in the Durban South group were significantly higher than the same genotype in Durban North (*$p < 0.05$ when compared to AA/GA in Durban North).

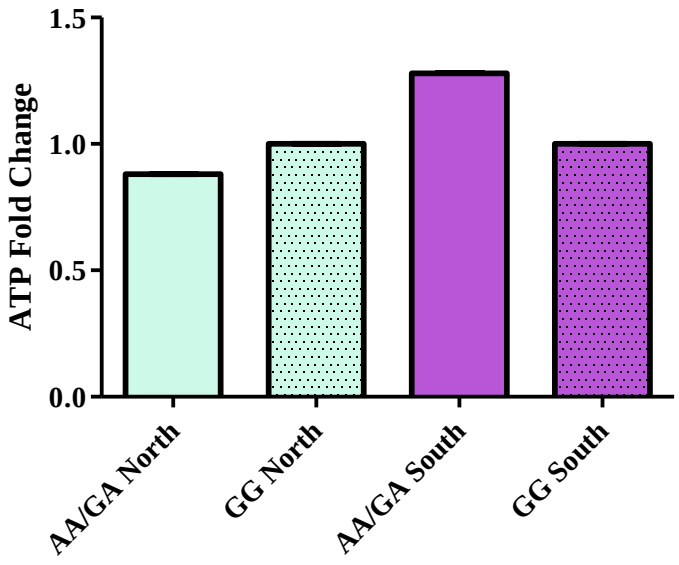

Figure 3.7: Fold change of ATP levels compared between UCP2 genotypes.

3.4. Mitochondrial Depolarisation

Mitochondrial depolarisation of PBMCs from the study group was measured by performing the JC-1 Mitoscreen. Results are reflected as a percentage (Fig 3.8). Mitochondrial depolarisation of PBMCs was slightly higher in the women from DS (45.3±17.2%) than the women from DN (44.1±25.6%; $p = 0.80$; Mann Whitney). The difference was not statistically significant ($p > 0.05$).

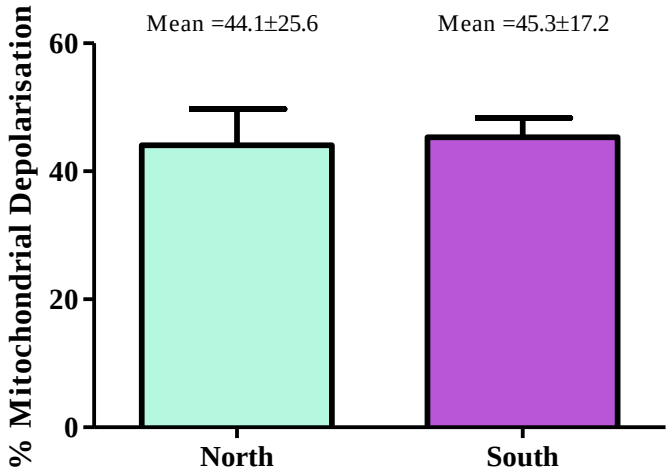

Figure 3.8: Percentage mitochondrial depolarisation of PBMCs from pregnant women in Durban North and Durban South ($p > 0.05$).

The results from the JC-1 Mitoscreen were then stratified according to UCP2 genotypes (Fig 3.9). The GG genotype displayed higher $\Delta\Psi$m in both DN (59.8±15.8%) and DS (47.4±14.2%) when compared to the AA/GA genotype in their respective groups ($p = 0.38$; ANOVA). No statistically significant differences were observed ($p > 0.05$).

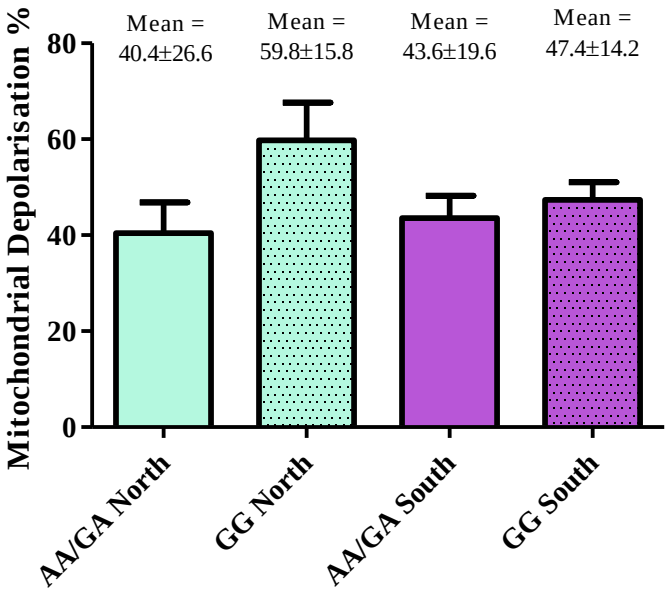

Figure 3.9: Percentage mitochondrial depolarisation of PBMCs from pregnant women in Durban North and Durban South stratified according to UCP2 genotype ($p > 0.05$).

3.5. Comet Assay

The comet assay was performed to evaluate DNA fragmentation in PBMCs of the pregnant women from DN and DS. Longer comet tail length is associated with higher DNA fragmentation. Figure 3.11 shows comet tails were significantly longer in PBMCs from women in DS (0.57±0.16µm) than women from DN (0.48±0.13µm; $p = 0.04$; Mann Whitney).

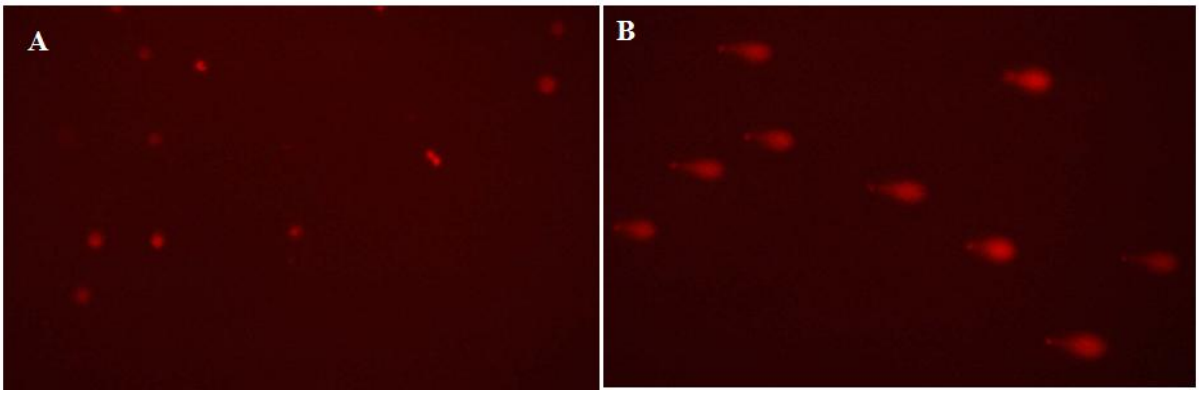

Figure 3.10 Comet tails of PBMCs in women from Durban North (A) and Durban South (B).

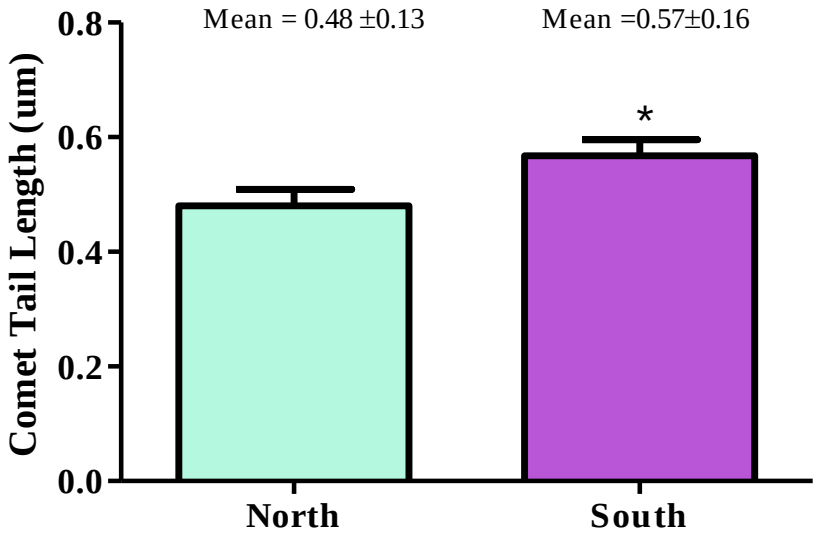

Figure 3.11: Comet tail length was significantly higher in PBMCs from women in Durban South than women from Durban North (*$p < 0.05$).

The comet assay results were then stratified according to the UCP2 genotypes in pregnant women from DN and DS (Fig 3.12). The GG genotype was found to have longer comet tails in DN (0.50±0.07µm) and DS (0.62±0.20µm) than the AA/GA genotype in their respective groups ($p = 0.07$; ANOVA).

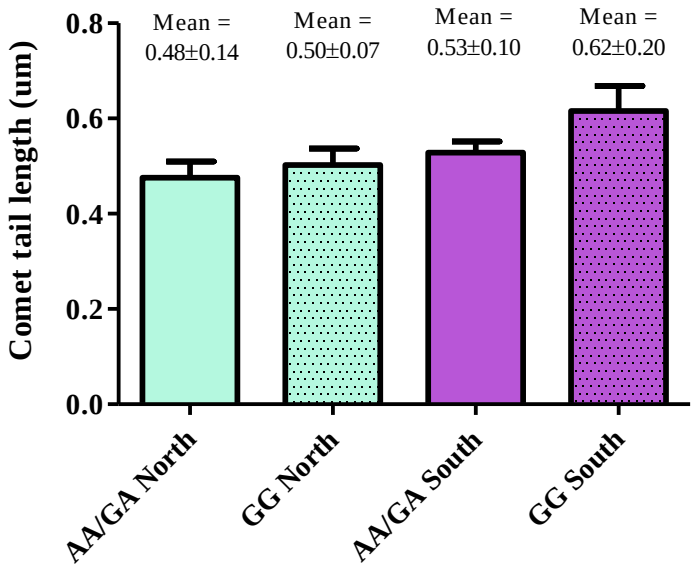

Figure 3.12: Comet assay results stratified to UCP2 genotypes. The GG genotype was associated with longer comet tail length in both Durban North and Durban South (*p* > 0.05).

3.6. Mitochondrial DNA damage

Mitochondrial DNA (mtDNA) damage was evaluated using qPCR to measure viable mtDNA. Greater mtDNA amplification is associated with more viable mtDNA. Results were calculated according to the Livak method (Livak 2001) and expressed as fold change ($2^{-\Delta\Delta Ct}$; Appendix 2). The women from DS displayed a 0.49 fold change in mtDNA amplification than the control group (Fig 3.13). Decreased mtDNA amplification can be associated with either a decline in the amount of viable mtDNA or unwinding of mtDNA due to gene expression.

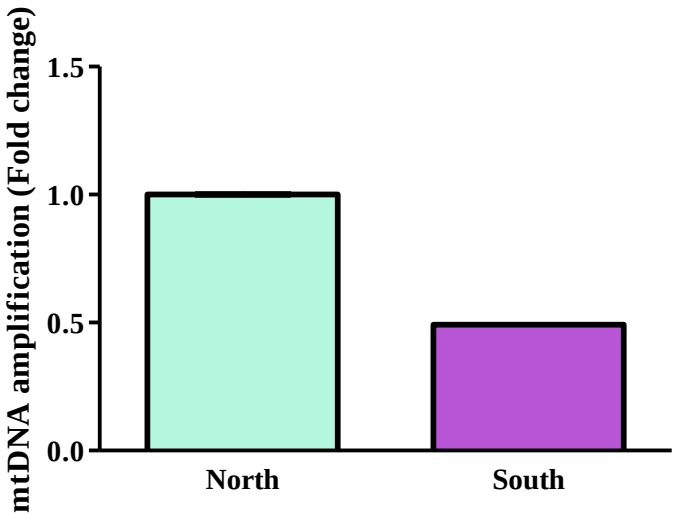

Figure 3.13: Pregnant women from Durban South displayed a 0.49 fold change in mtDNA amplification when compared to women from Durban North.

The Ct values from the mtDNA qPCR were then stratified according to the UCP2 genotypes. Fold change was calculated according to the Livak method ($2^{-\Delta\Delta Ct}$; Appendix 2) with the GG genotype being used as the control in each geographical group. The AA/GA genotype in DN showed a 0.69 decrease in mtDNA amplification. The same genotype had a 0.81 fold decrease in mtDNA amplification in DS when compared to the GG genotype (Fig 3.14).

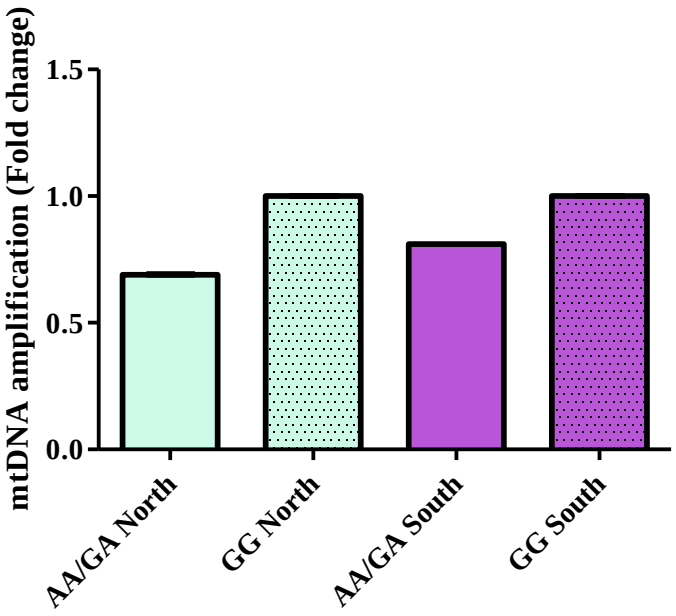

Figure 3.14: Fold change in mtDNA amplification in Durban North and Durban South stratified according to UCP2 genotypes

3.7. Uncoupling protein2 mRNA expression

Fold change in UCP2 mRNA expression was calculated using the Livak method ($2^{-\Delta\Delta Ct}$; Appendix 2). Then women from DS showed 1.58 fold higher UCP2 mRNA expression in their PBMCs when compared to the women from DN (Fig 3.15).

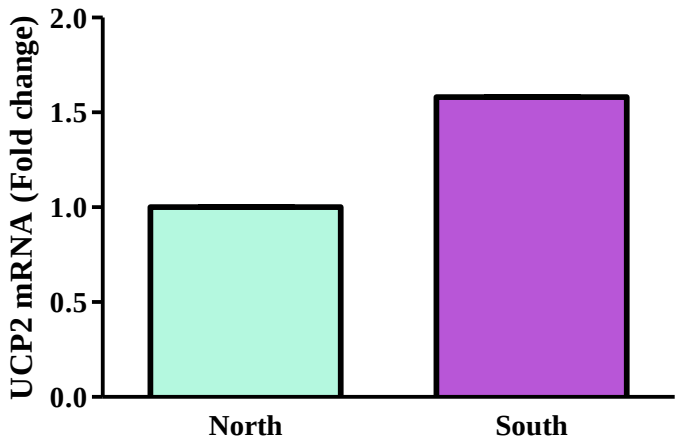

Figure 3.15: Uncoupling protein mRNA expression was 1.58 fold higher in PBMCs from women in Durban South than women from Durban North

The Ct values from the UCP2 qPCR were then stratified according to the UCP2 genotypes. The fold change was calculated according to the Livak method ($2^{-\Delta\Delta Ct}$; Appendix 2) with the GG genotype being used as the control in each geographical group. The AA/GA genotype exhibited lower UCP2 mRNA expression in both DN (0.72 fold) and DS (0.89 fold) when compared to the GG genotype in their respective groups (Fig 3.16).

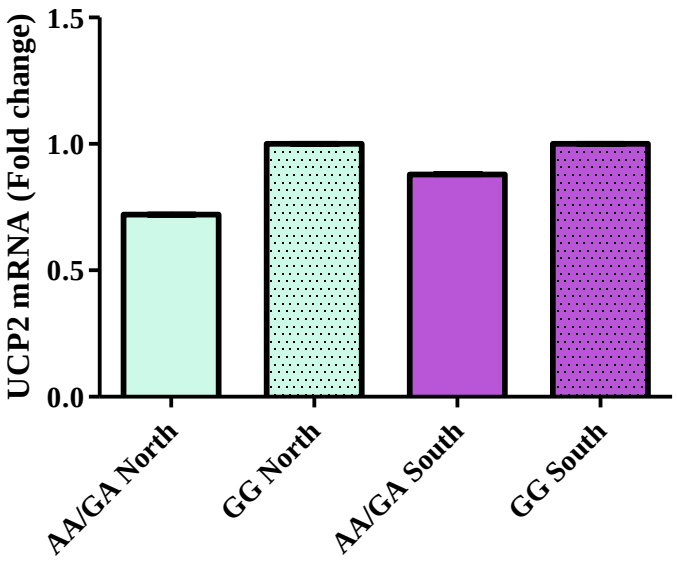

Figure 3.16: Uncoupling protein mRNA expression stratified according to UCP2 genotype. The AA/GA genotype exhibited lower mRNA expression in both Durban North and Durban South

3.8. Superoxide dismutase 2 mRNA expression

Fold change in SOD2 mRNA expression was calculated as $2^{-\Delta\Delta Ct}$ (Appendix 2). Pregnant women from DS showed 1.23 fold higher expression of SOD2 mRNA in their PBMCs than the women from the control group (Fig 3.17).

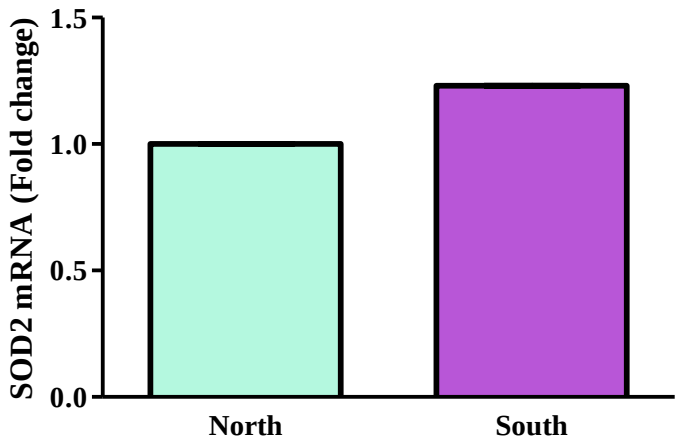

Figure 3.17: Women from Durban South displayed a 1.23 fold increase in SOD2 mRNA expression

The Ct values the SOD2 qPCR were then stratified according to the UCP2 genotypes. The fold change was calculated according to the Livak method ($2^{-\Delta\Delta Ct}$) with the GG genotype being used as the control in each geographical group (Appendix 2). Expression of SOD2 mRNA was up regulated in the AA/GA in DN (5.46 fold), but the same genotype was down regulated in DS (0.83 fold) in comparison to the GG genotypes in their respective groups (Fig 3.18).

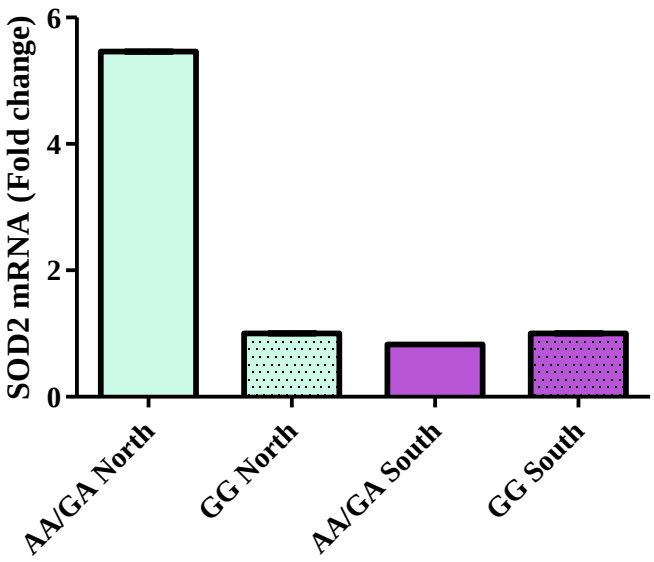

Figure 3.18: Fold change of SOD2 mRNA expression between genotypes in Durban North and Durban South

3.9. Nuclear erythroid related factor 2 (Nrf2) mRNA

The Ct values from the Nrf2 qPCR were used to calculate fold change. Fold change was calculated as $2^{-\Delta\Delta Ct}$ (Appendix 2). Pregnant women from DS had a 0.73 fold lower Nrf2 mRNA than women from DN (Fig 3.19).

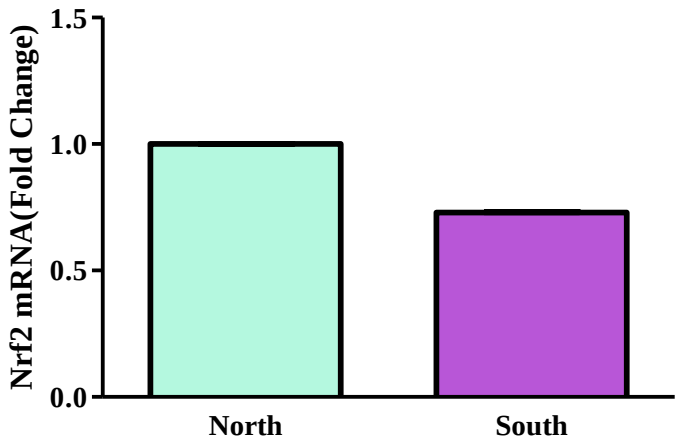

Figure 3.19: Pregnant women from Durban South displayed a 0.73 fold decrease in Nrf2 mRNA expression compared to women from Durban North

The Ct values the Nrf2 qPCR were then stratified according to the UCP2 genotypes. The fold change was calculated according to the Livak method ($2^{-\Delta\Delta Ct}$) with the GG genotype being used as the control in each geographical group. The AA/GA genotype showed a 3.38 fold increase in Nrf2 mRNA expression compared to the GG genotype in DN. In the DS group, the AA/GA genotype displayed 0.6 fold lower Nrf2 mRNA expression than the GG genotype (Figure 3.20)

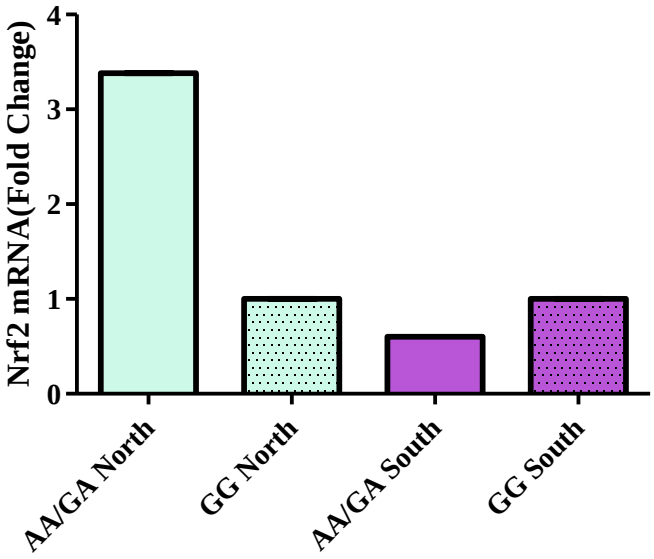

Figure 3.20: Fold change of Nrf2 mRNA expression between genotypes in Durban North and Durban South

3.10 Uncoupling protein2 protein expression

Protein expression of UCP2 was quantified by performing western blots. The results are reflected as RBI of the UCP2 probe divided by the RBI of the β-Actin probe (Figure 3.22). The PBMCs from pregnant women from DS had significantly higher UCP2 protein expression than women from the control group (DS: 0.08±0.03RBI vs DN: 0.05±0.01RBI; *p* = 0.049; Mann Whitney).

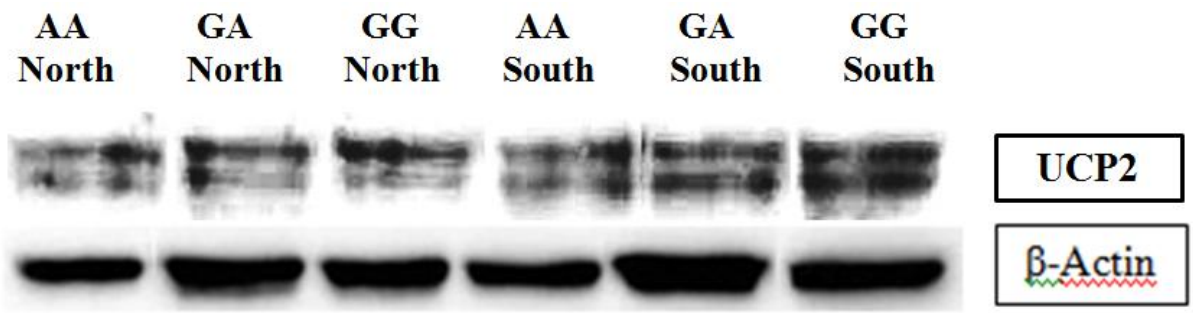

Figure 3.21: Western blot images for UCP2 expression and house-keeping protein

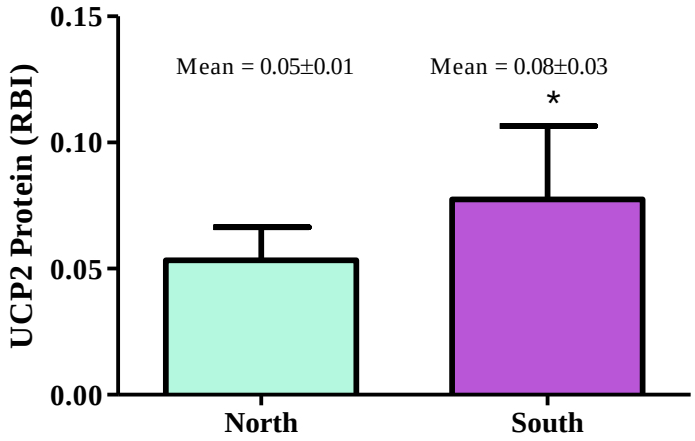

Figure 3.22 Protein expression of UCP2 in PBMCs from pregnant women in Durban South was significantly higher than women from Durban North; *$p < 0.05$.

The results from the UCP2 western blot were stratified according to the UCP2 genotypes of the women from DN and DS (Fig 3.23). No statistically significant differences were observed ($p > 0.05$). The GG genotype displayed higher UCP2 protein expression than the AA/GA genotype in DS (GG: 0.12±0.08 vs GG/GA: 0.10±0.08; $p = 0.53$; ANOVA).

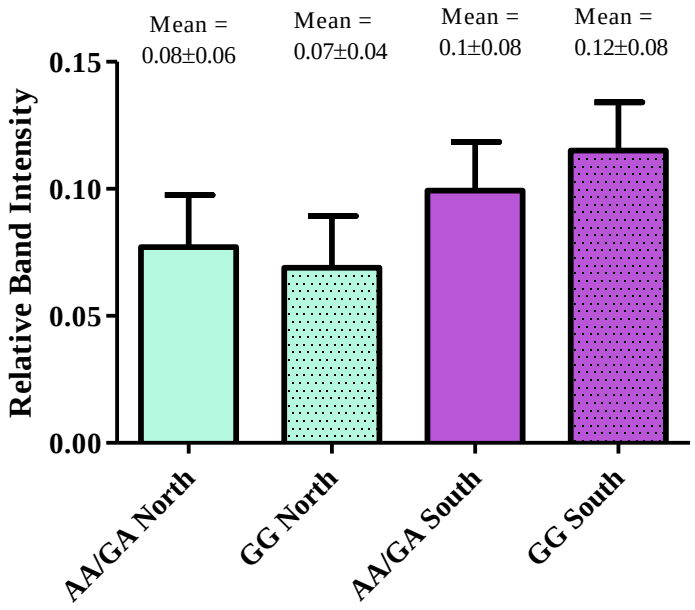

Figure 3.23: Protein expression of UCP2 in PBMCs from pregnant women in Durban North and Durban South stratified according to UCP2 genotype ($p > 0.05$)

3.11 Nuclear erythroid related factor 2 protein expression

The results of the Nrf2 western blot are reflected as Nrf2 RBI/ β-Actin RBI (Fig 3.25). Protein expression of Nrf2 in PBMCs from pregnant women from DS was significantly lower than women from DN (DS: 1.68±0.84RBI vs DN: 2.09±0.84RBI; $p = 0.03$; Mann Whitney).

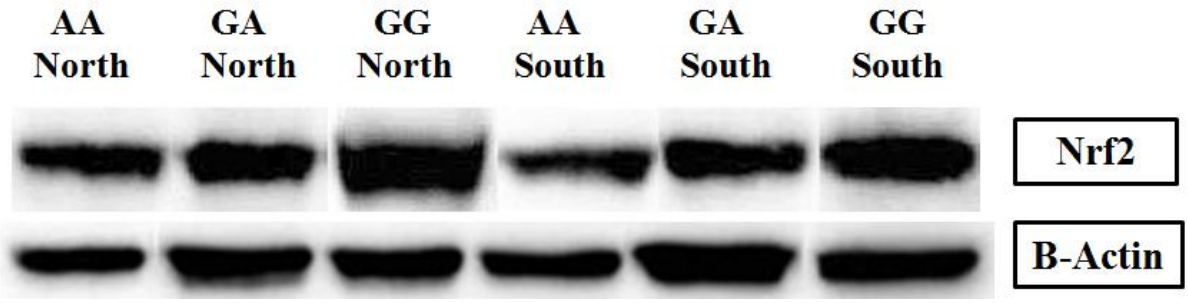

Figure 3.24: Western blot images for Nrf2 expression and house-keeping protein

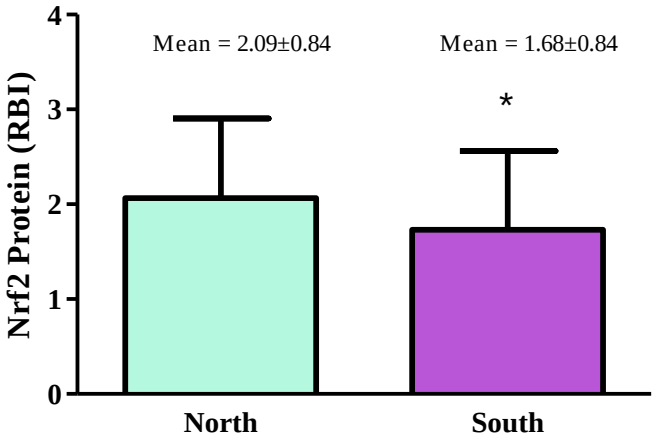

Figure 3.25: Protein expression of Nrf2 in PBMCs from pregnant women in Durban North and Durban South. Nrf2 protein expression was significantly lower in women from Durban South compared to Durban North (*$p < 0.05$)

The results from the Nrf2 western blot were stratified according to the UCP2 genotypes of the women from DN and DS (Fig 3.26). The GG genotype exhibited higher Nrf2 protein expression in both DN (2.41±0.72RBI) and DS (1.81±0.86RBI) when compared to the AA/GA genotype in within their respective groups ($p = 0.71$; ANOVA).

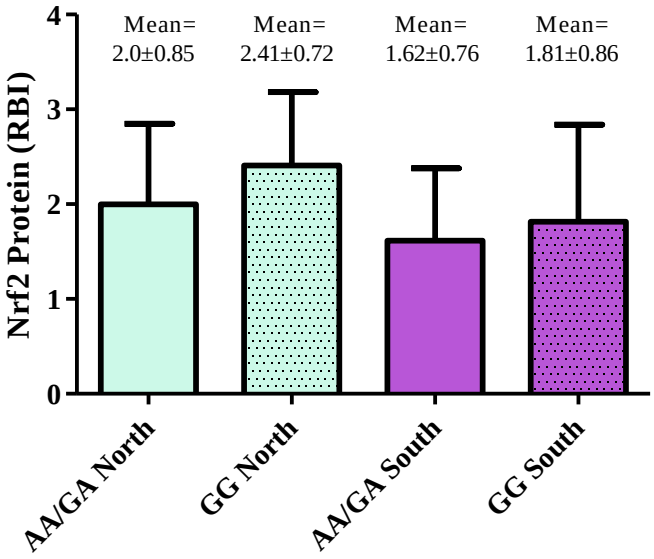

Figure 3.26: Protein expression of Nrf2 in PBMCs from pregnant women in Durban North and Durban South stratified according to UCP2 genotype ($p > 0.05$)

CHAPTER 4

DISCUSSION

The industrial basin in the south of Durban has been recognised as an area of concern since the 1960's. The petrol company and oil refinery situated in the DS industrial basin are the major contributors to AAP levels, emitting high levels of SO_2, NO_x and PM_{10}. SO_2 levels have exceeded limits set out by the World Health Organization until 2006 (Guastella 2007). Studies have found associations between these pollutants and the incidence of asthma in children attending the school situated between the two industries (Kistnasamy 2005; Niranjan 2005). The association of AAP exposure with adverse birth outcomes has not been investigated in DS.

The exact mechanism by which AAP causes adverse health outcomes is difficult to determine as interactions between pollutants and variations in pollutant levels between different environments need to be taken in to account. Oxidative stress has been identified as a molecular mechanism in AAP associated adverse health and birth outcomes (Wang, Ding et al. 1997; Maroziene and Grazuleviciene 2002; Maisonet, Correa et al. 2004; Sram 2005). If oxidative stress plays a role in AAP toxicity, genes involved in oxidative stress response could influence susceptibility to AAP associated health outcomes.

Women from DS are exposed to high levels of pollutants that are associated with inducing free radical production (Guastella 2007). Particulate matter has been recognised as a potent stimulus for mitochondrial ROS production via disruption of the mitochondrial ETC (Kamdar, Le et al. 2008). Sulphur dioxide was found to elevate MDA levels (Gokirmak, Yildirim et al. 2003) and deplete an important antioxidant, vitamin C, in plasma (Gumuslu, Korgun et al. 2000). Upon inhalation, NO_x dissolves in lung lining fluid and is converted to a free radical in solution (Kelly 2003). We set out to establish whether pregnant women from

DS displayed elevated markers for oxidative stress and damage than pregnant women from the less industrialized DN.

Pregnant women tend to display higher markers for lipid peroxidation products than non-pregnant women (Arikana 2001). Increased energy expenditure and changes in metabolic processes during pregnancy promote ROS production. TBARS results showed that women from DS had elevated levels of extracellular MDA when compared to women from DN (Fig 3.2). Malondialdehyde is a by-product of lipid peroxidation, a process initiated by oxidative damage to lipid membranes (Marnett 1999). Therefore elevated MDA levels are associated with increased levels of circulating free radicals. The elevated ATP levels (Fig 3.5) and higher $\Delta\Psi$m (Fig 3.8) observed in women from DS favour mitochondrial free radical production. Increased ATP production by mitochondria promotes $O_2^{\bullet-}$ anion radical production via the electron transport chain (Brand 2004). The higher ATP levels in women from the industrialized DS could be due to increased apoptosis or gene expression.

The longer PBMC comet tail lengths in women from DS (Fig 3.11) indicates increased DNA fragmentation or increased unwinding of DNA due to increased gene expression. Increased DNA fragmentation could be due to elevated circulating MDA, which has a high affinity for deoxyguanine and deoxyadenine in DNA. Pollutants such as SO_2 and PM_{10} can also increase DNA fragmentation due to their genotoxic effects (Kamdar, Le et al. 2008; Ziemann, Hansen et al. 2010). This could lead to DNA lesions and breaks, increasing DNA fragmentation. Furthermore, damage by oxidants can induce apoptosis, resulting in DNA fragmentation. Particle matter has been found to induce pro-apoptotic members of the BCl_2 family (Kamdar, Le et al. 2008). Apoptosis is an active process requires ATP, hence the increase in ATP production in women from DS.

The qPCR results showed women from DS only had half as much mtDNA amplification when compared to pregnant women from DN (Fig 3.13). Reduced mtDNA amplification could be due to mtDNA damage, as only viable mtDNA strands are amplified. Since mitochondria are the main site of ROS production, mtDNA is extremely susceptible to oxidative damage (de Souza 2012). Elevated ATP production in the women from DS will cause an increase in mitochondrial ROS production, possibly contributing to increased oxidative damage to mtDNA.

Aside from DNA damage, the longer comet tails and decreased mtDNA amplification in women from DS could be due to increased gene expression. Elevated ROS levels in these women would stimulate the expression of antioxidant response genes. In order for transcription to take place, dsDNA must unwind into ssDNA (Strachan 1999). Single stranded DNA would migrate from the nucleosome embedded in the LMPA gel, resulting in longer comet tails. These strands would also not be quantified during qPCR as the tracking dye, SYBR Green, only intercalates in dsDNA. Increased gene expression is supported by the higher levels of UCP2 (Fig 3.15), Nrf2 (Fig 3.19) and SOD2 (Fig 3.15) expression observed in women from DS.

The elevated ATP levels in this group favours $O_2^{\bullet-}$ anion radical production (Krauss, Zhang et al. 2002). Superoxide is a potent stimulator of UCP2 expression. When $O_2^{\bullet-}$ anion radical levels rise, UCP2 alters mitochondrial membrane proton conductance, to limit ATP production and reduce $O_2^{\bullet-}$ anion radical production (Echtay, Roussel et al. 2002). The major antioxidant enzyme involved in the detoxification of mitochondrial $O_2^{\bullet-}$ is SOD2, which is responsible for the conversion of $O_2^{\bullet-}$ anion radical to hydrogen peroxide (Limón-Pacheco and Gonsebatt 2009). Women in DS showed increased SOD2 mRNA expression (Fig 3.17), indicating these women were responding to higher levels of $O_2^{\bullet-}$ anion radicals than women in DN. Furthermore, decreased mtDNA viability in the women from DS can attenuate $O_2^{\bullet-}$

production and PM_{10} in particular has been found to cause blocks in the mitochondrial electron transport chain, resulting in elevated $O_2^{\bullet-}$ anion radical production (Kamdar, Le et al. 2008). This would explain the significantly higher expression of UCP2 mRNA (Fig 3.15) and protein (Fig 3.22) observed in women from DS.

The antioxidant response of women from DS was then evaluated. The transcription factor Nrf2 is regarded as the master regulator of antioxidant response genes. In its inactive form, Nrf2 remains in the cytoplasm bound to its inhibitor, Keap1. In the presence of ROS, the sulphydryl groups of Keap1 are disrupted and Nrf2 breaks free of Keap1 and enters the nucleus. Nrf2 heterodimerizes with small Maf proteins, binds to the ARE, and initiates the transcription of antioxidant genes such as GST, GP_x, CAT and SOD (Fig 1.5). Pregnant women from DS showed reduced levels of Nrf2 mRNA expression (Fig 3.19) and a significant decline in Nrf2 protein expression (Fig 3.25). The binding of Nrf2 to the ARE is an early response to oxidative stress (Lodovici 2011). The women from DS have been exposed to pro-oxidant air pollutants over a long period of time. Previous studies have found that long term exposure to oxidative agents causes reduced expression of an Nrf2 stabilizing protein ,DJ-1 (Malhotra, Thimmulappa et al. 2008). This protein also acts as a scavenger for free radicals; hence a possible reason for the decline in Nrf2 expression in women from DS could be due to depleted DJ-1.

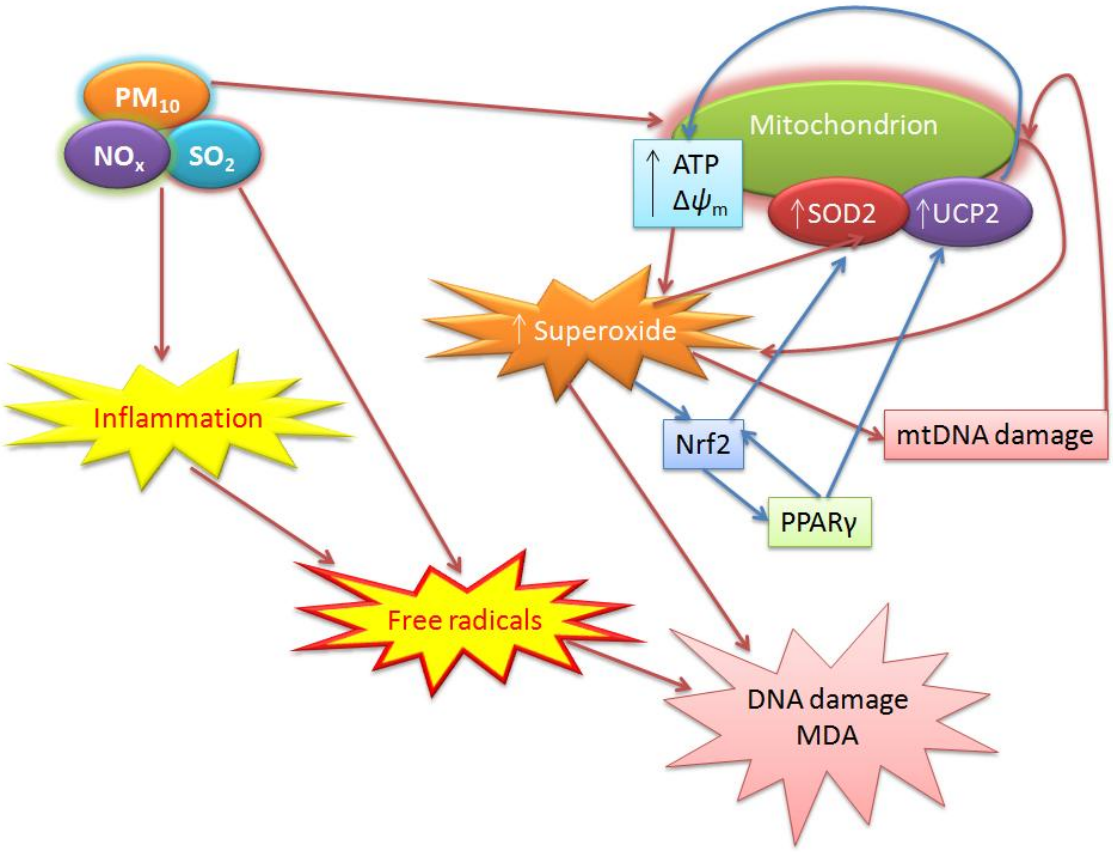

Figure 14.1. Oxidative stress response in pregnant women from DS. The red arrows show pro-oxidant events, while the blue arrows indicate antioxidant defence. Air pollutants induce free radical production directly, via the induction of inflammatory response aor by altering mitochondrial function. Women in DS had elevated ATP and ΔΨm, favouring the production of superoxide anion radical production. Superoxide and free radicals will then cause DNA lesions, as indicated by the increased comet tail length, and higher MDA levels through oxidation of lipids. Increased superoxide anion radical production by the mitochondrion will increase the risk of mtDNA damage. An increase in superoxide levels will stimulate antioxidant response (SOD2) and UCP2 expression. Increased UCP2 expression will act as a regulatory mechanism by increasing the proton conductance across the inner mitochondrial membrane, reducing ATP and ΔΨm, in turn reducing superoxide anion radical production.

The functional relevance of a common UCP2-866G/A polymorphism in the promoter of the gene in the oxidative stress response of pregnant women living in DS was then evaluated. The GG genotype was almost twice as frequent in women from DS, than women from DN (Table 3.1). Previous studies have found that this genotype is associated with higher mRNA and protein expression of UCP2 (Emre and Nubel 2010). However, it is not understood if higher protein expression is associated with protein function.

The GG genotype was found to have higher UCP2 protein (Fig 3.23) and mRNA (Fig 3.16) than the AA/GA genotype in women from DS. However, MDA levels (Fig 3.3), DNA fragmentation (Fig 3.12) and $\Delta\Psi$m (Fig 3.9) were all higher in the GG genotype when compared to the AA/GA genotype in women from DS. This indicates that this genotype could be less effective at reducing $\Delta\Psi$m, and thus attenuate mitochondrial free radical production. The AA/GA genotype in women from DS displayed elevated ATP levels (Fig 3.7) and decreased mtDNA amplification (Fig 3.14) than the GG genotype. This could indicate an increase in gene expression. All antioxidant response genes evaluated were up regulated in the GG genotype in women in DS when compared to the AA/GA genotype. SOD2 is one of the many antioxidant genes regulated by Nrf2, thus an increase in Nrf2 expression (Fig 3.20) is coupled with an increase in SOD2 expression (Fig 3.18) as seen in the GG genotype in DS and the AA/GA genotype in DN (Motohashi and Yamamoto 2004). The elevated SOD2 levels in the GG genotype in DS indicate that these women were possibly producing higher levels of $O_2^{\bullet-}$ anion radicals than women with the AA/GA genotype. This would explain the higher UCP2 expression and antioxidant response. Furthermore, elevated Nrf2 protein expression in the GG genotype in women from DS could be indirectly affecting UCP2 levels via PPARγ. Nrf2 expression will increase the transcription of ARE genes, including PPARγ, which further stimulates UCP2 expression (Malhotra, Thimmulappa et al. 2008; Polvani 2012).

Although the GG genotype is associated with higher UCP2 expression than the AA/GA genotype in women from DS, this genotype displayed higher markers for oxidative stress. Elevated $\Delta\Psi$m is characteristic of increased ROS production and the mechanism by which UCP2 reduces mitochondrial ROS production is by reducing $\Delta\Psi$m (Krauss, Zhang et al. 2002; Rousset, Mozo et al. 2007). We observed that the GG genotype, although being associated with higher UCP2 expression, is less functional and reducing $\Delta\Psi$m and mitochondrial free radical production than the AA/GA genotype.

CHAPTER 5

CONCLUSION

No studies have been done in Africa investigating gene-environment interactions associated with AAP exposure. The rapid expansion of industries in developing countries changes environmental conditions which can have an impact on health outcomes. Genetic variation in the proteins involved in stress response is likely to influence susceptibility to environment associated diseases and disorders.

Oxidative stress is a likely mechanism of toxicity in many adverse health outcomes associated with AAP exposure. Air pollution exposure resulting in oxidative stress during pregnancy has health implications for both the mother and foetus. Mitochondria play a pivotal role in ROS production and regulatory mechanisms can give insight into oxidative stress response. Genetic variability in genes involved in mitochondrial response to oxidative stress can provide genetic risk factors for oxidative stress associated health outcomes.

We found that women from the DS industrial basin did exhibit higher markers for oxidative stress, indicating an association with air pollution exposure and increased free radical production. Hence, we can say that women exposed to higher levels of air pollution are at increased risk for oxidative stress. The up-regulation of UCP2 in conditions that favour oxidative stress indicated a role in the oxidative response of pregnant mothers exposed to AAP. By identifying these women as having increased risk for oxidative stress, targeted therapies such as antioxidant administration, or the induction of the expression of UCP2 can be taken into account.

The GG genotype was found to be almost twice as frequent in women from DS as women from DN. This genotype is associated with higher expression of UCP2 at both the protein and

translational level. However, this genotype was less efficient at reducing mitochondrial membrane potential and free radical production. The functional relevance of the UCP2 polymorphism cannot be evaluated in isolation, as other antioxidant proteins, such as Nrf2 and SOD2 can compensate in response to compromised UCP2 function.

Genetic variability in the UCP2 gene could potentially play a role in oxidative susceptibility in pregnant women; however, other antioxidant and regulatory mechanisms need to be taken into account. Further studies regarding AAP associated oxidative stress can include epigenetic mechanisms such as microRNAs and histone modification in pregnant women exposed to air pollution. This would give a better understanding of molecular pathways involved in the pathogenesis of various AAP associated health outcomes.

REFERENCES

Al-Gubory, K. H., Fowler, P. A., Garrel, C. (2010). "The roles of cellular reactive oxygen species, oxidative stress and antioxidants in pregnancy outcomes." The International Journal of Biochemistry & Cell Biology **42**(10): 1634-1650.

Aoki, Y., Sato H., Nishimura, N., Takahashi, S., Itoh, K., Yamamoto, M. (2001). "Accelerated DNA adduct formation in the lung of the Nrf2 knockout mouse exposed to diesel exhaust." Toxicol Appl Pharmacol **173**: 154–160.

Arikana, S., Konukoğlua, D., Arıkanb, C.,Akçaya, T., Davas, I. (2001). "Lipid Peroxidation and Antioxidant Status in Maternal and Cord Blood." Gynecological and Obstetric Investigation **51**(3): 145-149.

Baffy, G. (2010). "Uncoupling protein-2 and cancer." Mitochondrion **10**: 243–252.

Barnes, P. J., Belvisi, M. G. (1993). "Nitric oxide and lung disease." Thorax **48**: 1034-1043.

Bigagli, M. L. a. E. (2011). "Oxidative Stress and Air Pollution Exposure." Journal of Toxicology **2011**.

Bo, H., Jiang, N., Ma, G., Qu, J., Zhang, G., Cao, D., Wen, L., Liu, S., Ji, L., Zhang, Y. (2008). "Regulation of mitochondrial uncoupling respiration during exercise in rat heart: Role of reactive oxygen species (ROS) and uncoupling protein 2." Free Radical Biology and Medicine **44**(7): 1373-1381.

Bobak, M. (2000). "Outdoor air pollution, low birth weight, and prematurity." Environ Health Perspect **108**(2): 173-176.

Bobak, R. J. S. B. B. J. D. M. (2005). "Ambient Air Pollution and Pregnancy Outcomes: A Review of the Literature." Environmental Health Perspectives **113**(4): 378-382.

Boss, O., Muzzin, P., Giacobino, J. (1998). "The uncoupling proteins, a review." European Journal of Endocrinology **139**: 1-9.

Brand, M. D., Affourtit, C., Esteves, T. C., Green, K., Lambert, A. J.,Miwa, S., Pakay, J. L.,Parker, N. (2004). "Mitochondrial superoxide: production, biological effects, and activation of uncoupling proteins." Free Radical Biology and Medicine **37**(6): 755-767.

Brunekreef, B., Holgate, S. T. (2002). "Air pollution and health." The Lancet **360**(9341): 1233-1242.

Cadenas, E. (2004). "Mitochondrial free radical production and cell signaling." Molecular Aspects of Medicine **25**(1–2): 17-26.

Campen, M. J. (2009). "Nitric Oxide Synthase: “Enzyme Zero” in Air Pollution–Induced Vascular Toxicity." Toxicological Sciences **110**(1): 1-3.

Castro-Giner, F., Künzli, N., Jacquemin, B., Forsberg, B., de Cid, R., Sunyer, J., Jarvis, D., Briggs, D., Vienneau, D., Norback, D., González, J. R.., Guerra, S., Janson, Christer.,

Antó, J., Wjst, M., Heinrich, J., Estivill, X., Kogevinas, M. (2009). "Traffic-Related Air Pollution, Oxidative Stress Genes, and Asthma (ECHRS)." Environ Health Perspect **117**(12).

Chahine, T., Baccarelli, A., Litonjua, A., Wright, R. O., Suh, H., Gold, D. R., Sparrow, D., Vokonas, P., Schwartz, J. (2007). "Particulate Air Pollution, Oxidative Stress Genes, and Heart Rate Variability in an Elderly Cohort." Environ Health Perspect **115**(11).

Chomczynski, P., Sacchi, N. (1987). "Single-step method of RNA isolation by acid guanidinium thiocyanate-phenol-chloroform extraction." Analytical Biochemistry **162**(1): 156-159.

De Souza, B. M., Assmann, T. S., Kliemann, L. M., Marcon, A. S., Gross, J. L., Canani, L. H., Crispim, D. (2012). "The presence of the -866A/55Val/Ins haplotype in the uncoupling protein 2 (UCP2) gene is associated with decreased UCP2 gene expression in human retina." Experimental Eye Research **94**: 49-55.

de Souza, B. M., Assmann, T. S., Kliemann, L. M., Marcon, A. S., Gross, J. L., Canani, L. H., Crispim, D. (2012). "The presence of the -866A/55Val/Ins haplotype in the uncoupling protein 2 (UCP2) gene is associated with decreased UCP2 gene expression in human retina." Exp Eye Res **94**(1): 49-55.

De Souza, C. T., E. P. Araújo, et al. (2007). "Inhibition of UCP2 expression reverses diet-induced diabetes mellitus by effects on both insulin secretion and action." The FASEB Journal **21**(4): 1153-1163.

Dejmek, J., Solanský, I., Benes, I., Lenícek, J., Srám, R. J. (2000). "The impact of polycyclic aromatic hydrocarbons and fine particles on pregnancy outcome." Environ Health Perspect. **108**(12): 1159-1164.

Echtay, K. S., D. Roussel, et al. (2002). "Superoxide activates mitochondrial uncoupling proteins." Nature **415**(6867): 96-99.

Emre, Y. and T. Nubel (2010). "Uncoupling protein UCP2: when mitochondrial activity meets immunity." FEBS Lett **584**(8): 1437-1442.

Fleury, C. and D. Sanchis (1999). "The mitochondrial uncoupling protein-2: current status." The International Journal of Biochemistry & Cell Biology **31**(11): 1261-1278.

Giaime, E., Yamaguchi, H., Gautier, C. A., Kitada, T., Shen, J. (2012) "Loss of DJ-1 Does Not Affect Mitochondrial Respiration but Increases ROS Production and Mitochondrial Permeability Transition Pore Opening." **7** DOI: 10.1371/journal.pone.0040501.

Giardina, T. M., J. H. Steer, et al. (2008). "Uncoupling protein-2 accumulates rapidly in the inner mitochondrial membrane during mitochondrial reactive oxygen stress in macrophages." Biochim Biophys Acta **1777**(2): 118-129.

Gokirmak, M., Z. Yildirim, et al. (2003). "The role of oxidative stress in bronchoconstriction due to occupational sulfur dioxide exposure." Clinica Chimica Acta **331**(1–2): 119-126.

Guastella, L., Knudsen, S. (2007). South Durban Basin Multi-Point Plan: Case Study Report. Output A2: DEAT AQA Implementation: Air Quality Management Planning. E. A. a. Tourism. Republic of South Africa, Governance Information. **C**.

Gumus, S., Kipmen Korgun, D., Bilmen, S., Yargicog, P., Ag, A. (2000). "Effects of Sulfur Dioxide Inhalation on Plasma Vitamin C and Ceruloplasmin in Ageing Rats." Industrial Health **38**: 319–322.

Gumuslu, S., D. K. Korgun, et al. (2000). "Effects of sulfur dioxide inhalation on plasma vitamin C and ceruloplasmin in ageing rats." Industrial Health **38**(3): 319-322.

Hensley, K., K. A. Robinson, et al. (2000). "Reactive oxygen species, cell signaling, and cell injury." Free Radical Biology and Medicine **28**(10): 1456-1462.

Hurtaud, C., C. Gelly, et al. (2006). "Translation control of UCP2 synthesis by the upstream open reading frame." Cellular and Molecular Life Sciences **63**(15): 1780-1789.

Ishii, T., Itoh, K.,Takahashi, S., Sato, H., Yanagawa, T., Katoh, Y., Bannai, S., Yamamoto, M. (2000). "Transcription Factor Nrf2 Coordinately Regulates a Group of Oxidative Stress-inducible Genes in Macrophages." The Journal of Biological Chemistry **275**(May 26): 16023–16029.

Jaggernath, J. (2010). "Durban Basin: Integrating residents' perceptions and concerns resulting from air pollution." AJCR **10**(2).

Ježek, P. and L. Hlavatá (2005). "Mitochondria in homeostasis of reactive oxygen species in cell, tissues, and organism." The International Journal of Biochemistry & Cell Biology **37**(12): 2478-2503.

Jun, H. S., I. K. Kim, et al. (2008). "Effects of UCP2 and UCP3 Variants on the Manifestation of Overweight in Korean Children." Obesity **17**(2): 355-362.

Jung, K. A., Kwak, M. (2010). "The Nrf2 System as a Potential Target for the Development of Indirect Antioxidants." Molecules **15**: 7266-7291.

Kamdar, O., W. Le, et al. (2008). "Air pollution induces enhanced mitochondrial oxidative stress in cystic fibrosis airway epithelium." FEBS Letters **582**(25–26): 3601-3606.

Kelly, F. J. (2003). "Oxidative stress: its role in air pollution and adverse health effects." Occupational and Environmental Medicine **60**(8): 612-616.

Kim, J. H. and Y. C. Hong (2012). "GSTM1, GSTT1, and GSTP1 Polymorphisms and Associations between Air Pollutants and Markers of Insulin Resistance in Elderly Koreans." Environ Health Perspect **120**(10): 1378-1384.

Kistnasamy, E. J. (2005). The relationship between asthma and outdoor air pollutant concentrations of sulphur dioxide (SO2), oxides of nitrogen (NOx), ozone (O3) total reduced sulphates (TRS), carbon monoxide (CO) and respirable particulate matter less than 10 microns (PM10) in learners and teachers at Settlers Primary School in

Merebank, south Durban. Masters in Technology: Environmental Health, Durban University of Technology.

Kistnasamy, M. B., Knapp, M. (1991). "The relationship between location of residency and respiratory symptoms of primary school pupils." [Unpublished].

Kovacs, P., Ma, L., Hanson, R. L., Franks, P., Stumvoll, M., Bogardus, C., Baier, L. J. (2005). "Genetic variation in UCP2 (uncoupling protein-2) is associated with energy metabolism in Pima Indians." Diabetologia **48**: 2292-2295.

Krauss, S., C. Zhang, et al. (2002). "A significant portion of mitochondrial proton leak in intact thymocytes depends on expression of UCP2." Proceedings of the National Academy of Sciences **99**(1): 118-122.

Künzli, N., R. Kaiser, et al. (2000). "Public-health impact of outdoor and traffic-related air pollution: a European assessment." The Lancet **356**(9232): 795-801.

Lee, H., H. Ryu, et al. (2008). "Associations between polymorphisms in the mitochondrial uncoupling proteins (UCPs) with T2DM." Clinica Chimica Acta **398**(1–2): 27-33.

Li, N., Alam, J., Venkatesan, M. I., Eiguren-Fernandez, A., Schmitz, D., Di Stefano, E., Slaughter, N., Killeen, E., Wang, X., Huang, A., et al. (2004). "Nrf2 is a key transcription factor that regulates antioxidant defense in macrophages and epithelial cells: protecting against the proinflammatory and oxidizing effects of diesel exhaust chemicals." J Immunol **173**(3467–3481).

Li, N., M. Hao, et al. (2003). "Particulate air pollutants and asthma. A paradigm for the role of oxidative stress in PM-induced adverse health effects." Clin Immunol **109**(3): 250-265.

Li, N., Hao, M., Phalen, R. F., Hinds, W. C., Nel, A. E. (2003). "Particulate air pollutants and asthma: A paradigm for the role of oxidative stress in PM-induced adverse health effects." Clinical Immunology **109**: 250-265.

Li, N., C. Sioutas, et al. (2002). "Ultrafine Particulate Pollutants Induce Oxidative Stress and Mitochondrial Damage." Environ Health Perspect **111**(4).

Li, X. Y., Gilmour, P. S., Donaldson, K., MacNee, W. (1996). "Free radical activity and pro-inflammatory effects of particulate air pollution (PM10) in vivo and in vitro." Thorax **51**(12): 1216-1222.

Lim, J. H., Ko, M. M., Lee, H., Go, H. Y., Moon, T., Cha, M. H., Lee, M. S. (2012). "Differential Association of Uncoupling Protein 2 Polymorphisms with Pattern Identification among Korean Stroke Patients: A Diagnostic System in Traditional Korean Medicine." Evidence-Based Complementary and Alternative Medicine **2012**: 9.

Limón-Pacheco, J. and M. E. Gonsebatt (2009). "The role of antioxidants and antioxidant-related enzymes in protective responses to environmentally induced oxidative stress." Mutation Research/Genetic Toxicology and Environmental Mutagenesis **674**(1–2): 137-147.

Liu, L., R. Poon, et al. (2008). "Acute Effects of Air Pollution on Pulmonary Function, Airway Inflammation, and Oxidative Stress in Asthmatic Children." Environ Health Perspect **117**(4).

Livak, K. J., Schmittgen, T. D. (2001). "Analysis of Relative Gene Expression Data Using Real-Time Quantitative PCR and the 2−ΔΔCT Method." Methods **25**(4): 402-408.

Lodovici, M., Bigagli, E. (2011). "Oxidative Stress and Air Pollution Exposure." Journal of Toxicology **2011**.

Loh, E., J. S. Stamler, et al. (1994). "Cardiovascular effects of inhaled nitric oxide in patients with left ventricular dysfunction." Circulation **90**(6): 2780-2785.

Maisonet, M., A. Correa, et al. (2004). "A review of the literature on the effects of ambient air pollution on fetal growth." Environmental Research **95**(1): 106-115.

Malhotra, D., R. Thimmulappa, et al. (2008). "Decline in NRF2-regulated antioxidants in chronic obstructive pulmonary disease lungs due to loss of its positive regulator, DJ-1." Am J Respir Crit Care Med **178**(6): 592-604.

Marnett, L. J. (1999). "Lipid peroxidation-DNA damage by malondialdehyde." Mutat Res **424**(1-2): 83-95.

Maroziene, L. and R. Grazuleviciene (2002). "Maternal exposure to low-level air pollution and pregnancy outcomes: a population-based study." Environmental Health: A Global Access Science Source **1**(1): 6.

Masaki, T., H. Yoshimatsu, et al. (1999). "Up-regulation of uterine UCP2 and UCP3 in pregnant rats." Biochim Biophys Acta **1440**(1): 81-88.

Masaki, T., Yoshimatsu, H., Chiba, S., Kurokawa, M., Sakata, T. (1999). "Up-regulation of uterine UCP2 and UCP3 in pregnant rats." Biochimica et Biophysica Acta (BBA) - Bioenergetics **1440**(81-88).

Matsuzaki, S., P. A. Szweda, et al. (2009). "Regulated production of free radicals by the mitochondrial electron transport chain: Cardiac ischemic preconditioning." Advanced Drug Delivery Reviews **61**(14): 1324-1331.

Meng, Z. and W. Bai (2004). "Oxidation damage of sulfur dioxide on testicles of mice." Environmental Research **96**(3): 298-304.

Meng, Z., G. Qin, et al. (2003). "Oxidative damage of sulfur dioxide inhalation on lungs and hearts of mice." Environmental Research **93**(3): 285-292.

Meng, Z., Qin G., Bai J., Zhang J., Zhang X., Yang Z. (2007). "Alterations of gene expression profiles induced by sulfur." Front. Biol. China **2**(4): 369–378.

Motohashi, H. and M. Yamamoto (2004). "Nrf2–Keap1 defines a physiologically important stress response mechanism." Trends in Molecular Medicine **10**(11): 549-557.

Nedergaard, J., D. Ricquier, et al. (2005). "Uncoupling proteins: current status and therapeutic prospects." EMBO Rep **6**(10): 917-921.

Negre-Salvayre, A., Hirtz, C., Carrera, G., Cazenave, R., Troly, M., Salvayre, R., Penicaud, L., Casteilla, L. (1997). "A role for uncoupling protein-2 as a regulator of hydrogen peroxide generation." FASEB J. **11**: 809-815.

Niranjan, I. (2005). A case of environmental health in the South Durban Basin. Masters in Public Administration, University of KwaZulu Natal.

Nordberg, J. and E. S. J. Arnér (2001). "Reactive oxygen species, antioxidants, and the mammalian thioredoxin system." Free Radical Biology and Medicine **31**(11): 1287-1312.

Pecqueur, C., M. Alves-Guerra, et al. (2001). "Uncoupling Protein 2, in Vivo Distribution, Induction upon Oxidative Stress, and Evidence for Translational Regulation." Journal of Biological Chemistry **276**(12): 8705-8712.

Polvani, S., Tarocchi, M., Galli, A. (2012). "PPARγ and Oxidative Stress: Con(β) Catenating NRF2 and FOXO." PPAR Research **2012**: 15.

Pope, C., Burnett R. T., Thun M. J., et al. (2002). "Lung cancer, cardiopulmonary mortality, and long-term exposure to fine particulate air pollution." JAMA: The Journal of the American Medical Association **287**(9): 1132-1141.

Poston, L. and M. T. M. Raijmakers (2004). "Trophoblast Oxidative Stress, Antioxidants and Pregnancy Outcome—A Review." Placenta **25**: S72-S78.

Quyyumi, A. A., Dakak, N., Andrews, N. P., Husain, S., Arora, S., Gilligan, D. M., Panza, J. A., Cannon, R. O. (1995). "Nitric oxide activity in the human coronary circulation. Impact of risk factors for coronary atherosclerosis." J Clin Invest. **95**(4): 1747–1755.

Rahman, M., Lane, A., Swindle, A., Bartram, S. (2006). Introduction to Flow Cytometry. Serotec Ld. Endevour House. A. Serotec. Langford Lane, Kidlington, Oxford, Seotec Ltd.

Rangasamy, T., Guo, J., Mitzner, W. A,. Roman, J., Singh, A., Fryer, A. D., Yamamoto, M., Kensler, T. W., Tuder, R. M., Georas, S. N., et al. (2005). "Disruption of Nrf2 enhances susceptibility to severe airway inflammation and asthma in mice." J Exp Med **202**: 47-59.

Reis, A. F., D. Dubois-Laforgue, et al. (2004). "A polymorphism in the promoter of UCP2 gene modulates lipid levels in patients with type 2 diabetes." Molecular Genetics and Metabolism **82**(4): 339-344.

Risom, L., P. Møller, et al. (2005). "Oxidative stress-induced DNA damage by particulate air pollution." Mutation Research/Fundamental and Molecular Mechanisms of Mutagenesis **592**(1–2): 119-137.

Rousset, S., J. Mozo, et al. (2007). "UCP2 is a mitochondrial transporter with an unusual very short half-life." FEBS Letters **581**(3): 479-482.

Rudofsky, G., Jr., A. Schroedter, et al. (2006). "Functional polymorphisms of UCP2 and UCP3 are associated with a reduced prevalence of diabetic neuropathy in patients with type 1 diabetes." Diabetes Care **29**(1): 89-94.

Salpea, K. D., P. J. Talmud, et al. (2010). "Association of telomere length with type 2 diabetes, oxidative stress and UCP2 gene variation." Atherosclerosis **209**(1): 42-50.

Sanjuán-Pla, A., A. M. Cervera, et al. (2005). "A targeted antioxidant reveals the importance of mitochondrial reactive oxygen species in the hypoxic signaling of HIF-1α." FEBS Letters **579**(12): 2669-2674.

Sastre-Serra, J., Company, M. M., Garau, I., Oliver, J., Roca, P. (2010). "Estrogen down-regulates uncoupling proteins and increases oxidative stress in breast cancer." Free Radical Biology & Medicine **48**: 506–512.

Schwartz, J. (2004). "Air Pollution and Children's Health." Pediatrics **113**(Supplement 3): 1037-1043.

Seifried, H. E., D. E. Anderson, et al. (2007). "A review of the interaction among dietary antioxidants and reactive oxygen species." The Journal of Nutritional Biochemistry **18**(9): 567-579.

Shrey, K., A. Suchit, et al. (2011). "Air pollutants: The key stages in the pathway towards the development of cardiovascular disorders." Environmental Toxicology and Pharmacology **31**(1): 1-9.

Sies, H. (1991). "Role of reactive oxygen species in biological processes." Journal of Molecular Medicine **69**(21): 965-968.

Sies, H. (1997). "Oxidative stress: oxidants and antioxidants." Experimental Physiology **82**(2): 291-295.

Smith, P. K., R. I. Krohn, et al. (1985). "Measurement of protein using bicinchoninic acid." Analytical Biochemistry **150**(1): 76-85.

Södergren, E. (2000). Lipid peroxidation in vivo. Evaluation and application of methods for measurement. . Doctor of Medical Science in Geriatrics - Clinical Nutrition, Acta Universitatis Upsaliensis.

Space, L. (2012). "Animals at the extremes: Hibernation and torpor." The Open University, 2012, from http://openlearn.open.ac.uk/mod/oucontent/view.php?id=398616&section=3.6.

Sram, R. J., Binkova, B., Dejmek, J., Bobak, M. (2005). "Ambient air pollution and pregnancy outcomes: a review of the literature." Environmental Health Perspectives **113**(4): 375-382.

Stephens, J. W., Bain, S. C., Humphries, S. E. (2008). "Gene–environment interaction and oxidative stress in cardiovascular disease." Atherosclerosis **200**(2): 229-238.

Stephens, J. W., S. S. Dhamrait, et al. (2008). "Interaction between the uncoupling protein 2 −866G/A gene variant and cigarette smoking to increase oxidative stress in subjects with diabetes." Nutrition, Metabolism and Cardiovascular Diseases **18**(1): 7-14.

Strachan, T., Read A. P. (1999). Human Molecular Genetics. Chapter 1: DNA structure and gene expression. Wiley-Liss. New York, Garland Science.

Suh, J. H., S. V. Shenvi, et al. (2004). "Decline in transcriptional activity of Nrf2 causes age-related loss of glutathione synthesis, which is reversible with lipoic acid." Proceedings of the National Academy of Sciences of the United States of America **101**(10): 3381-3386.

Taguchi, K., Motohashi, H., Yamamoto, M. (2011). "Molecular mechanisms of the Keap1–Nrf2 pathway in stress response and cancer evolution." Genes to Cells **16**(123-140).

Thannickal, V. J. and B. L. Fanburg (2000). "Reactive oxygen species in cell signaling." American Journal of Physiology - Lung Cellular and Molecular Physiology **279**(6): L1005-L1028.

Turrens, J. F. (2003). "Mitochondrial formation of reactive oxygen species." The Journal of Physiology **552**(2): 335-344.

Vogler, S., Goedde, R., Miterski, B., Gold, R., Kroner, A., Koczan, D., Zettl, U., Rieckmann, P., Epplen, J. T., Ibrahim, S. M. (2005). "Association of a common polymorphism in

the promoter of UCP2 with susceptibility to multiple sclerosis." J Mol Med **83**: 806-811.

Wang, X., H. Ding, et al. (1997). "Association between air pollution and low birth weight: a community-based study." Environ Health Perspect **105**(5): 514-520.

Xu, Z., X. Xu, et al. (2011). "Ambient particulate air pollution induces oxidative stress and alterations of mitochondria and gene expression in brown and white adipose tissues." Particle and Fibre Toxicology **8**(1): 20.

Yang, W. and S. T. Omaye (2009). "Air pollutants, oxidative stress and human health." Mutation Research/Genetic Toxicology and Environmental Mutagenesis **674**(1–2): 45-54.

Ziemann, C., T. Hansen, et al. (2010). "Genotoxicity testing of sulfur dioxide (SO2) in a mouse bone marrow micronucleus test complemented with hematological endpoints." Mutat Res **697**(1-2): 38-46.

Ziqiang Meng, G. Q., Bo Zhang, Hong Geng, Quli Bai, Wei Bai, Chengyun Liu (2003). "Oxidative damage of sulfur dioxide inhalation on lungs and hearts of mice." Environmental Research **93**: 285–292.

APPENDIX 1

Protein standards for BCA assay

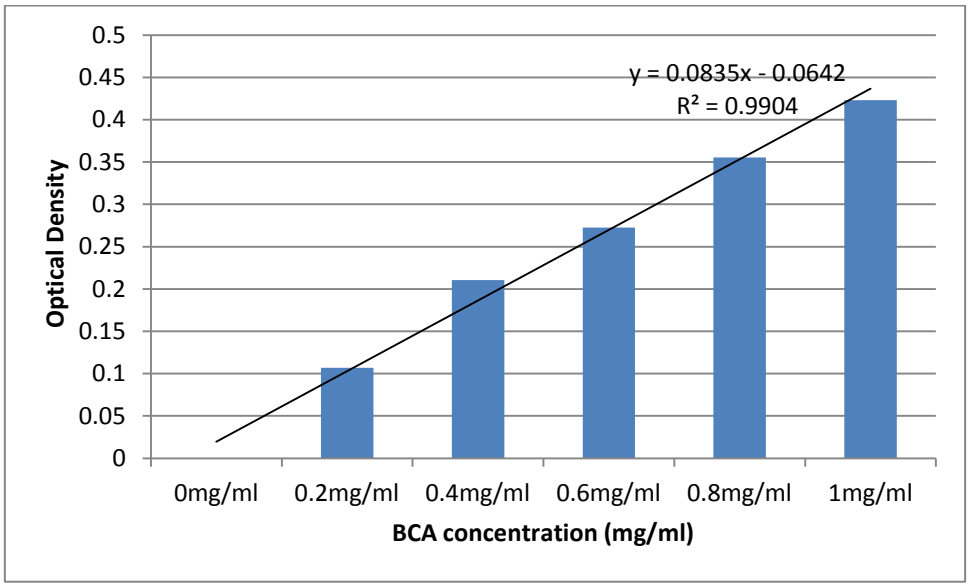

APPENDIX 2

Quantitative PCR calculations (Livak method)

ΔC(t) = Gene (Ct) – Housekeeping gene (Ct)

ΔΔC(t) = Experimental group (ΔCt) – Control (ΔCt)

Fold change = $2^{-\Delta\Delta Ct}$

	Nrf2	Nrf2	House keeping	House keeping		
	North C(t)	**South C(t)**	**North C(t)**	**South C(t)**	**North ΔC(t)**	**South ΔC(t)**
AA	31.38	28.78	16.01	11.99	15.37	16.79
AA	31.23	29.9	16.18	11.72	15.05	18.18
GA	30.04	30.18	13.37	12.7	16.67	17.48
GA	29.91	30.19	13.51	13.08	16.4	17.11
GG	33.9	30.11	15.99	13.78	17.91	16.33
GG	33.55	30.73	16.16	15.11	17.39	15.62
				Average	**16.465**	**16.91833333**

ΔΔC(t) = 16.92 – 16.47 = 0.45

Fold change = $2^{-\Delta\Delta Ct} = 2^{-(0.45)} = 0.73$

Similarly fold change between genotypes:-

Average ΔCt (GG) - Average ΔCt (AA/GA) = ΔΔC(t)

		Nrf2 Ct	Housekeeping gene Ct	ΔCt	ΔΔCt	$2^{-\Delta\Delta Ct}$
	AA/GA	30.605	14.65	15.955	-1.755	3.375263185
North	**GG**	33.86	16.15	17.71	0	1
	AA/GA	29.7625	12.3125	17.45	0.735	0.600818025
South	**GG**	30.42	13.705	16.715	0	1

	SOD2	SOD2	House keeping	House keeping		
	North C(t)	**South C(t)**	**North C(t)**	**South C(t)**	**North ΔC(t)**	**South ΔC(t)**
AA	29.65	26.52	16.01	11.99	13.64	14.53
AA	29.68	26.61	16.18	11.72	13.5	14.89
GA	28.93	28.95	13.51	13.08	15.42	15.87
GA	29.13	28.93	13.26	12.66	15.87	16.27
GG	33.48	28.83	15.99	13.78	17.49	15.05
GG	32.34	28.84	16.16	15.11	16.18	13.73
				Average	**15.35**	**15.05666667**

North vs South

$\Delta\Delta C(t) = 15.05 - 15.35 = -0.29$

Fold change = $2^{-\Delta\Delta Ct} = 2^{-(-0.29)} = 1.23$

Genotypes

Average ΔCt (GG) - Average ΔCt (AA/GA) = ΔΔC(t)

		SOD2 Ct	Housekeeping gene Ct	ΔCt	ΔΔCt	$2^{-\Delta\Delta Ct}$
	AA/GA	29.38	14.65	14.73	-2.45	5.464161027
North	**GG**	33.33	16.15	17.18	0	1
	AA/GA	27.7525	12.34166667	15.41083	0.280833	0.82311543
South	**GG**	28.835	13.705	15.13	0	1

	UCP2			Average Ct	Housekeeping gene			Average Ct
AA North	27.58	27.94	27.88	27.8	20.13	20.44	20.3	20.3
GA North	26.01	26.03	26.1	26.0	19.67	19.69		19.7
GG North	31.06	31.1	32.26	31.5	24.91	25.18	24.95	25.0
AA South	24.63	24.48	24.76	24.6	18.59	18.32	18.46	18.5
GA South	26.04	26.21	26.23	26.2	20.15	19.91	19.86	20.0
GG South	27.15	26.96	27.33	27.1	21.44	20.37	21.61	21.1

UCP2		House keeping gene					
Average Ct North	**Average Ct South**	**Average Ct North**	**Average Ct South**	**ΔCt North**	**ΔCt South**	**ΔΔCt**	**$2^{-\Delta\Delta Ct}$**
28.4	26.0	21.7	19.9	6.8	6.1	-0.7	1.57886617

		UCP2	Housekeeping gene			
		Average Ct	**Average Ct**	**ΔCt**	**ΔΔCt**	**$2^{-\Delta\Delta Ct}$ (FOLD CHANGE)**
North	**AA/GA**	26.9	20.0	6.9	0.5	0.717806388
	GG	31.5	25.0	6.5	0.0	1
South	**AA/GA**	25.4	19.2	6.2	0.2	0.888842681
	GG	27.1	21.1	6.0	0.0	1

mtDNA Ct		House keeping gene					
Average Ct North	**Average Ct South**	**Average Ct North**	**Average Ct South**	**ΔCt North**	**ΔCt South**	**ΔΔCt**	**$2^{-\Delta\Delta Ct}$**
25.61428571	26.13516129	24.15714286	23.65580645	1.5	2.5	1.0	0.492361

		mtDNA Ct	Housekeeping gene			
		Average Ct	**Average Ct**	**ΔCt**	**ΔΔCt**	**$2^{-\Delta\Delta Ct}$ (FOLD CHANGE)**
North	**AA/GA**	25.42083333	23.88666667	1.534166667	0.5	0.688168296
	GG	26.775	25.78	0.995	0.0	1
South	**AA/GA**	26.04428571	23.46761905	2.576666667	0.3	0.811314587
	GG	26.326	24.051	2.3	0.0	1